⑫

CHEMICAL
RESEARCH,
DEVELOPMENT &
ENGINEERING
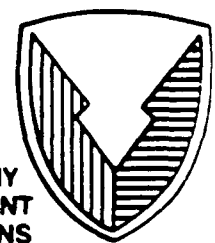# CENTER

AD-A229 912

CRDEC-CR-084
(GC-TR-1728-008)

MECHANISMS AND KINETICS OF CATALYTIC REACTIONS

Stephanie M. Garlick

GEO-CENTERS, INC.
Newton Center, MA 02159

August 1990

DTIC
ELECTE
DEC 11 1990
S
B
D

U.S. ARMY
ARMAMENT
MUNITIONS
CHEMICAL COMMAND

Aberdeen Proving Ground, Maryland 21010-5423

90 12 10 166

Disclaimer

The findings in this report are not to be construed as an official Department
of the Army position unless so designated by other authorizing documents.

Distribution Statement

Approved for public release; distribution is unlimited.

REPORT DOCUMENTATION PAGE

1. AGENCY USE ONLY (Leave blank)	2. REPORT DATE 1990 August	3. REPORT TYPE AND DATES COVERED Final, 88 Dec - 90 May

4. TITLE AND SUBTITLE Mechanisms and Kinetics of Catalytic Reactions	5. FUNDING NUMBERS C-DAAA15-87-D-0007
6. AUTHOR(S) Garlick, Stephanie M.	

7. PERFORMING ORGANIZATION NAME(S) AND ADDRESS(ES) GEO-CENTERS, Inc. 7 Wells Avenue Newton Centre, MA 02159	8. PERFORMING ORGANIZATION REPORT NUMBER CRDEC-CR-084 (GC-TR-90-1728-008)

9. SPONSORING/MONITORING AGENCY NAME(S) AND ADDRESS(ES) CDR, CRDEC, ATTN: SMCCR-RSC-C, APG, MD 21010-5423	10. SPONSORING/MONITORING AGENCY REPORT NUMBER

11. SUPPLEMENTARY NOTES

12a. DISTRIBUTION/AVAILABILITY STATEMENT Approved for public release; distribution is unlimited.	12b. DISTRIBUTION CODE

13. ABSTRACT (Maximum 200 words)

Second order rate constants, K_{IBA} have been determined for unsubstituted and 4-alkyl substituted o-iodosobenzoate catalyzed hydrolysis of the simulant p-nitrophenyl-diphenyl phosphate in microemulsions containing surfactants: cetyltrimethyl-ammonium bromide/chloride, or cetylpyridinium chloride; cosurfactants: 1-alkyl-2-pyrrolidinones, N,N-dialkylformamides, tetraalkylammonium chloride/bromide; oils: hexadecane, toluene, 4-tert-butyltoluene, and perchloroethylene. Additional cosurfactants containing N-C=O functionality, double-tailed surfactants, and aromatic N-alkyl oils have also been employed. Phase diagrams and maps have been constructed. The kinetics were optimized by varying component concentrations. Complex ruthenium molecules were synthesized and steady-state and time-resolved luminescence quenching techniques was employed to measure the aggregation number for eleven different microemulsions. The studies indicate that the time-resolved quenching technique is valid for most of the cases examined. However, the static method is unsuccessful for most cases.

14. SUBJECT TERMS Microemulsion media Luminescence quenching Catalysts Kinetics Physical studies Phase Maps Chemical studies			15. NUMBER OF PAGES 113
			16. PRICE CODE

17. SECURITY CLASSIFICATION OF REPORT UNCLASSIFIED	18. SECURITY CLASSIFICATION OF THIS PAGE UNCLASSIFIED	19. SECURITY CLASSIFICATION OF ABSTRACT UNCLASSIFIED	20. LIMITATION OF ABSTRACT UL

Blank

PREFACE

The use of trade names or manufacturers' names in this report does not constitute an official endorsement of any commercial products. This report may not be cited for purposes of advertisement.

Reproduction of this document in whole or in part is prohibited except with permission of the Commander, U.S. Army Chemical Research, Development and Engineering Center (CRDEC), ATTN: SMCCR-SPS-T, Aberdeen Proving Ground, Maryland 21010-5423. However, the Defense Technical Information Center and the National Technical Information Service are authorized to reproduce the document for U.S. Government purposes.

This report has been approved for release to the public.

Acknowledgments

Accession For	
NTIS GRA&I	☑
DTIC TAB	☐
Unannounced	☐
Justification	
By	
Distribution/	
Availability Codes	
Dist	Avail and/or Special
A-1	

iii

Blank

CONTENTS

MECHANISMS AND KINETICS OF CATALYTIC REACTIONS

1. INTRODUCTION

The hydrolysis of phosphate esters in microemulsion media has been studied and well documented. Mackay and Hermansky have studied the reactions of the phosphate esters, p-nitrophenyldiphenyl phosphate (PNDP), p-nitrophenyldihexyl phosphate, and p-nitrophenyldiethyl phosphate with hydroxide ion (OH⁻) and with fluoride ion (F⁻) in media consisting of water, n-hexadecane (HEX), 1-butanol (BuOH), and cetyltrimethylammonium bromide (CTAB).[1] Mackay, Longo, Knier, and Durst have studied o-iodosobenzoate (IBA) catalyzed hydrolysis in mildly basic, microemulsion media,[2] and have discovered that, at pH 9.2, IBA is a more effective nucleophile than OH⁻. (In fact, $k_{IBA} \geq 100 \times k_{OH}$ at pH 9.2.) Since the pK_a of IBA is 7.02,[2] the iodoso oxygen is negatively charged in mildly basic solutions. This research has, therefore, been directed toward the study of the catalyzed hydrolysis of the phosphate ester p-nitrophenyldiphenyl phosphate (PNDP).

Since microemulsions are effective chemical reactors, primarily because they bring together materials of widely different polarities, we have measured second order rate constants, k_{IBA}, for the IBA catalyzed hydrolysis of the agent simulant PNDP in microemulsions containing the surfactants: cetyltrimethylammonium bromide or chloride, or cetylpyridinium chloride (CPC); the cosurfactants: 1-alkyl-2-pyrrolidinones, N,N-dialkylformamides, tetraalkyl (C_1-C_8) ammonium chlorides and bromides; the oils: hexadecane, toluene, 4-tert-butyltoluene, perchloroethylene, o-xylene, or cumene. Furthermore, we have studied the substituted cosurfactants that contain the >N-C=O functionality, double-tailed surfactants, and aromatic N-alkyl oils in these systems. Ternary phase diagrams and pseudo-ternary phase maps have been constructed for these media. We have attempted to select concentrations of components that optimize the kinetics and minimize environmental hazards.

Second order rate constants have been measured for the catalyzed hydrolysis of PNDP in microemulsion media by 4-alkyl-substituted IBA derivatives. We have conducted a literature search for catalytic IBA derivatives, tabulated the results, and ordered the effectiveness of these derivatives.

We have determined hydrolysis rates of PNDP by photolyzed IBA in buffer and in microemulsion media.

A static, steady state method[3] was proposed by Turro and Yekta to determine micelle aggregation number (number of surfactant molecules/aggregate, N) from luminescence quenching measurements of a donor molecule. The method assumes that the dominant quenching mechanism of donor by acceptor is static or active-sphere quenching.[4] We have synthesized ruthenium complex donor molecules and have conducted steady-state luminescence quenching experiments and measured N for several media.

Time-resolved luminescence quenching measurements were used to either validate steady-state results or obtain additional information that could be used to calculate N. We employed an equation developed by Infelta, Grètzel, and Thomas to describe the kinetics of quenching reactions in micelles.[5]

2.   EXPERIMENTAL PROCEDURES

This section includes a brief description of the instrumentation used in the experiments and an outline of the procedures followed to complete them.

The procedures include phase map construction, kinetics determination of the rates of hydrolysis of PNDP in microemulsion media and in solutions, measurement of donor luminescence using steady-state and time-resolved techniques to determine N, and the ultraviolet irradiation of IBA. The syntheses of 4-alkyl-2-iodoso-benzoate catalysts and of donor molecules are diagrammed. A list of chemicals and abbreviations used in this report is included in Appendix A.   Figures are included in Appendix B; tables are included in Appendix C.

2.1   Phase Diagrams/Maps

Solutions and media were prepared by mass percentages and were stirred or sonicated and heated during titrant addition.   Increments of titrant weighed between 0.01 - 0.02 grams.   Sufficient time was allowed for equilibrium to be established between additions.   The aqueous phase (AQ) was 0.03 M borate buffer, pH 9.2.   Mixtures of surfactant (S) and cosurfactant (CoS) are termed emulsifier (E).   A high intensity lamp was used to examine solutions for the Tyndall effect exhibited by aggregate media. Solutions and mixtures were inspected in a polariscope for liquid crystals.

Ternary phase diagrams were constructed by titrating mixtures of S and AQ with CoS and by titrating mixtures of S and CoS with AQ along constant mass ratio titration lines (Figure 1).   Pseudo-ternary phase maps were constructed by titrating mixtures of E and oil (O) with AQ and by titrating mixtures of E and AQ with O (Figure 2).

Clear regions on the phase maps consist of either homogeneous solutions or microemulsion media, while turbid regions consist of macroemulsions or two or three phase heterogeneous solutions. Four component systems are designated as S/CoS/O/AQ. Three component systems are designated as S/CoS/AQ.

2.2 Kinetics

Kinetics rates were measured on a Gilford single beam spectrophotometer by measuring the absorbance of a hydrolysis product, p-nitrophenoxide ion, at 402 nm. Four cuvettes are automatically cycled and positioned every two minutes. The cell carriage is thermostatted and the temperature was maintained at 25.0 ± 0.1°C with a circulating water bath. The spectrophotometer is interfaced to an Apple IIe computer via an Adalab interface card for "real time" data acquisition. Apple IIe software programs, Precise Input 1.72 and Auto Algernon 1.1, were used to acquire and generate rate data.[6] The program, Precise Input 1.72, measures the absorbance in each cuvette every 2 minutes (dwell time). The absorbance is read twenty times during the dwell time and averaged. The program, Auto Algernon 1.1, analyzes the data and calculates the second order rate constant for each reaction.

Kinetics solutions were prepared in the following manner. An aliquot of a stock concentrated solution of catalyst in AQ was added to 5 mL of microemulsion media. Two mL of catalyzed microemulsion were added to one cuvette. Catalyzed microemulsion was diluted one to two, one to four, and one to eight with uncatalyzed microemulsion and 2 mL were added to three more cuvettes. Final IBA concentrations ranged from 1×10^{-3} M to 2×10^{-4} M and were selected to ensure a reaction half life $\leq$ 5 minutes.

The cuvettes were capped, thoroughly mixed, and equilibrated at 25°C. Following equilibration, 15 to 20 μL of a 3×10^{-3} M solution of PNDP in acetonitrile (ACN) were added to each cuvette. The cuvettes were capped and mixed, placed in the cell compart-

4

ments, and data acquisition was initiated. The concentration of PNDP in each cuvette ranged from 2×10^{-5} M to 3×10^{-5} M. The rate of hydrolysis of PNDP by OH⁻ in microemulsion media was determined similarly, however, equilibration time was 3-4 hours. [OH⁻] ranged from 2.7×10^{-2} M to 3.2×10^{-3} M.

Hydrolysis rates of PNDP by 1-methyl-2-pyrrolidinone (MP) and by 1-isopropyl-2-pyrrolidinone (iso-PP) were measured in AQ. A 1 $\times 10^{-2}$ M solution of pyrrolidinone in AQ was adjusted to pH 11.55. Two mL of this solution were placed in one cuvette. Cuvettes two, three, and four contained MP solution that had been diluted one to two, one to four, and one to eight with AQ.

The pH of all microemulsion media was measured before and after a kinetics run. Since the concentration of PNDP in the cuvette was low, the pH remained constant during the kinetics experiment.

2.3 Syntheses of Donor Molecules

Donor complexes were synthesized[7] by a method that Sutin[8] had adapted from procedures used by Braddock and Meyer,[9] and by Dwyer.[10] For ease, we designate: ruthenium (2⁺) tris (2,2'bipyridine-N, N')-dichloride, Ru(bpy)₃Cl₂:6H₂O, as I; ruthenium (2⁺) tris (1,10-phenanthroline-N¹,N¹⁰)-dichloride as II; ruthenium (2⁺) tris (4,7-diphenyl-1,10-phenanthroline-N¹,N¹⁰) dichloride hexahydrate, Ru [phen(ph)₂]₃Cl₂:6H₂O as III; †.is [[(1,10-phenanthroline-4,7-diyl) bis[benzene sulfonato]] (2⁻)-N,N']-tetrasodium ruthenate (4⁻) hexahydrate as IV; tris [[(1,10-phenanthroline-4,7-diyl) bis[benzenesulfonato]] (4/3⁻-N,N']-discdium ruthenate (2⁻) decahydrate as V.

A half gram of dipotassium aquopentachlororuthenate (III), K₂RuCl₅: x H₂O, was dissolved in 50 mL of hot water containing a drop of 6 N HCl. A stoichiometric quantity of the ligand, 1,10-phenanthroline, was added. The mixture was boiled for 10 - 20

minutes or until the solution turned dark green. A 1.2 mL volume of 30% hypophosphorus acid was neutralized with 3 - 4 mL of 2 N NaOH, and added to the green solution. This mixture was refluxed for ~ 30 minutes to give an orange-red mixture which was heated, filtered, acidified with 10 mL of 6 N HCl and evaporated. The ruthenium (2⁺) tris(1,10-phenanthroline-N^1,N^{10})-dichloride (II) was recrystallized several times from hot water. An identical synthetic procedure was followed less successfully for IV and V. Donors IV and V were eluted from a Sephadex LH-20 column with water and with a 15% aqueous solution of acetone to increase their purity. A similar procedure was followed to synthesize donor complex III. A stoichiometric quantity of the ligand, 4,7-di-phenyl-1,10-phenanthroline (DPPhen) was dissolved in 30 mL of DMF, added to the ruthenium (III) solution, boiled, and filtered. Hypophosphorus acid was added to the filtrate, and the solution was refluxed and filtered. Hydrochloric acid (6 N) was slowly added to the filtrate. The solution was evaporated, and the crystals (III) were washed 2 x with water. Elemental analysis by Schwartzkopf Laboratories indicated that the donor complexes were 70-99% pure.

2.4 Steady-State Luminescence Experiments

Steady-state luminescence was measured at 25.0°C on a Perkin Elmer MPF-66 computer-controlled spectrofluorimeter. Three mL of microemulsion media were added to a cuvette, and 20 µL of 2.0 x 10^{-3} M to 7.2 x 10^{-3} M donor solution in water (I, II, IV, V) or in MP (III) were added. The cuvette was capped, mixed thoroughly, and purged with nitrogen for ≥ 15 minutes.[11] The cuvette was positioned in the spectrofluorimeter and the intensity (I_o) was measured. Ten µL of 6.16 x 10^{-2} M solution of 9-methylanthracene (MeA) in ACN were added to the cuvette. The cuvette was capped, mixed thoroughly, purged for 3 minutes and the luminescence intensity (I) was measured. Another 10 µL of MeA were added to the cuvette and the process was repeated. The concentration range of MeA, in the cuvette was 2.033 x 10^{-4} M to 1.003 x 10^{-3} M. Data is analyzed with the equation[3]:

$$\ln \left(\frac{I_o}{I}\right) = \frac{([Q] N)}{([Surfactant] - [cmc])} \qquad \text{(1)}$$

A plot of ln (Io/I) versus [Q] results in a graph whose slope times the quantity, ([Surfactant] - [cmc]), equals the number average aggregation number, N. The critical micelle concentrations (cmc) for the surfactants were determined by light scattering or by solubility experiments.

Excitation/emission wavelengths used for the donors were 453/629 nm (I), 465/597 nm (II), 463/615 nm (III), and 469/612 nm (IV, V).

Emission intensities were measured in the ratio mode to compensate for time lags in the volt~ ~e applied to the detector, and to eliminate the wavelength depenuency of the gratings and the source.[65] Spectral correction factors were applied to the luminescence intensities to eliminate instrumental artifacts such as the wavelength dependent properties of the gratings, the source, and the detector. Excitation and emission correction factors were generated weekly. Steady-state luminescence measurements were collected in triplicate for each sample. When possible, concentrations of stock solutions were determined spectrophotometrically from reported absorptivities.

2.5 Time-Resolved Luminescence Experiments

Time-resolved fluorescence was measured at 532 nm by equipment diagrammed in Figure 3. Emission wavelengths used were 629 nm (I), 597 nm (II), 615 nm (III), and 612 nm (V). Three mL of micro-emulsion media were added to a cuvette and 20 µL of 2.0 x 10^{-3} M to 7.2 x 10^{-3} M solution of donor in water (I, III, IV, V) or in MP (III) were added. The cuvette was capped, mixed thoroughly, purged with nitrogen for ≥ 15 minutes,[11] and positioned in the illumina-

tor/sample chamber. Sample assembly and optics are physically aligned by viewing photomultiplier output on an oscilloscope. Data is collected by a transient recorder. Typically, for one curve, 512 points are collected at 0.02 µsec intervals. Data are saved on a floppy disc for transfer to a personal computer and subsequent data analysis by Asyst.[12]

A 25 µL sample of 6.16 x 10^{-2} M MeA in ACN is then injected into the cuvette. The cuvette is mixed thoroughly, purged for 3 minutes, and placed in the illuminator/sample chamber for lifetime and intensity measurements.

Equation 2[5] was used to estimate the zero time channel in the pulsed experiments, and to calculate the quenching constant, the average number of quencher molecules per aggregate, and the aggregation number:

$$F(t) = F(0) \exp (-A_2 t - A_3 (1 - \exp (A_4 t)))$$ (2)

Infelta's method[5] assumes that the quenching rate in an aggregate containing n quencher molecules is n times the quenching rate in a micelle containing one quencher molecule.[13]

A complete expression, assuming an immobile quencher, is provided by:

$$F(t) = F(0) \exp \{\frac{-t}{\tau_o} + \eta (e^{-k_q' t} - 1)\}$$ (3)

where A_2 equals $-1/\tau_o$, A_3 equals $-\eta$, and A_4 equals $- k_{q'}$, the first order rate constant for luminescence quenching of a donor by one

8

quencher in an aggregate. Intensity/time data sets are analyzed by Asyst which iterates on the values of F (t), η, and k_q until acceptable values are obtained. Once η has been determined, N is determined using the following equations:

$$\eta = \frac{[Q]}{[M]} \tag{4}$$

$$[M] = \frac{([Surfactant] - [free\ monomer])}{N} \tag{5}$$

Equation 3 is solved satisfactorily when the r^2 value is $\geq$ 0.99.

2.6 Ultraviolet Irradiation of IBA

Twenty mL of 1 x 10^{-3} M IBA in AQ were placed in a shallow glass beaker and irradiated with a low intensity ultraviolet (UV) lamp for 130 minutes. Light was incident to the solution's surface. Samples were removed at timed intervals and diluted 1:2 with media containing 36% CTAB/36% BuOH/8% HEX/20% AQ to give media containing 18% CTAB/18% BuOH/ 4% HEX/60% AQ and 5 x 10^{-4} M irradiated IBA. Hydrolysis rates of PNDP were measured in diluted sample. Uncatalyzed hydrolysis rates were determined in 18% CTAB/18% BuOH/4% HEX/60% AQ as baseline values.

The experiment was repeated with high intensity UV. Samples were removed at timed intervals for 25 minutes. One mL samples were removed and similarly diluted. The hydrolysis rate of PNDP was measured.

Twelve mL of 1 x 10^{-3} M IBA in AQ were placed in a sealed quartz tube and positioned in the sun for 8.5 days. Duplicate 1 mL

samples were removed and diluted with microemulsion concentrate. The rate of hydrolysis of PNDP was measured in each sample.

Since photolyzed solutions were brown, a starch solution was prepared to test for I_2. Starch (0.5 g) was added to 20 mL of formamide and heated. Photolyzate was added to an aqueous solution of I^-. Two drops of cooled starch solution were added to this solution and to 2 mL of a control solution of I_2/I^-. For NMR and mass spectroscopy studies, 120 mL of 1 x 10^{-3} M IBA in water were irradiated in 20 mL volumes by low intensity UV. Irradiated volumes were combined, evaporated to dryness, and submitted for analysis.

2.7 Syntheses of IBA Derivatives

Several 4-alkyl-2-iodosobenzoic acid derivatives were synthesized.[14] These were 2-iodoso-4-methylbenzoic acid, 2-iodoso-4-ethylbenzoic acid, 2-iodoso-4-n-propylbenzoic acid, 2-iodoso-4-n-pentylbenzoic acid, 2-iodoso-4-n-octylbenzoic acid. Attempts to synthesize 2-iodoso-4-n-butylbenzoic acid and 2-iodoso-4-n-hexylbenzoic acid were unsuccessful. Synthetic schemes have not been included for priority reasons.

A weighed sample of derivative was added to 4 mls of distilled water. A molar equivalent of standard 0.2 N NaOH solution was added and the mixture was allowed to stand until conversion to the sodium salt was complete. Less than 100 uL of catalyst was added to 5 mL of control microemulsion containing 8% CTAB/8% MP/4% TOL/80% AQ. The PNDP hydrolysis rate was measured and compared to rate constant data obtained for unsubstituted IBA.

3. EXPERIMENTAL RESULTS

Experiments were selected to improve our assessment of how different components and structural features of microemulsions affect PNDP hydrolysis and to devise more efficient, environmentally safe systems for decontamination.

3.1 CTAC/N,N-Dialkylformamide/HEX/AQ

Satisfactory rate constants for PNDP hydrolysis have been obtained in CTAC/DBF/HEX/AQ microemulsions.[15,16] The excellent solubilizing potential of N,N-dialkylformamides has prompted us to test additional N,N-dialkylformamides as cosurfactants in microemulsion aggregates.[17]

3.1.1 Phase Maps

An appreciable clear area exists on the CTAC/DMF/AQ ternary phase diagram (Figure 4) in the water rich region. Clear media are reasonably fluid, and therefore, suitable for kinetics measurements. There is a liquid crystalline region, and approximately 40% of the diagram is turbid.

When the E ratio is equal to 1.0 in the CTAC/DMF/HEX/AQ system, the phase map is completely turbid. A phase map for the CTAC/DMF/HEX/AQ system with the E ratio equal to 2.0 is shown in Figure 5. Liquid crystals form in the low AQ, low O, high S region. No clear regions exist.

A phase diagram of the CTAC/DIPF/AQ system is shown in Figure 6. This diagram is similar to CTAC/DMF/AQ diagram, however, a larger liquid crystalline region is observed.

Phase maps obtained in the CTAC/DBF/HEX/AQ system[16] indicate that clear regions on the phase maps decrease in size as the E ratio increases. Also, as the E ratio increases, the viscosity

increases. Therefore, clear regions containing non-viscous microemulsions should occur at low E ratios in the CTAC/DIPF/HEX/AQ system. A phase map was constructed for this system at an E ratio of 0.5 (Figure 7). Most of the map is turbid. Small turbid liquid crystalline and clear areas are observed in the low AQ, low O, high E region.

3.1.2 Kinetics

Values for k_{IBA}, as a function of E ratio, were obtained in CTAC/ DMF/AQ systems, and are presented in Table 1. In this experiment, the % AQ remained constant as the E ratio decreases from 9.0 to 1.0 to 0.11. When E ratio is 0.11, a rate constant of 21.47 $sec^{-1}M^{-1}$ is measured. However, when the E ratio is 9.0, the rate constant decreases to 8.53 $sec^{-1}M^{-1}$.

Second order rate constants for the catalyzed hydrolysis of PNDP were measured in 8% CTAB/8% N,N-dialkylformamide/4% TOL/80% AQ systems (Table 2). Clear media could not be prepared with 8% DBF.

3.1.3 Conclusions/Discussion

The CTAC/N,N-dialkylformamides/AQ systems that we have studied are easy to prepare, are non-viscous, and exhibit good rate constants for the catalyzed hydrolysis of PNDP. However, phase map studies indicate that the solubility of HEX in these systems is low.

The clear regions obtained on the pseudo-ternary phase maps containing CTAC/N,N-dialkylformamides/HEX/AQ are small, and liquid crystalline regions occur in the medium to low % AQ regions of the maps. Clear areas, however, appear on the four component phase maps, and increase in size as the length of the N-alkyl group of the CoS increases.

Kinetics results indicate that the rate constant decreases in CTAC/ DMF/AQ systems as the E ratio decreases at constant % AQ.

With 3% CTAC, the solution is probably micellar, which explains the higher rate constant. With 27% S, the aggregates may be non-spherical.[18] Since the hydrolysis of PNDP has previously been suggested[17] as occurring at the water/oil interface, hydrolysis rates should increase as aggregate interfacial area increases. This may explain the lower rate constant obtained with 27% CTAC.

When TOL replaces HEX in these systems, the hydrolytic effectiveness of the dialkylformamides tested in the 8% CTAC/8% N,N-dialkylformamide/4% TOL/80% AQ system is ordered: DMF > DEF > DIPF > DBF.

Phase map studies have indicated that N,N-dialkylformamides are not practical as cosurfactants in microemulsions containing HEX. However, when TOL replaces HEX, clear media can be prepared.

3.2 CTAB/1-Alkyl-2-Pyrrolidinone/HEX/AQ

The 1-alkyl-2-pyrrolidinones were tested as cosurfactants for several reasons. First, their structures are similar to the N,N-dialkylformamides which have previously been employed as cosurfactants.[15] Both structures contain the >N-C=O functionality and have similar resonance forms. The N-alkyl-2-pyrrolidinones are probably zwitterionic at pH 9.2. Their high polarity is a result of resonance stabilization. Second, the 1-alkyl-2-pyrrolidinones are aprotic liquids and are miscible with water and conventional organic solvents.[19] Third, the 1-alkyl-2-pyrrolidinones are non-corrosive and stable at environmental extremes. They are also unreactive to the microemulsion components used.

The N-alkyl-2-pyrrolidinones are biodegradable and non-toxic. The LD_{50} value for MP in white rats is 4.2 grams/kg. When ^{14}C and ^{3}H labeled MP is injected into rats, 90% of the isotope appears in the urine within twenty four hours. MP has been determined to be biodegradable by measuring the oxygen uptake in Warburg respirome-

13

try tests.[20]   The vapor pressure of MP is 0.29 mm at 20°C, there-
fore, the risk of exposure by inhalation is minimal.

3.2.1   Phase Maps

A ternary phase diagram of the CTAB/MP/AQ system was
completed. Mixtures of CTAB and MP, and CTAB and AQ were titrated
respectively with AQ (Figure 8) and with MP (Figure 9). When CTAB
and MP were titrated with AQ the phase diagram contained turbid,
gelled, turbid liquid crystalline, and clear regions. When CTAB
and AQ were titrated with MP the phase diagram contained turbid and
clear regions. Gelled solutions did not clear on standing. The
gels "melted" and cleared when heated, but re-gelled on cooling.
The constant mass ratio titration lines are indicated on both
figures to indicate the direction of the titrations. In general,
the appearance of a phase map or a phase diagram does not depend on
the order of mixing of the components.[21] However, in this case, two
different diagrams were obtained.

Phase diagrams in CTAB/EP/AQ (Figure 10), CTAB/Iso-PP/AQ
(Figure 11), and CTAB/CHP/AQ (Figure 12) systems are similar in
appearance and contain comparable clear regions.

Pseudo-ternary phase maps were constructed in these systems.
The phase map of the CTAB/MP/HEX/AQ system with an E ratio equal to
0.11 is turbid. Solutions prepared at higher E ratios in this
system were also turbid or gelled. Phase maps of the CTAB/EP/HEX/
AQ system with E ratios equal to 0.11 and 0.67 are turbid. A small
clear region appears on the CTAB/Iso-PP/HEX/AQ phase map (Figure
13) when E ratio equals 1.0.

Phase maps for the CTAB/CHP/HEX/AQ system with the E ratio
equal to 0.11 (Figure 14), 0.25 (Figure 15), 0.43 (Figure 16), 0.67
(Figure 17), 1.5 (Figure 18), and 4.0 were constructed. When the
E ratio varies from 0.11 to 0.67 a narrow clear region appears
along the 60% E/40% AQ titration line. No explanation is offered

for this result. When the E ratio is equal to 1.5, a small clear area occurs at high AQ. At an E ratio of 4.0, the phase map is turbid.

3.2.2 Kinetics

Rate constants for k_{IBA} were measured in CTAB/1-alkyl-2-pyrrolidinone/AQ systems (Table 3). Media contained either identical mass % but different pyrrolidinones or increasing % EP. Rate constants for k_{OH} and k_{hyd} were determined in CTAB/EP/AQ and CTAB/CHP/AQ systems. Values of k_{IBA}, k_{OH}, and k_{hyd} were measured in CTAB/CHP/HEX/AQ systems. In four media, % AQ was constant and E ratio varied (Table 4). Values for k_{hyd} are ¯ 0.

A k_{IBA} value of 4.03 $sec^{-1}M^{-1}$ was obtained in media containing 25.6% CTAB/17.0% CHP/2.2% HEX/55.2% AQ. When CTAC was substituted for CTAB in this formulation, k_{IBA} increased. Both microemulsions were viscous.

3.2.3 Conclusions/Discussion

The CTAB/1-alkyl-2-pyrrolidinone/AQ phase diagrams are all similar in appearance. Ternary systems tested became turbid when HEX was added. Small clear regions, however, appear on the phase maps as one proceeds from MP to CHP as CoS. Phase maps obtained in the CTAB/CHP/HEX/AQ systems cannot be adequately explained at this time.

The k_{IBA} values obtained in CTAB/1-alkyl-2-pyrrolidinone/AQ systems decrease as the bulk of the N substituent increases. At constant % AQ and % HEX in the CTAB/CHP/HEX/AQ systems, k_{IBA} values increase as E ratio increases. Rate constants for PNDP hydrolysis by OH¯ in the CTAB/CHP/HEX/AQ system with E ratios of 0.11 and 0.43 are identical. Similar k_{OH} values are obtained in the CTAB/CHP/AQ and the CTAB/EP/AQ systems.

15

Results obtained from the phase map and kinetics studies indicate that systems containing CTAB/1-alkyl-2-pyrrolidinone/AQ provide an effective environment for the hydrolysis of phosphate esters. When the oil HEX is added, small clear regions are obtained only on the phase maps containing CHP as CoS. These results agree with results obtained when N,N-dialkylformamides function as cosurfactants. Increasing the hydrophobicity of the N-alkyl groups increases the compatibility of the cosurfactant with the oil. Since the 1-alkyl-2-pyrrolidinones are not sufficiently compatible with the oil HEX, and the rates of PNDP hydrolysis in CTAB/CHP/HEX/AQ systems are slow, these systems are not suitable for the hydrolysis of phosphate esters.

3.3   CPC/1-Alkyl-2-Pyrrolidinone/HEX/AQ

Instead of substituting a different oil for HEX in the CTAB/ 1-alkyl-2-pyrrolidinone/HEX/AQ systems, it was first decided to substitute the surfactant CPC for CTAB. It was anticipated that the aromatic ring and the hexadecyl tail of CPC could increase the solubility of HEX in these systems.

3.3.1   Phase Maps

Ternary phase diagrams consisting of CPC/MP/AQ (Figure 19) and CPC/CHP/AQ (Figure 20) were completed. Clear regions on these diagrams are similar in size and location to clear regions obtained in the CTAB/EP/AQ, the CTAB/Iso-PP/AQ and the CTAB/CHP/AQ systems. Clear, three component systems, however, became turbid when HEX was added.

3.3.2   Kinetics

In order to ascertain the relative effectiveness of CPC systems as media for PNDP hydrolysis, CPC and CTAB microemulsions of 12% S/10% MP/78% AQ were prepared. Rate constants for k_{IBA} equal to 14.09 ± 0.12 $sec^{-1}M^{-1}$ and to 14.05 ± 0.35 $sec^{-1}M^{-1}$ (See Table 3) were obtained in the CPC and in the CTAB system. No other studies were completed in this system.

3.3.3 Conclusions/Discussion

Three component systems containing CPC/1-alkyl-2-pyrrolidin-one/AQ and four component systems containing CPC/1-alkyl-2-pyrroli-dinone/HEX/AQ offer no advantage when compared to similar three and four component systems containing CTAB surfactant. When CPC was substituted for CTAB, HEX solubility in these systems did not improve.

3.4 CTAB/1-Alkyl-2-Pyrrolidinone/TOL/AQ

Since previously tested four component systems containing the oil HEX were turbid, TOL was tested in CTAB/CHP/OIL/AQ systems. The vapor pressure of toluene is 40 mm at 31.8°C and environmental-ly unacceptable, even in a mixture. Other oils, therefore, were tested first in the CTAB/CHP/OIL/AQ system. These oils included ʋ-xylene (10 mm at 32.1°C), cumene (10 mm at 38.3°C), phenylhexane (˜ 1 mm at 102°C), phenyldecane (˜ 1 mm at 110°C), and 4-tert-butyl-toluene (˜ 1 mm at 25°C).[22,23]

3.4.1 Phase Maps

Pseudo-ternary phase maps were constructed in the CTAB/MP/TOL/AQ system at E ratios equal to 0.5 (Figure 21), 0.76 (Figure 22), 1.0 (Figure 23), and 1.5 (Figure 24). Clear regions increase in size as the E ratio increases. At an E ratio of 0.76, a small, clear, liquid crystalline region exists at ˜ 90% AQ; at high % TOL a small microemulsion island, probably water in oil (W/O), and a larger gel region are observed. At an E ratio of 1.0, a narrow, turbid liquid crystalline region is observed between ˜70% and 90% AQ. A large gel region occurs when the E ratio is equal to 1.5.

Maps were constructed for the CTAB/CHP/t-BuTOL/AQ system with E ratios equal to 0.5 (Figure 25), 0.76 (Figure 26), 1.0 (Figure 27), and 1.5 (Figure 28). In this system, the clear microemulsion regions decrease in size as the E ratio increases from 0.76 to 1.5. When the E ratio is equal to 0.76, a small, turbid, liquid crystalline area occurs at high O. Considerable gel regions exist

at the higher E ratios. A phase map of the CTAB/CHP/TOL/AQ system at an E ratio of 1.0 (Figure 29) was constructed for comparison with the CTAB/MP/TOL/AQ system. A large, clear region extends from low to high % AQ.

A phase map was constructed in the CTAB/CHP/XY/AQ (Figure 30) system. This map is similar in appearance to the phase map of the CTAB/ CHP/TOL/AQ system. Clear regions contained reasonably fluid media.

To determine if the 1-alkyl-2-pyrrolidinones were functioning as cosurfactants, a phase diagram consisting of CTAB/TOL/AQ was constructed. This diagram was turbid. Systems with the potential to form microemulsions, however, usually clear when CoS is added. When selected turbid mixtures of CTAB, TOL, and AQ are titrated with MP or with CHP, clear microemulsions form. This indicates that MP and CHP are probably functioning as cosurfactants.

The double-tailed surfactants Variquat K300, Arosurf TA-101, and Adogen 442 were tested in these systems. Arosurf TA-101 and Adogen 442 were insoluble. Variquat K300 was soluble in several MP/TOL/AQ systems, however, contains ~25% isopropanol. Rate constants for PNDP hydrolysis in 8% CTAB/8% MP/4% TOL/80% AQ decreased from 11.06 ± 0.11 sec^{-1}M^{-1} to 8.72 ± 0.02 sec^{-1}M^{-1} when 2.5% isopropanol was added.

1-Phenylhexane and 1-phenyldecane were tested as oils. Several clear microemulsions were prepared in CTAB/1-alkyl-2-pyrrolidinone/PhHEX/AQ systems (Table 5). When the oil was 1-phenyldecane, media were turbid.

3.4.2 Kinetics

Rate constants for IBA catalyzed PNDP hydrolysis were measured in microemulsions containing equal mass % (Table 6) or equal moles (Table 7) of 1-alkyl-2-pyrrolidinones. At 8% CoS, k_{IBA} values

18

ranged from 11.06 $sec^{-1}M^{-1}$ for MP to 5.01 $sec^{-1}M^{-1}$ for VP. With equimolar cosurfactant, the rate constant ranged from 11.06 $sec^{-1}M^{-1}$ for MP to 3.26 $sec^{-1}M^{-1}$ for CHP.

To determine how % AQ affects the rate constants, k_{obsd} values were measured in the MP system as a function of % AQ (Table 8). As % AQ varies from 81.1% to 74.5% in 8% CTAB/MP/4% TOL/AQ systems (first section, Table 8), k_{obsd} decreases from 5.73 sec^{-1} at 6.9% MP and 81.1% AQ to 4.99 sec^{-1} at 13.5% MP and 74.5% AQ. Values of k_{obsd} with different pyrrolidinones as cosurfactants decrease from 4.84 sec^{-1} for 2-P to 1.66 sec^{-1} for CHP (second section, Table 8). Because microemulsions prepared with the cosurfactants CHP and MP provided the extremes in our preliminary kinetics studies, we investigated the IBA catalyzed hydrolysis of PNDP in CTAB micro-emulsions containing MP and CHP in detail over a wide range of compositions.

In CTAB/MP/TOL/AQ systems, as E varies from 0.50 to 1.75 (first section, Table 9) at constant % O and % AQ, the second order rate constants, k_{IBA}, do not significantly change. At an E ratio of 1.0 (second section, Table 9), the k_{IBA} values measured at an E to O mass ratio of either 3 or 9, range from 4.0 $sec^{-1}M^{-1}$ to 6.3 $sec^{-1}M^{-1}$ as % AQ increases from 35% to 60%. When % AQ increases from 65% to 85%, the k_{IBA} values increase dramatically from 7.31 $sec^{-1}M^{-1}$ to 17.3 $sec^{-1}M^{-1}$ at an E ratio of 1.0. A k_{IBA} value of 25.1 $sec^{-1}M^{-1}$ was measured in media containing 90% AQ and 1% O, suggesting that the system probably contains micellar aggregates. (Since PNDP is not water soluble, an accurate k_{IBA} value cannot be measured in 100 % AQ.) In the last section of Table 9, rate constants decrease at increasing % TOL and decreasing % AQ.

Rate constants change only slightly when 4-tert-butyltoluene (t-BuTOL) substitutes for TOL in CTAB/MP/TOL/AQ systems, or when TOL is substituted for t-BuTOL (Table 10) in CTAB/CHP/t-BuTOL/AQ systems. Therefore, TOL was replaced by the less volatile t-BuTOL

in *systems containing CHP.* In CTAB/CHP/t-BuTOL/AQ systems, k_{IBA} values (first section, Table 10) increase only slightly as the E ratio increases from 0.50 to 1.75. With a constant E ratio of 1.0, increasing % AQ at an E to O ratio of 9, results in ¯ constant k_{IBA} values ranging from 3.43 $sec^{-1}M^{-1}$ at 20% AQ to 3.94 $sec^{-1}M^{-1}$ at 60% AQ (second section, Table 10). The k_{IBA} values increase to 12.6 $sec^{-1}M^{-1}$ when % AQ increases to 90%. As % t-BuTOL varies from 11% to 23%, only slight variations in k_{IBA} values are noted (last section, Table 10).

Values of k_{IBA} were determined in CTAB/CHP/OIL/AQ systems with the oils toluene, o-xylene, or cumene. Similar k_{IBA} values were measured in these oils (Table 11). Also, as % TOL, % XY, or % CUM increases and % AQ decreases at constant E ratio, k_{IBA} values decrease only slightly.

The structure and the hydrolytic effectiveness of microemulsions containing 1-alkyl-2-pyrrolidinones suggested that these materials may function as nucleophiles in PNDP hydrolysis. However, experiments in our laboratory indicate that MP and iso-PP are not directly involved in PNDP hydrolysis in AQ. As pyrrolidinone concentration varies from 0.001 M to 2.5 M, pseudo first order rate constants for PNDP hydrolysis remain constant at 3.87 ± 1.97 x 10^{-5} sec^{-1} for MP and 5.01 ± 0.67 x 10^{-5} sec^{-1} for iso-PP. CTAB/1-phenyl-2-pyrrolidinone/O/AQ systems were prepared. When TOL is the oil, investigated media were turbid. When the oil is 1-phenylhexane, microemulsions formed only on heating.

Additional compounds containing the >N-C=O functionality were tested as cosurfactants. These included: 1,3-dimethyl-3,4,5,6-tetrahydro-2 (1H-) pyrimidinone (DMP); 1,1,3,3-tetramethylurea (TMU); 1-pyrrolidine carboxaldehyde (1-PC); 1,3-dimethyl-2-imidazolidinone (DMIZ); 1-formyl piperidine (1-FP); and N,N-dimethylacetamide (DMAC). Several N,N-dialkyl formamides and MP were also included for comparison. Two sets of microemulsions were prepared.

20

Set 1 contained 8% CTAB/8% CoS/4% TOL/80% AQ, and set 2 contained 8% CTAB/0.8073 M CoS/4% TOL/AQ. Rate constants for the catalyzed PNDP hydrolysis were measured (Table 12). At 8% CoS, rate constants ranged from 11.67 $sec^{-1}M^{-1}$ for DMP and 11.26 $sec^{-1}M^{-1}$ for DMIZ to 3.83 $sec^{-1}M^{-1}$ for DIPF. At 0.8073CoS, a value of 12.56 $sec^{-1}M^{-1}$ was obtained for DMAC. These systems were not investigated further.

Several 1-phenyl-2-pyrrolidinones (PhP) were synthesized.[14] These were 4-n-butyl-PhP, 4-methoxy-PhP, and 4-tetramethylammonium-PhP. When O was TOL or PhHEX, systems tested were turbid, even when heated to 100°C.

3.4.3 Conclusions/Discussion

Results of phase map studies indicate that the 1-alkyl-2-pyrrolidinones tested are suitable as cosurfactants in CTAB/1-alkyl-2-pyrrolidinone/O/AQ systems containing TOL or t-BuTOL as oil. Clear microemulsions form in CTAB systems containing the oils TOL, t-BuTOL, and HEX with CHP as cosurfactant, and in CTAB systems containing TOL and t-BuTOL with MP as cosurfactant.

Results of kinetics studies imply that the N-alkyl substituent of the pyrrolidinone cosurfactants affects the kinetics in CTAB/1-alkyl-2-pyrrolidinone/TOL/AQ microemulsions. From Tables 6 and 7, the order of hydrolytic effectiveness of the microemulsions is: MP > 2-P > EP > iso-PP ≈ AP > CHP.

Rate constants decrease as the bulk of the alkyl group increases. First order rate constants obtained in 8% CTAB/MP/4% TOL/AQ systems indicate that a slight variation in % AQ in the systems does not significantly affect the rate constants. Therefore, the differences in the measured rate constants of the pyrrolidinones reflect the nature of the N-alkyl substituent. However, since the rate constants show a definite dependence on the nature of the N-alkyl substituent, but are independent of pyrroli-

21

dinone concentration, the function of the pyrrolidinone in the microemulsion may involve factors which only indirectly influence PNDP hydrolysis: the size and shape of the microdroplet and/or the nature of the aggregate interface. With the exception of VP, pyrrolidinone polarity and second order rate constants are similarly ordered.

Lower rate constants are obtained when CHP is substituted for MP in microemulsions containing TOL or t-BuTOL as oil (Tables 9 and 10). Also, as % AQ increases in CTAB/MP or CHP/TOL or t-BuTOL/AQ systems, rate constants measured for catalyzed PNDP hydrolysis increase. In similar systems,[15,16] rate constants generally increase as % AQ increases. At 100% AQ, the microemulsion frequently breaks and the solutions become turbid.

Due to limited solubility in water, the double-tailed surfactants tested cannot replace CTAB or CTAC in S/1-alkyl-2-pyr-rolidinone/O/AQ systems.

Toluene, o-xylene, and cumene are effective oils in CTAB/1-alkyl-2-pyrrolidinone/OIL/AQ systems (Table 11). The slight differences of these oils have little effect on measured rate constants. Therefore, the oils t-BuTOL, o-XY, and CUM can replace TOL in CTAB/CHP/O/AQ systems. Furthermore, the vapor pressure of these oils (neat) at 25°C is ≤ 5 mm.

Additional compounds tested were all effective as cosurfactants in CTAB/CoS/TOL/AQ systems. Rate constants measured for catalyzed PNDP hydrolysis (Table 12), were all comparable to values obtained with 1-alkyl-2-pyrrolidinone cosurfactants. Rate constants determined in systems containing cosurfactants (DMP, DMIZ, TMU) with a carbonyl group adjacent to two nitrogens are higher than those obtained in systems containing cosurfactants with only the >N-C=O functionality.

22

The N-alkyl-2-pyrrolidinones, as a class, clarify CTAB and CTAC microemulsions, and, therefore, behave like alcoholic cosurfactants. Since rates of phosphate ester hydrolysis are dependent on the specific nature of the N-alkyl group, we can infer that the pyrrolidinones are present at the reaction site, but are not directly involved in PNDP hydrolysis. Furthermore, since the N-alkyl-2-pyrrolidinones are water and oil soluble, these compounds may be appropriate as reaction media, and may function as oils in S/CoS/O/AQ systems.

In conclusion, microemulsions containing 1-alkyl-2-pyrrolidinones as cosurfactants provide media in which the hydrolysis of phosphate esters is rapid. The oil dissolving power of microemulsions is greatly enhanced when 1-alkyl-2-pyrrolidinones are employed as cosurfactants; such systems are, therefore, very attractive as microreactors and as decontamination media.

3.5 CTAC/Tetraalkylammonium Halide/PERC/AQ

The MCBD (Multipurpose Chemical and Biological Decontaminant) microemulsion[24] has been investigated as a potential decontamination media. The MCBD microemulsion contains 16.5% CTAC/11.6% TBAOH, 1.4% Adogen 464 (Ad)/7.5% PERC/63.0% H_2O. Since the pH of this system is $\geq$ 13.5 it is necessary to add ~ 0.25 M H_3BO_3 to adjust the pH to 11.2. However, if the pH falls below ~ 11, cetyltrimethylammonium borate salts precipitate.

Tetraalkylammonium (C_4 to C_{10}) hydroxides and halides (TAAX) function as phase-transfer catalysts in organic synthesis,[26-28] and have been employed as hydrotropes[38] to improve the solubility of organic compounds in water.[66] It has previously been demonstrated that, while TAAX function as CoS in CTAC/Ad/HEX/AQ[15-17] and in CTAC/TAAX/PERC/AQ[31] systems, tetraalkylammonium (C_4 to C_{10}) ions do not form aggregates.[31-34] Instead, TAAX may increase the rate of hydrolysis of phosphate esters by: providing an hydrophobic environment that allows the substrate and the nucleophile to form

a tight ion-pair;[33] forming nonmicellar aggregates that could be catalytically active,[34] simple salt effects;[34] solvent effects.[35,36]

Since the MCBD formulation is complex and unstable (salts precipitate on standing[59]), we attempted to simplify the MCBD composition. Simplification techniques included: substituting other TAAX for TBAOH and Ad; determining the minimum concentration of TBAX necessary for microemulsion formation and good hydrolysis rates of PNDP; determining if E ratio and % AQ affect microemulsion formation; acsertaining the importance of Ad. TAAX tested as cosurfactants contained four identical N-alkyl substituents.

3.5.1 Phase Maps

Because OH⁻ effectively hydrolyzes PNDP at pH 11, we conducted IBA catalyzed kinetics studies at pH 9.2. Also, because TBAOH was received as a 40% aqueous solution, we determined pseudo-ternary phase maps for CTAC/TBACl, Ad/PERC/AQ systems. TBACl and Ad, mass ratio 8.2, TBACl to Ad, were cosurfactants. The E ratio in the MCBD microemulsion is 1.26.

Pseudo-ternary phase maps were constructed in CTAC/TBACl, Ad/PERC/AQ systems at emulsifier ratios of 0.5 (Figure 31), 0.76 (Figure 32), and 1.25 (Figure 33). Clear regions, whose areas seem independent of E ratio, extend from 20% to 80% S and from low to moderate (~50%) oil. The map is turbid, except for gel regions in low % AQ, high % O.

3.5.2 Kinetics

We have measured second order rate constants, k_{IBA}, for IBA catalyzed PNDP hydrolysis in CTAC/TBACl, Ad/PERC/AQ microemulsions. With E to O ratio of ~ 4, k_{IBA} values (first section, Table 13) increase from 4.99 sec⁻¹M⁻¹ to 6.37 sec⁻¹M⁻¹ at 50% AQ and 10% O, and from 5.90 sec⁻¹M⁻¹ to 8.05 sec⁻¹M⁻¹ at 60% AQ and 8% O as the E ratio increases from 0.50 to 1.25. As % AQ increases from 20.0% to 79.7% with E ratio of 0.76 (second section, Table 13), k_{IBA} values

24

increase from 4.53 $sec^{-1}M^{-1}$ to 12.5 $sec^{-1}M^{-1}$. In Figure 34, k_{IBA} is plotted versus % AQ.

Since previous kinetics studies in the MCBD microemulsion were completed at pH 11.2 with a different substrate, we measured k_{IBA} for PNDP hydrolysis in the MCBD microemulsion at pH 11 for comparison. A k_{IBA} value of 17.6 $sec^{-1}M^{-1}$ was measured (Table 14). When TBACl replaced TBAOH, k_{IBA} was 10.1 $sec^{-1}M^{-1}$. When 11.6% TBAOH was added to an 8% CTAB/8% MP/4% TOL/68.4% AQ microemulsion, k_{IBA} was 10.3 $sec^{-1}M^{-1}$. At 13.0% TBACl and pH 9.4, k_{IBA} was 1.67 ± 0.27 $sec^{-1}M^{-1}$ for catalyzed PNDP hydrolysis in AQ.

First order rate constants, k_{obsd}, for catalyzed PNDP hydrolysis in AQ containing TBACl (Table 15), increase from 4.63 x 10^{-4} sec^{-1} to a constant value of ~ 12 x 10^{-4} sec^{-1} at % TBACl > 4 - 5%.

Fifty mg of PNDP were added to 5 mL of AQ at pH 9.4 and at pH 11.2 with and without 13% TBACl. The solutions appeared clear. After centrifugation, 1mL volumes of supernatant were removed at 10, 60, and 180 minutes and diluted 1:2 with water. Absorbances were measured at 402 nm (Table 16).

Solutions of AQ containing ≤ 4 to 5% of either THABr or TBABr and 3 x 10^{-5} M PNDP were turbid.[59] However, since solutions containing 3 x 10^{-5} M PNDP in AQ and > 4 - 5% TAAX were not visually turbid, second order rate constants were measured in systems containing 15.9% CTAC/4.8% TAAX/8.5% PERC/70.8% AQ (Table 17). When Ad is not added, k_{IBA} values range from 13.3 $sec^{-1}M^{-1}$ to 9.4 $sec^{-1}M^{-1}$ with different TAAX. Due to the low solubility of TOAX in water, only microemulsions containing ≤ 2.5% TOABr could be prepared. In fact, gels formed at higher % TOABr. Clear media could not be prepared with 4.8% TMACl. Values for k_{IBA} of 13.8 $sec^{-1}M^{-1}$ and 13.3 $sec^{-1}M^{-1}$ were measured in similar CTAC/~4% TBACl/ PERC/AQ with and without Ad.

3.5.3 Conclusions/Discussion

Phase maps indicate that the MCBD microemulsion is suitable for kinetics studies when the E ratio equals 0.50, 0.76, or 1.26. Formulations tested have been reasonably fluid, and can be prepared without Ad (Table 17). Longer mixing times, however, are required for media without Ad to clear.

Second order rate constants for catalyzed PNDP hydrolysis (Table 13) increase as E ratio increases at constant % AQ and % O. When at constant E ratio, k_{IBA} values increase as % AQ increases. In 15.9% CTAC/4.8% TAAX/8.5% PERC/70.8% AQ, measured rate constants (Table 17) are independent of the N-alkyl substituents in TAAX. Slightly larger rate constants, however, are obtained when chloride replaces bromide as X (See TBAX, THAX).

As % TBACl, Ad increases from 4.8% to 13.0% at decreasing % AQ, k_{IBA} values range from 13.8 sec^{-1}M^{-1} to 10.1 sec^{-1}M^{-1}. Similarly, k_{IBA} decreases slightly as % THABr increases from ¯ 1.1% to 4.8%. As % TOABr increases from 0.6 to 2.5% at ¯ constant % S, % AQ, and % O, k_{IBA} values are constant.

First order rate constants, k_{obsd}, for catalyzed PNDP hydrolysis in AQ are independent of the % TBACl above ¯ 4 to 5% (Table 15). Since 3 x 10^{-5} M PNDP solutions appear turbid when TBACl < 4%, and since conductivity and kinetics studies indicate medium sized tetraalkyl-ammonium ions do not aggregate to form micelles,[31-34] it can be concluded that, when CTAX is absent, tetraalkylammonium ions may function as hydrotropes for PNDP. Results (Table 16) indicate that uncatalyzed PNDP hydrolysis rates are similar at pH 9.4 and pH 11.2 without TBACl. However, when 13% TBACl is added to AQ, PNDP hydrolysis rates increase. At pH 11.2, the rate increase is even more dramatic. The reaction between PNDP and OH¯ is accelerated by the presence of TBACl. Similar results have been reported for other hydrophobic ammonium ions.[31-34] We may, therefore, infer that, since rates of phosphate ester hydrolysis in aqueous solutions of

26

hydrophobic ammonium ions surpass rates obtained in micellar CTAB,[31,32,38] and since tetraalkylammonium ions (C_2 - C_8) do not form micellar aggregates,[31-35] they may instead form sub-micellar aggregates that provide an environment suitable for uncharged substrate (PNDP) and anionic nucleophilic catalyst (IBA) to interact at close proximity. Since TAAX (C_2 - C_8) are only slightly soluble in water,[59,38] they are probably functioning as cosurfactants in CTAC/TAAX/PERC/AQ systems. When THABr, TBABr, or Ad is added to a mixture of PERC and AQ, the PERC droplets are immediately dispersed. Also, it has previously been reported that tri-n-octyl-ethylammonium bromide (TOEABr), chloride (TOEACl), and tri-n-octyl-ethylammonium mesylate (TEAMs) comicellize with CTAX.[31,38] The function of TAAX in media tested cannot be established. Clearly, they serve as cosurfactants, however, they may be acting as hydrotropes as well.

In conclusion, studies in CTAC/TAAX/PERC/AQ systems have provided us with the following information. Tetraalkylammonium halides (C_2 - C_8) may be substituted for TBACl as cosurfactants in these systems. The concentration of TBAX necessary for microemulsion formation and for good PNDP hydrolysis rates in microemulsions seems to be independent of the nature of the N-alkyl groups in tetraalkylammonium ions (C_2 - C_7), however gels form at mass % of TOABr > 2.5%.

At an E ratio of 0.76, reasonable rate constants are obtained for PNDP hydrolysis in fluid, non-viscous, microemulsion media. Also, if sufficient mixing time is allowed for microemulsion formation, it is not necessary to include Adogen 464 as an additional cosurfactant. Since isopropanol decreases the rate constant measured for PNDP hydrolysis, and is included (10% - 15%) in the industrial formulation of Ad, it is undesirable to include Ad.

3.6 IBA and IBA Derivatives

Previous work has documented IBA, o-iodoxybenzoic acid (IBX) and their derivatives as catalysts in the hydrolysis of phosphate esters (Table 18, Table 19). Moss originally described IBA as a turnover catalyst, and proposed that its catalytic activity occurs because IBA exists in water as a cyclized valence tautomer, 1-hydroxy-1,2-benzio-doxolin-3-one.[39,40] The iodoso oxygen is deprotonated at pH 9.2 and is a nucleophile in phosphate ester hydrolysis.[41] Few IBA derivatives tested as catalysts for phosphate ester hydrolysis are substituted in the 4 position and only with carboxy or nitro groups. The 4-alkyl-IBA derivatives have therefore been synthesized and evaluated as catalysts.[14]

3.6.1 Kinetics

Following conversion to sodium salts, second order rate constants for catalyzed PNDP hydrolysis were measured in the 8% CTAB/8% MP/4% TOL/80% AQ system. Results (Table 20) were compared to rate constant data obtained for unsubstituted IBA.

Values for k_{IBA} increase to 18.6 $sec^{-1}M^{-1}$ and 22.9 $sec^{-1}M^{-1}$ when a methyl or an ethyl substituent is introduced at the 4 position of the benzene ring. Low values for the rate constants are obtained when the 4-alkyl substituent is an n-propyl or an n-pentyl. We could not prepare the sodium salt when the substituent was an n-octyl group.

3.6.2 Conclusions/Discussion

The IBA derivatives with the smaller 4-alkyl substituents are significantly better catalysts than those with larger 4-alkyl substituents, and even better than unsubstituted IBA. The 4-n-propyl and 4-n-pentyl derivatives are poorer catalysts possibly due to incorporation into the interface of the microemulsion aggregates. The 4-n-octyl derivative may be too lipophilic for the sodium salt to be prepared in water. The increase in the rate constant for the 4-alkyl derivative relative to unsubstituted IBA

28

can be explained by electron donating properties of the alkyl groups. The iodoso oxygen becomes a better nucleophile as iodine assumes a more negative charge. The explanation is strengthened by the rate constant obtained for 5-MIBA relative to IBA in micellar solutions (Table 19).

To better visualize the differences of the catalytic IBA/IBX derivatives, second order rate constants for PNDP hydrolysis have been tabulated (Table 20). The source of the data, and experimental conditions, are listed. In several instances, second order rate constants have been obtained by dividing pseudo-first order rate constants by experimental catalyst concentration.

Several observations are evident. First, second order rate constants measured in micellar solutions[39,42,44] are several orders of magnitude larger than values obtained in microemulsion media.[16,40,45] Second order rate constants for PNDP hydrolysis catalyzed by IBA derivatives are comparable to rate constants measured when catalyzed by IBX derivatives.[41] Moss has previously indicated[39] that a kinetic a⌐ ɩtage of ˜ 3.6 is obtained for iodoso- versus iodoxybenz ɔʅ ɘ at pH 8 in CTAC micelles (Table 19) when the substra⁺ɘ is PNDP. This is probably due to a pK_a value of 7.4 for IBX-H compared to a pK_a value of 7.2 for IBA-H. Also, second order rate constants obtained from slope of plots of pseudo-first order rate constants versus catalyst concentration[41] are considerably different than those obtained by dividing a measured first order rate constant by a single catalyst concentration.[39]

It is difficult to obtain trends in the data because each series of rate constants was obtained under different experimental conditions. However, some experimental trends can be noted. The 4-NIBA and 4-NIBX structures exhibit rate constants twice those measured for 5-NIBA and 5-NIBX in micellar and in microemulsion media. This can easily be explained by drawing valence bond canonical structures for 5-NIBA and for 5-NIBX that decrease the

negative charge and the nucleophilicity of the iodoso oxygen. Similar structures cannot be drawn for 4-NIBA and for 4-NIBX. This explains the magnitude of the rate constants for 4-NIBA and 5-NIBA.[16]

Rate constants measured for 5-BXIBA, 5-OXIBA, and 5-DDXIBA and for 5-BXIBX, 5-OXIBX, and 5-DDXIBX in micellar media are comparable,[41] and we may, therefore, infer that the nature of the 5-alkoxy (R) substituent is inconsequential. There is no mesomeric effect[46] between the lone pair of electrons on the alkoxy oxygen adjacent to the bicyclic structure. No stable resonance structures can be drawn for either 4-RO- or 5-RO-IBA/IBX.

A carboxyl group in the 4 or 5 position of IBA or IBX exhibits a negative mesomeric effect that decreases the nucleophilicity of the oxygen by diminishing its negative charge resulting in lower rate constants than IBA.[16,41] The catalytic activity of IBA at pH 9.2 results from its bicyclic structure. Rate constants measured for o-, m-, and for p-iodosobenzoate are compared in Table 21. The lower rates[47] when iodoso is m- or p- probably occurs because these molecules cannot exist as bicyclic valence tautomers in solution.

In conclusion, since the catalytic effectiveness of IBA/IBX derivatives is: 5-BXIBA ≈ 5-OXIBA ≈ 5-DDXIBA ≈ 5-BXIBX ≈ 5-OXIBX ≈ 5-DDXIBX > 4-NIBA ≈ 4-NIBX > 5-MIBA ≈ 5-MIBX > 5-NIBA ≈ 5-NIBX > IBA > 4-CXIBA in CTAC micelles,[41] and 4-NIBA > IBA > 4-MIBX > 5-OXIBA > 5-CXIBA in CTAC/Ad/HEX/AQ microemulsion media,[16] additional rate constants should be measured in aqueous CTAC and in microemulsion media under similar conditions with some of the better catalysts. Also, the superb rate constant obtained with CHDA-IBA in CTAC micelles[48] warrants further investigation.

3.7 Ultraviolet Irradiation of IBA

It has previously been determined that the catalytic activity of IBA is pH dependent.[39,40] To assess the sensitivity of the

30

catalytic activity of IBA to radiation, buffer solutions, pH 9.2, containing 1×10^{-3} M IBA were exposed to UV radiation. Since the dielectric constant in an O/W microemulsion aggregate extends from ≈ 2 in the oily interior to ≈ 78 in the aqueous continuous phase, results may possibly suggest the location of the IBA in the aggregates.

3.7.1 Kinetics

Rate constants measured in microemulsion media consisting of 18% CTAB/18% n-BuOH/4% HEX/60% AQ after exposure to low intensity ultraviolet radiation are listed in Table 22. When exposed to low intensity UV radiation for periods of time ranging from 4 minutes to 130 minutes, the pseudo first order rate constant, k_{obsd}, decreases from 3.6×10^{-4} sec^{-1} to ≈ 0.24×10^{-5} sec^{-1}. The rate of hydrolysis of PNDP in uncatalyzed microemulsion media containing 18% CTAB, 18% BuOH, 4% HEX, and 60% AQ was determined as a control baseline value. The value of k_{obsd}, based on an average of four determinations, was 2.63×10^{-5} sec^{-1}.

The catalyzed rate of hydrolysis of PNDP was measured in identical microemulsion media following exposure of the IBA to high intensity UV radiation. The results are tabulated in Table 23. When exposed to high intensity radiation from 30 seconds to 25 minutes the k_{obsd} values range from 4.9×10^{-4} sec^{-1} to ≈ 0.25×10^{-4} sec^{-1}. Due to the low concentration of IBA in the irradiated solutions, the pH of the solutions did not change during the experiments.

The rate of hydrolysis of PNDP in IBA/AQ that had been naturally irradiated for 8.5 days and diluted 1:2 with microemulsion concentrate was measured as 0.26×10^{-4} sec^{-1}, which is < 4% of the initial catalytic activity.

Since the solutions turned brown when irradiated, the photolyzates were tested for the presence of I_2. A control

solution containing I_2/I^- turned blue. When tested under similar conditions, the photolyzate remained colorless.

3.7.2 NMR and Mass Spectroscopy

Six 20 mL volumes of a solution containing 1×10^{-3} M IBA in water were irradiated for 150 minutes with low intensity UV. The first order rate constant for the hydrolysis of PNDP, k_{obsd}, in a irradiated sample/microemulsion concentrate mixture was 2.12×10^{-5} sec^{-1}. Irradiated samples were combined, evaporated to dryness, and submitted for NMR analysis. A more concentrated solution of IBA in water or in AQ did not completely photolyze when irradiated with low intensity UV radiation.

^{13}C spectra in deuterated dimethyl sulfoxide indicated that a fully photolyzed sample of IBA contained twenty-seven separate peaks. Tentatively, the sample is a mixture of four compounds: 45% o-hydroxy-benzoic acid, 27% o-iodobenzoic acid, 9% 2-iodo-4-hydroxybenzoic acid, and 19% of an unknown compound.

Direct probe mass spectroscopy confirmed the existence of o-hydroxybenzoic acid and of o-iodobenzoic acid in the mixture. The typical patterns for the breakdown of o-hydroxybenzoic acid and of o-iodobenzoic acid are readily identified on the mass spectrum.

3.7.3 Conclusions/Discussion

Aqueous solutions of IBA undergo photolysis that decreases the catalytic activity of IBA in $\approx$ 60 - 70 minutes (low) or $\approx$ 20 minutes (high) upon exposure to ultraviolet radiation. Natural UV radiation destroys the catalytic activity of IBA within several days when stored out-of-doors in sealed quartz vessels. It is therefore necessary, from a practical point of view, to store formulations containing IBA in UV-opaque containers. Also, because IBA photolyzes when exposed to UV radiation, it is difficult to accurately study the solvent shifts associated with the lumines-

cence of IBA and to pinpoint the approximate location of the IBA in a microemulsion aggregate.

3.8 Aggregation Numbers

We initially attempted to determine the aggregation number of microemulsion aggregates using a steady-state luminescence technique[3] that was proposed by Turro and Yekta in 1978 to determine number average aggregation number from luminescence quenching measurements with a probe molecule. Duplicate results obtained with Turro's method were, however, lacking in precision, and, therefore, suspect.

We, therefore, applied a time-resolved luminescence technique developed by Infelta, et. al.[5] that had previously been used to determine aggregation number or several micellar and microemulsion systems.[13]

However, before it was possible to apply either the steady-state or the time-resolved luminescence technique, it was necessary to insure that several important criteria were satisfied. By definition, the luminescence properties of fluorescence and phosphorescence probes must change and be readily measurable when the immediate environment surrounding the probe molecule changes.[128] The concentration of the probe must be low ($\leq 7.2 \times 10^{-5}$ M)[3] to minimize multiple occupancy and self quenching. In addition, other basic assumptions of Turro's method, as the method applies to micelles, include:[49]

1) donor and quencher molecules must associate with the micelles

2) the residence times of donor and quencher molecules in the micelles must be longer than donor unquenched lifetime

3) excited donor is quenching primarily by acceptor

4) the quenching of donor by acceptor is static

33

5) the micelles are approximately spherical

6) the probability of finding a specific number of donor and quencher molecules in a micelle is given by the Poisson distribution

The assumptions inherent in Turro's steady-state method are, with the exception of #4, identical to the propositions intrinsic in the time-resolved luminescence technique.

3.8.1 Luminescence of Donor Molecules

Absorption spectrum for the donor molecules in water (I, II, V) and in MP (III) are presented in Figures 35 and 36. Values of measured and reported absorption maxima and donor lifetimes are presented in Table 24. In all cases, reported absorption maxima and donor lifetimes agree with measured values. Measured and reported absorption spectra of the donor molecules in water exhibit either two distinct peaks (I, V), or one peak and a shoulder (II, III). At 25°C these peaks are broad, extending from ⁻ 550 nm to ⁻ 780 nm, and exhibit one primary peak, one long wavelength shoulder, and either one or two short wavelength shoulders. The intense visible absorption of the polypyridine and the polyphenanthroline ruthenium (2^+) complexes results from charge transfer from the d orbitals of the ruthenium ion to the π^* orbitals of the ligand.[8,49]

3.8.2 Location of Donor Molecules

Donor molecules I, II, and V are water soluble, while donor III is water insoluble, but soluble in polar organic solvents. The quencher molecule, 9-methylanthracene, is insoluble in water and soluble in most oils, and is, therefore, associated with the oily, hydrocarbon core of an O/W aggregate. For donor luminescence to be quenched, the donor and the quencher must be in close physical proximity. Since the dielectric constant extends from ⁻ 78 in the bulk aqueous phase to ⁻ 2 in the dispersed hydrocarbon core, the donor molecules are probably positioned in the interface of the aggregate.

While it would be logical to assume that positively or negatively charged donor molecules would bind to aggregates consisting, respectively, of negatively charged (SDS) or positively charged surfactant molecules (CTAC, CTAB), this is not necessarily the case. We have found that effective quenching of donor luminescence occurs, not only in aggregates oppositely charged to the donor molecules, but, in several instances, in aggregates similarly charged to che donor molecules. Donors I and II are effectively quenched in SDS micelles[59,3,60] and in 5.53% SDS/10.28% 1-pentanol/5.14% n-dodecane/79.05% water microemulsion media[62] (AμE), however no quenching is observed in 8% CTAB/8% MP/4% TOL/80% AQ microemulsion media (1A) or in CTAC micelles.[59] (The quenching phenomenon is independent of aggregate size). Donor III, surprisingly, is efficiently quenched in microemulsion 1A[59] as well as in SDS micelles.[61] Donor V is successfully quenched in SDS micelles,[60] in CTAC micelles,[59,62] and in 1A.[59] Also, aggregation numbers measured in identical cationic microemulsion media[59] with donors I and III and in SDS micelles[59,62] with donors I and V are similar (± 5%).

Demas has suggested that cationic (I, II, III) and anionic (V) photosensitizers such as ruthenium complexes bind strongly to anionic,[62] cationic, and non-ionic[64] micelles due to an hydrophobic interaction of the ligands with the micellar hydrocarbon core. Repulsive effects between negatively charged surfactant and donor V are diminished by the diffuseness of the donor.[61] Identical reasoning may be applied to cationic aggregates (1A) with III.

Some spectroscopic evidence was obtained to verify donor binding to aggregates. To obtain each spectrum, 15 to 20 mL of aqueous solutions containing 7.27 x 10^{-3} M of either donor I or V were added to 3 mL of media. Absorption spectra of I were measured in 0.03 M borate buffer, in 8% CTAB/8% MP/4% TOL/80% AQ microemulsion medium, and in 5 x 10^{-2} M CTAB/AQ and of V in AQ, and in 5 x 10^{-2} M CTAB/AQ. On comparison, the peak shifts obtained in micellar

35

and in microemulsion media relative to buffer indicate that the probes experience a different environment in aggregate containing media.

3.8.3 Quenching of Donor Molecules

The quencher, 9-methylanthracene, is an hydrophobic molecule that is water insoluble. In order to ensure that the quencher was primarily associated with the oily, hydrocarbon core of the O/W aggregates, the distribution coefficient, K_D, of 9-methylanthracene between a mixture of toluene and a solution of MP and 0.03 M borate buffer was determined. A sample of ~ 120 mg of 9-methylanthracene was placed in 10 mL of TOL/MP/AQ (2/1/1). The mixture was mixed well and incubated at 25°C overnite. The concentration of quencher in each phase was determined spectrophotometrically at 348 nm. 98.9% of solubilized quencher was found in the toluene phase. Assuming equal volumes for the two phases, K_D equals 10.4. If phase volumes are considered, as in microemulsion 1A, K_D equals 365. The quencher, therefore, is primarily associated with the hydrocarbon core of the aggregates.

Since 9-methylanthracene absorbs in the UV, energy transfer by donor to quencher cannot be verified. However, luminescence lifetimes of the donor molecules decrease in the presence of quencher molecules, indicating that the excited state of the donor molecules is affected by the presence of quencher.

3.8.4 Steady-State Luminescence Quenching Measurements

The steady-state (S-S) quenching technique was applied to media to determine N. This technique involves quenching measurements of a probe as [9-MeA] is increased. Compositions and results using Turro's technique are listed (Table 25). N values are imprecise for duplicate and triplicate sample measurements. To test our procedure, the method[3] was applied to AμE to duplicate the N value of 100 ± 10 that Thomas[63] obtained with Turro's method. N

equal to 122.4, 147.1, 158.9, 151.1, 144.7, 153.6 and 116.2 were obtained.

Since the method was originally tested in 0.045 M SDS/water with (I) and MeA, this experiment was repeated. Measured N of 58 and 63 agree with Turro's value of 60 ± 2.[3] In addition, Turro's method was applied to 0.02 M phosphate buffered, pH 8.0, 0.08 M NaCl, CTAC solutions with V. Measured N agree (± 10%) with N calculated from diffusion coefficient measurements.[63]

3.8.5 Lifetimes of Donor Molecules

Luminescence lifetimes of donor molecules in water and in micro- emulsion media were determined in the absence of quencher (Table 26). Results indicate that S-S measurements can not meaningfully and confidently be applied to microemulsion aggregates in media containing > 8% S and < 80% bulk phase. In fact, N values obtained in media containing 4.5 to 8% S and 80 to 90% bulk phase should be critically evaluated, especially if N ≥ 300.

3.8.6 Time-Resolved Luminescence Quenching Measurements

Time-resolved (T-R) luminescence quenching measurements have been used to determine N (Table 27) for microemulsions listed in Table 26.

3.8.7 Conclusions/Discussion

Results presented in Table 25 indicate that the S-S luminescence quenching technique of Turro may be unsuitable to determine N when N > 200 to 250. This technique proved to be unsuccessful for all microemulsion media except those that could be termed as swollen micelles. This corresponds to aggregates in O/W microemulsion media containing > 8% S and < 80% AQ. Duplicate and triplicate measurements of N in larger aggregates lack precision. Turro's method, then, may only be applied, with accuracy, to micellar media.

When the T-R luminescence quenching technique is employed to determine N in microemulsion media, and Infelta's equation is used to facilitate the calculations, the success rate increases. Decreasing % S and increasing % AQ into the region where only small microemulsion aggregates or swollen micelles exist, ensures precise results in ≥ 70 % of the cases tested. When results in Tables 25, 26, and 27 are combined, and presented in Table 28, it is obvious that precise results have only been obtained in 4.5% S/4.5% CoS/1.0% Oil/90.0% AQ media. N values determined from S-S measurements agree with N values determined from T-R measurements only for media 3, 6, and 8. Data obtained in systems containing CHP or DIPF as CoS could not solve Infelta's equation or resulted in N values with large standard deviations. Also, despite numerous attempts, satisfactory results were not obtained for AμE.

When results presented in Table 28 are combined with second order rate constants for the catalyzed hydrolysis of PNDP, it can be concluded that no direct relationship exists between the rate constants obtained for the catalyzed hydrolysis of PNDP and the N. An additional parameter, such as aggregate surface charge density, may be more directly related to the rate constants.

It has, therefore, been established that the T-R luminescence quenching technique is valid for ≥ 70 % of the cases studied. It can also been concluded that, for Infelta's method to be applicable, the aggregates should be spherical and have a narrow size distribution. The failure of the T-R technique, as, for example, in the large uncertainty in the N values for media 4 and 9, provides some evidence of a broad size distribution and/or very large aggregates.

In addition, as S concentration increases from 4.5% to 9.0% in several microemulsions, the luminescence decay fit a single exponential rather than the Infelta equation. Close inspection of this equation reveals that it reduces to a single exponential decay

function as the quenching rate decreases and k_q becomes very small. Since $k_q \leq 2 \times 10^{-7}$/sec for media 4 and 9 (Table 27), this would be consistent with the presence of very large, possibly non-spherical aggregates. As S concentration increases (Table 25, Table 28), larger aggregates form. Therefore, based on our results, it can be concluded that N can probably only be determined precisely from luminescence quenching measurements in media containing low % S, high % bulk phase.

4.   SUMMARY/RECOMMENDATIONS

The studies reported here were conducted to develop systems that will effectively penetrate polymers, solubilize phosphate esters, and provide media in which phosphate esters hydrolyze rapidly. From the results of studies in mildly basic (pH ~ 9) microemulsion media prepared with cationic surfactant, we conclude that:

1) substituting chloride for bromide as surfactant counter ion increases the PNDP hydrolysis rate by ~ 20 %

2) increasing % AQ and/or decreasing % S increases PNDP   hydrolysis rate

3) increasing the % O has little effect on the hydrolysis rate of PNDP

4) increasing the E ratio at 50% AQ does not affect hydrolysis rate

5) increasing the polarity of the cosurfactant increases the hydrolysis rate in identical composition microemulsion media

6) decreasing the N-alkyl chain length of the 1-alkyl-2-pyrrolidinones or of the N,N-dialkylformamide cosurfactants increases the hydrolysis rate: methyl > ethyl > n-isopropyl > n- butyl > cyclohexyl

9) the addition of a 4-alkyl substituent to o-iodosobenzoate increases the rate of catalysis of PNDP; 4-ethyl IBA > 4-methyl IBA > unsubstituted IBA

10) increasing the alkyl chain length in tetraalkylammonium cosurfactants has little effect on the hydrolysis rate in identical composition microemulsion media

11) N values obtained do not correlate with PNDP hydrolysis rates.

In addition, based on kinetics rates, phase diagrams and phase maps, environmental toxicity, investigation of component availabil-

ity, cost, and component biodegradability, further study is recommended of the following systems:

CTAC/MP/AQ

CTAC/EP/AQ

CTAC/DMF/AQ

CTAC/DEF/AQ

CTAC/Adogen 464/AQ

CTAC/MP/TOL/AQ

CTAC/DMF/TOL/AQ

It is suggested that these systems be studied at low E ratios and that 1-alkyl-2-pyrrolidinones or N,N-dialkylformamides be tested as the continuous phase.

Based on luminescence quenching results, we propose that our studies involving the physical properties of microemulsion aggregates, with extended investigation into methods to accurately determine surface charge density and structures of surfactant solutions at the microscopic level, be continued.

REFERENCES

1. C.G. Hermansky, "Reactions in and Characterization of Oil in Water Microemulsions", PhD Thesis, Drexel University, Phil., PA, 1980.

2. R.A. Mackay, F.R. Longo, B.L. Knier, H.D. Durst, J. Phys. Chem. 1987, 91, 861-864.

3. N.J. Turro, A. Yekta, J. Am. Chem. Soc. 1978, 100, 5951-5952.

4. M.F. Perrin, M.J. Perrin, Comp. Rend. Heb. des Seances de l'Acad. de Sci. 1924, 178, 1978-80.

5. P.P. Infelta, M. Grètzel, J.K. Thomas, J. Phys. Chem. 1974, 78, 190-195.

6. Programs developed by B. L. Knier. Address available on request.

7. Syntheses completed by K. G. Haddaway, U.S. Army CRDEC, GEO-CENTERS, INC., Fort Washington, MD 20744.

8. C-T. Lin, W. Böttcher, M. Chou, C. Creutz, N. Sutin, J. Am. Chem. Soc. 1976, 98, 6536-6544.

9. J.N. Braddock, T.J. Meyer, J. Am. Chem. Soc. 1973, 95, 3159-3162.

10. F.P. Dwyer, J.E. Humpoletz, R.S. Nyholm, Proc. Roy. Soc. N.S. Wales, 1947, 80, 212-216.

11. N.J. Turro, K.-C. Liu, M.-F. Chow, P. Lee, Photochem. and Photobiol. 1978, 27, 523-529.

12. Developed by Adaptable Laboratory Software, 2024 West Henrietta Road, Rochester, NY 14623; Available through Macmillan Software Company, 866 Third Avenue, New York, NY 10022; 1986.

13. M. Almgren, J-E. Lofroth, J. Coll. Int. Sci. 1981, 81, 486-499.

14. Syntheses developed and completed by C. A. Panetta, NRC-CRDEC Research Associate, University of Mississippi, Oxford, MS 38677.

15. R.A. Mackay, B.A. Burnside, S.M. Garlick, B.L. Knier, H.D. Durst, P.M. Nolan, F.R. Longo, J. Disp. Sci. and Tech. 1989, 9, 493-510.

16. B.A. Burnside, B.L. Knier, R.A. Mackay, H.D. Durst, F.R. Longo, J. Phys. Chem. 1988, 92, 4505-4510.

17. S.M. Garlick, B.A. Burnside, R.A. Mackay, B.L. Knier, H.D. Durst, P.M. Nolan, K.G. Haddaway, F.R. Longo, Proc. U.S. Army CRDESCS Chem. Def. Res. 1989, 3.

18. P.A. Winsor, Chem. Rev. 1968, 68, 1-40.

19. Pamphlet published by BASF Corporation N-Methylpyrrolidone (NMP); West Germany, 1985.

20. Pamphlet published by GAF Corp. M-Pyrol; Wayne, New Jersey, 1986.

21. R.A. Mackay, Encyclopedia of Emulsion Technology, Vol III, P. Becher, Ed., Marcel Dekker, Inc., New York, 1988, 223-237.

22. J.A. Dean, Ed., Lange's Handbook of Chemistry, McGraw-Hill, Inc., New York, 1979, 10-37 to 10-54.

23. R.C. Weast, Ed., Handbook of Chemistry and Physics, The Chemical Rubber Co., Cleveland, OH, 1972, D151-D170.

24. Developed by J. R. Hovanic, U.S. Army CRDEC, APG., MD 21010-5423.

25. J. March, Advanced Organic Chemistry, McGraw Hill, New York, NY, 1977, 357-358.

26. J. Dockx, Synthesis 1973, 441-456.

27. E.V. Dehmlow, Angew. Chem. Inter. Edit. 1974, 13, 170-179.

28. A.W. Herriott, D. Picker, J. Am. Chem. Soc. 1963, 96, 2345-2349.

29. S.M. Garlick, R.A. Mackay, H.D. Durst, F.R. Longo, "Catalytic Hydrolysis of Phosphate Esters in Microemulsions. VIII. Tetraalkylammonium Halides as Cosurfactants," in preparation.

30. M. Tadros, K. Bridger, A. Berrier, R. Hearns, Report MML #TR 87-28(c), Martin Marietta Laboratories, 1988.

31. Y. Okahata, R. Ando, T. Kunitake, J. Am. Chem. Soc. 1977, 99, 3067-3072.

32. C.A. Bunton, Y.S. Hong, R.S. Romsted, C. Quan, J. Am. Chem. Soc. 1981, 103, 5788-5794.

33. C.A. Bunton, C. Quan, J. Org. Chem. 1985, 50, 3230-3232.

34. F.A. Long, W.F. McDevit, Chem. Rev. 1952, 51, 119-157.

35. A.S.C. Lawrence, J.T. Pearson, Proceedings of the 4th International Congress on Surface Active Substances, Vol 2; J. Th. G. Overbeek, Ed., Gordon and Breach, New York, 1967; 709-719.

36. C. Neuberg, Biochem. Z. 1916, 76, 107.

37. C.A. Bunton, Y.S. Hong, L.S. Romsted, C. Quan, J. Am. Chem. Soc. 1981, 103, 5784-5788.

38. C.A. Bunton, personal communication, Gordon Conference, 1987.

39. R.A. Moss, K.W. Alwis, J-S. Shin, J. Am Chem. Soc. 1984, 106, 2651-2655.

40. R.A. Moss, K.W. Alwis, G.O. Bizzigotti, J. Am. Chem. Soc. 1984, 105, 1681-1687.

41. A.R. Katritzky, B.L. Duell, H.D. Durst, B.L. Knier, J. Org. Chem. 1988, 53, 3972-3978.

42. P.S. Hammond, J.S. Forster, C.N. Lieske, H.D. Durst, J. Am. Chem. Soc. 1989, 111, 7860-7866.

43. R.A. Moss, S. Chatterjee, B. Wilk, J. Org. Chem. 1986, 51, 4303-4306.

44. B.A. Burnside, B.L. Knier, R.A. Mackay, H.D. Durst, F.R. Longo, J. Phys. Chem. 1988, 92, 4505-4510.

45. B.A. Burnside, "The Hydrolysis of p-Nitrophenyl Diphenyl Phosphate Ester in Microemulsion Media", Ph.D Thesis, Drexel University, Philadelphia, PA, 1987.

46. N.S. Isaac, "Reactive Intermediates in Organic Chemistry", John Wiley and Sons, New York, 1979, 30-38.

47. Synthesized in A. Katritzky's laboratory at the University of Florida. Rate constants measured by F.R. Longo, CRDEC, Edgewood, MD.

48. Communication by A. Katritzky's laboratory at the Univ. of Florida.

49. J-E. Lofroth, M. Almgren, "Surfactants in Solution, Vol. 1," K.L. Mittal, and B. Lindman, Ed., Plenum Press, New York, 1984, 627-643.

50. F.E. Lytle, D.M. Hercules, J. Am. Chem. Soc. 1969, 91, 253-257.

51. B.L. Knier, H.D. Durst, B.A. Burnside, R.A. Mackay, F.R. Longo, J. Soln. Chem. 1988, 17, 77-81.

52. J.D. Miller, R.H. Prince, J. Chem. Soc.(A) 1966, 1048-1052.

53. D. Meisel, M.S. Matheson, J. Rabani, J. Am. Chem. Soc. 1978, 100, 117-122.

54. G.D. Hager, G.A. Crosby, J. Am. Chem. Soc. 1975, 97, 7031-7037.

55. S. Oishi, K. Tajime, I. Shiojima, J. Mol. Cat. 1982, 14, 383-386.

56. D.M. Klassen, G.A. Crosby, J. Chem. Phys. 1968, 48, 1853-1858.

57. J.N. Braddock, T.J. Meyer, J. Am. Chem. Soc. 1973, 95, 3158-3162.

58. F.E. Lytle, D.M. Hercules, J. Am. Chem. Soc. 1969, 91, 253-257.

59. Experimentally determined value; personal observation.

60. B.L. Hauenstein, Jr., W.J. Dressick, S.L. Buell, J.N. Demas, B.A. DeGraff, J. Am. Chem. Soc. 1983, 105, 4251-4255.

61. J.D. Bolt, N.J. Turro, Photochem. and Photobiol. 1982, 35, 305-310.

62. M. Almgren, F. Grieser, J.K. Thomas, J. Am. Chem. Soc. 1980, 102, 3188-3193.

63. R.A. Mackay, N.S. Dixit, R. Agarwal, R.P. Seiders, J. Disp. Sci. Tech. 1983, 4, 397-407.

64. K. Mandal, B.L. Hauenstein, Jr., J.N. Demas, J. Phys. Chem. 1983, 87, 328-331.

65. Instrument Manual, Part 3, Perkin Elmer, Norwalk, CT, pp 3-1 to 3-83.

66. J.T. Pearson, J. Coll. Int. Sci. 1971, 37, 509-520.

Abbreviations

1-PC	1-pyrrolidinecarboxaldehyde
1A	8% CTAB/8% MP/4% TOL/80% AQ microemulsion media
4-CXIBA	4-carboxy-2-iodosobenzoate
4-MIBX	4-methyl-2-iodoxybenzoate
4-NIBA	4-nitro-2-iodosobenzoate
5-BXIBA	5-(n-butoxy)-2-iodosobenzoate
5-BXIBX	5-(n-butoxy)-2-iodoxybenzoate
5-CXIBA	5-carboxy-2-iodosobenzoate
5-DDXIBA	5-(n-dodecyloxy)-2-iodosobenzoate
5-DDXIBX	5-(n-dodecyloxy)-2-iodoxybenzoate
5-MIBA	5-methyl-2-iodosobenzoate
5-MXIBA	5-(methoxy)-2-iodosobenzoate
5-NIBA	5-nitro-2-iodosobenzoate
5-NIBX	5-(n-octyloxy)-2-iodoxybenzoate
[M]	([Surfactant] - [free monomer])/N
A	absorbance
ACN	acetonitrile
Ad	Adogen 464; cosurfactant
Adogen 442-100P	dihydrogenated-tallow dimethylammonium chloride
AµE	5.53% SDS/10.28% 1-pentanol/5.14% n-dodecane/79.05% water
AP	1-allyl-2-pyrrolidinone
AQ	0.03 M borate buffer
Arosurf TA-101	distearyldimethylammonium chloride
BuOH	n-butanol
BuPhP	4-n-butyl-N-phenyl-2-pyrrolidinone
CHDA-IBA	4-(cetyl-2-hydroxyethyldimethyl ammonium)-2-iodoso-benzoate
CHP	1-cyclohexyl-2-pyrrolidinone
CMC	critical micelle concentration
CoS	cosurfactant
CPC	cetylpyridinium chloride
CTAB	cetyltrimethylammonium bromide
CTAC	cetyltrimethylammonium chloride
CTAX	cetyltrimethylammonium halide (chloride, bromide)
CUM	cumene
DBF	N,N-dibutylformamide
DDEC	n-dodecane
DEF	N,N-diethylformamide
DIPF	N,N-diisopropylformamide
DMAC	N,N-dimethylacetamide
DMF	N,N-dimethylformamide
DMIZ	1,3-dimethyl-2-imidazolidinone
DMP	1,3,dimethyl-3,4,5,6-tetrahydro-2 (1H-) pyrimidinone
DPP	diphenylphosphate anion
DPPhen	4,7-diphenyl-1,10-phenanthroline
DTAC	dodecyltrimethylammonium chloride

E/AQ	emulsifier/aqueous
E/O	emulsifier/oil
E	emulsifier (surfactant/cosurfactant)
EP	1-ethyl-2-pyrrolidinone
F (t)	luminescence intensity at time t
F^-	fluoride ion
FP	1-formylpiperidine
H	bis (2-chloroethyl) sulfide; mustard
HEX	n-hexadecane
Hex	n-hexane
I	luminescence intensity at time t
IBA	2-iodosobenzoic acid
IBX	2-iodoxybenzoic acid
I_o	luminescence intensity at time zero
iso-PP	1-isopropyl-2-pyrrolidinone
k_{hyd}	pseudo first order rate constant for the background hydrolysis of PNDP in water
k_{IBA}	second order rate constant for the IBA-dependent hydrolysis of PNDP
k_{obsd}	overall pseudo first order rate constant observed for the IBA catalyzed hydrolysis of PNDP in a basic aqueous solution
k_{OH}	second order rate constant for the hydroxide dependent hydrolysis of PNDP
M	total number of aggregates
MCBD	multipurpose chemical and biological decontaminant µE
µE	microemulsion
MeA	9-methylanthracene
MeOPhP	4-methoxy-N-phenyl-2-pyrrolidinone
MP	1-methyl-2-pyrrolidinone
MPF-66	fluorescence spectrophotometer used for steady-state measurements
N	number average aggregation number
Nd:YAG	neodymium doped, yttrium aluminum garnet laser
NPIPP	p-nitrophenylisopropylphenyl phosphinate
O/W	oil in water; type of aggregates
o-XY	o-xylene
OH^-	hydroxide ion
O	oil; any water insoluble organic liquid
OXIBA	5-(n-octyloxy)-2-iodosobenzoate
PERC	tetrachloroethylene
PhDEC	1-phenyldecane
Phen	1,10-phenanthroline
PhHEX	1-Phenylhexane
PhP	1-Phenyl-2-pyrrolidinone
PNDB	p-nitrophenyldibutyl phosphonate
PNDEP	p-nitrophenyldiethyl phosphate
PNDEP	p-nitrophenyldiethyl phosphate
PNDHP	p-nitrophenyldihexyl phosphate
PNDP	p-nitrophenyldiphenyl phosphate
PNP	p-nitrophenoxide ion
Ru [phen(ph)$_2$(4/3SO$_3$)]$_3$Na$_2$:10H$_2$O	donor molecule (V)

Ru [phen(ph)$_2$]$_3$Cl$_2$:6H$_2$O   donor molecule (III)
Ru [phen(phSO$_3$)$_2$]$_3$Na$_4$:6H$_2$O   donor molecule (IV)
Ru(bpy)$_3$Cl$_2$:6H$_2$O   donor molecule (I)
Ru(phen)$_3$Cl$_2$:6H$_2$O   donor molecule (II)

|	
S	surfactant
S-S	steady-state
SDS	sodium dodecyl sulfate
t-BuTOL	4-tert-butyltoluene
T-R	time-resolved
TAAX	tetraalkylammonium (C$_4$ to C$_{10}$) hydroxides and halides
TBABr	tetra-n-butylammonium bromide
TBACl	tetra-n-butylammonium chloride
TBAOH	tetra-n-butylammonium hydroxide
TDTAC	tetradecyltrimethylammonium chloride
TEACl	tetraethylammonium chloride
TEAMs	tri-n-octylethylammonium mesylate
THABr	tetra-n-hexylammonium bromide
THACl	tetra-n-hexylammonium chloride
τ_o	the radiative lifetime for a molecule in the absence of quencher
TMACl	tetramethylammonium chloride
TMAPhP	4-tetramethylammonium-N-phenyl-2-pyrrolidinone
TMU	1,1,3,3-tetramethylurea
TOABr	tetra-n-octylammonium bromide
TOAX	tetraoctylammonium halide (chloride, bromide)
TOEABr	tri-n-octylethylammonium bromide
TOEACl	tri-n-octylethylammonium chloride
TOL	toluene
TPABr	tetra-n-pentylammonium bromide
TPrACl	tetra-n-propylammonium chloride
Variquat K 300	dicocodimethylammonium chloride
VP	1-vinyl-2-pyrrolidinone
W/O	water in oil; type of aggregates

Blank
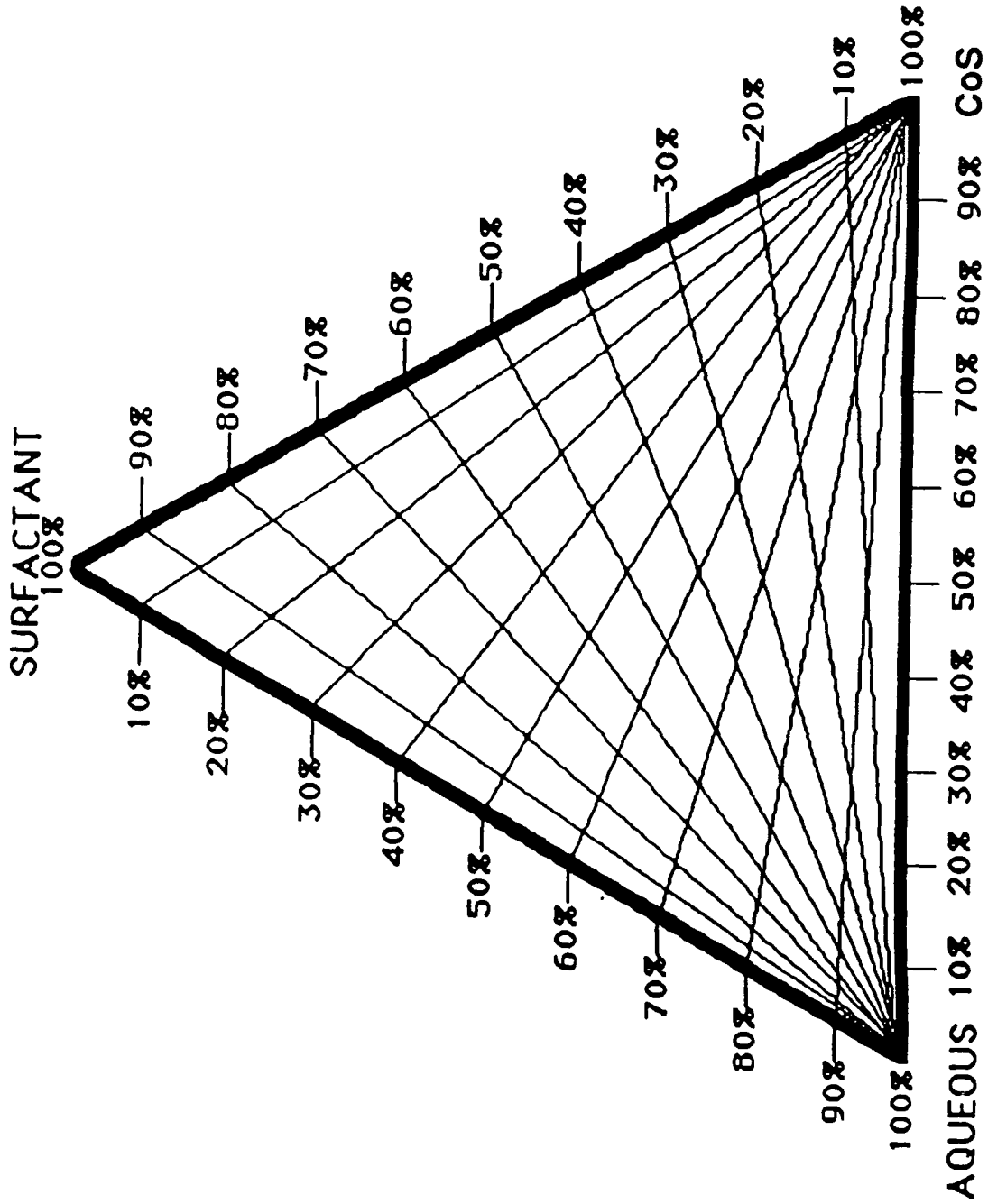
Figures

Figure 1. Ternary phase diagram depicting the titration of constant mass ratios of S/CoS and S/Aq respectively with AQ and CoS along constant ratio titration lines.

EMULSIFIER
100%

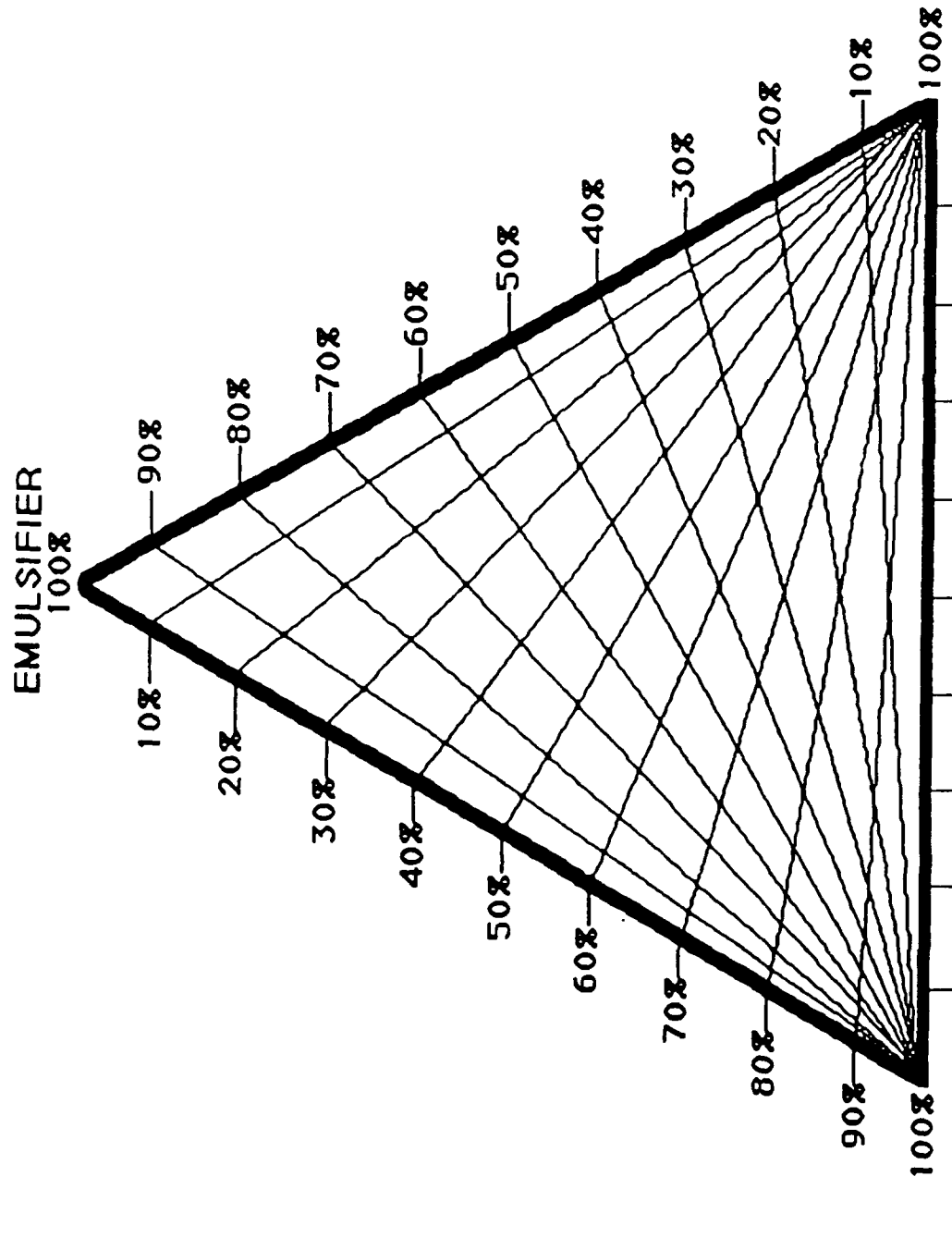AQUEOUS 10% 20% 30% 40% 50% 60% 70% 80% 90% OIL

Figure 2. Pseudo-ternary phase map depicting the titration of constant mass ratios of E/O and E/AQ respectively with AQ and Oil along constant ratio titration lines.

A. Nd:YAG Laser
B. KDP Doubling Crystal
C. Mirrors
D. Spex 1459 Illuminator
E. Lenses
F. Sample Mount Assembly
G. Spex 1403 Double Monochromator
H. Entrance Slits
I. Exit Slits
J. RCA 31043A Photomultiplier Tube
K. LeCroy 3500 Transient Recorder
L. Tektronix PG 508 Pulse Generator
M. Floppy Disk
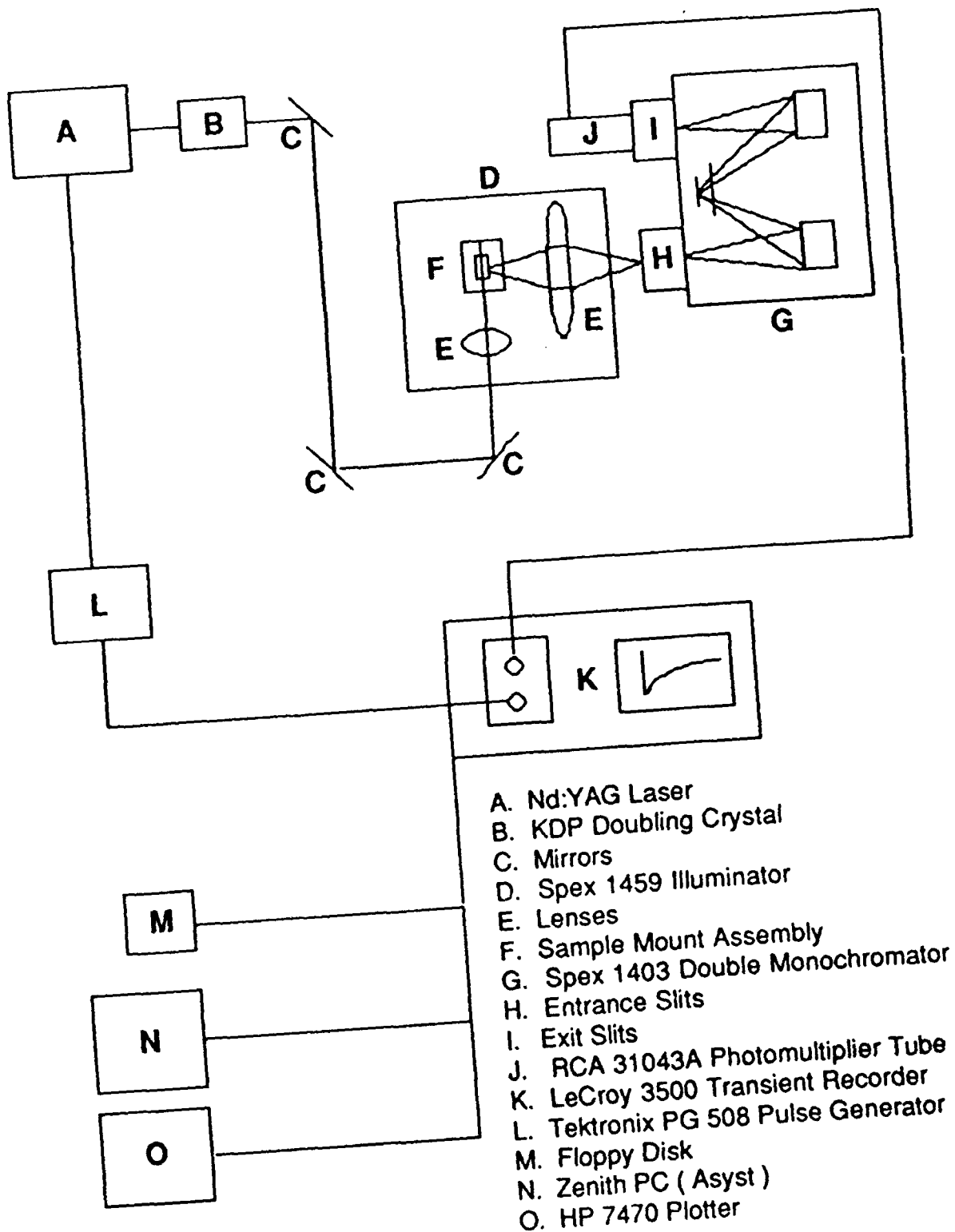N. Zenith PC (Asyst)
O. HP 7470 Plotter

Figure 3. Diagram of the apparatus used in the time-resolved luminescence studies. Details are given in the text.

Figure 4. Ternary phase diagram. Clear ○; turbid ○; turbid liquid crystalline ☺.

CTAC/DMF=2.0

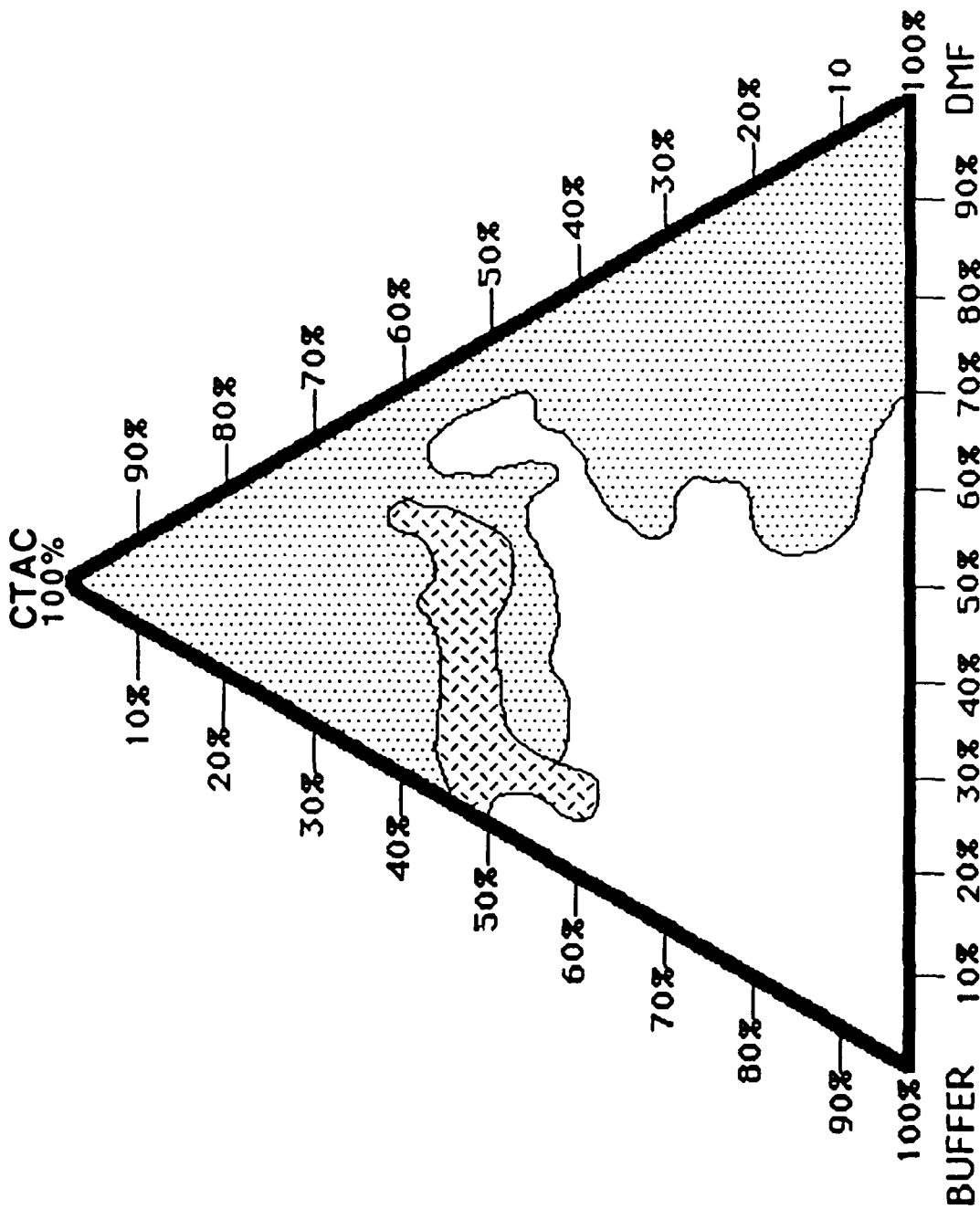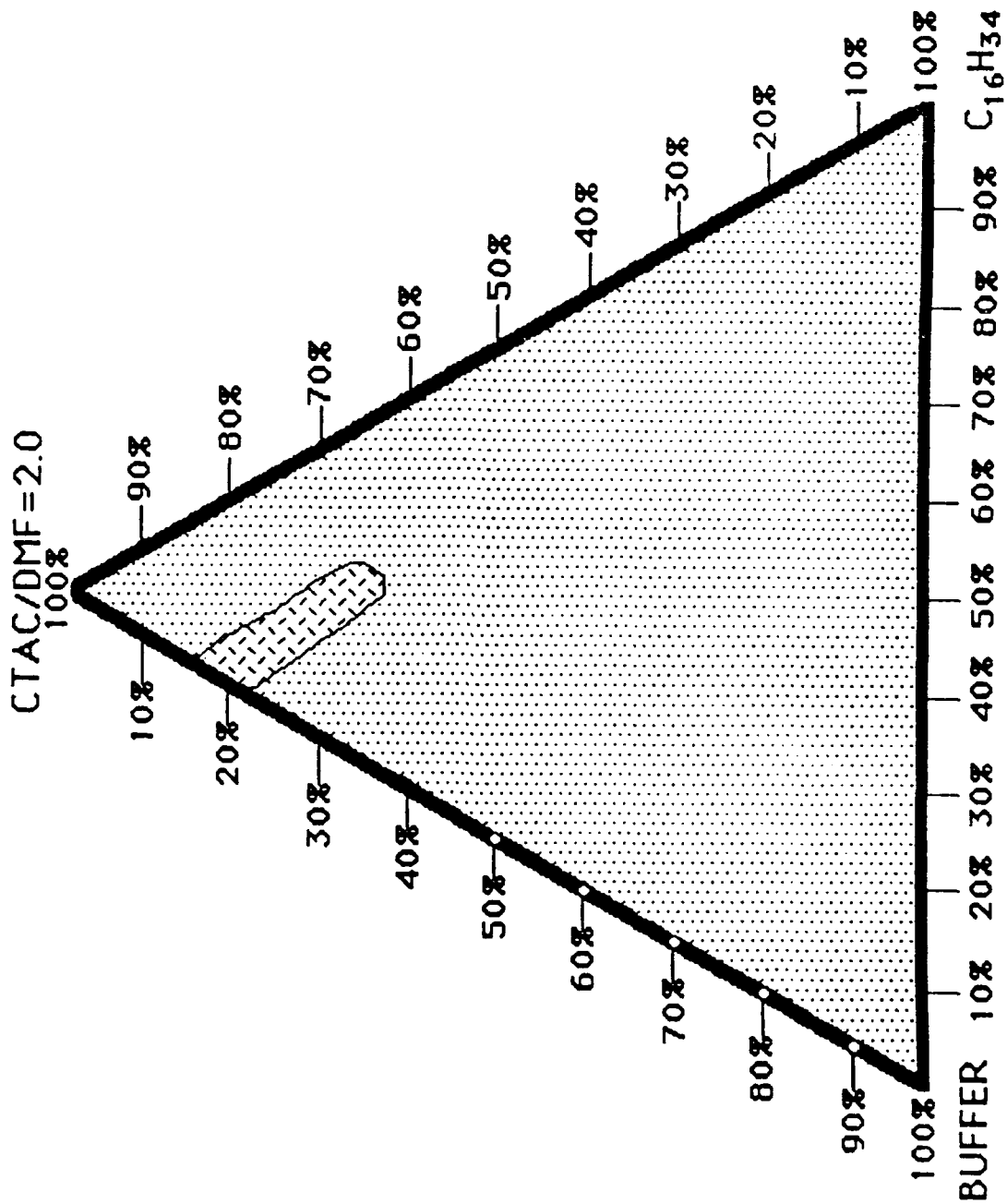Figure 5. Pseudo-ternary phase map. Clear ◯ ; turbid ◯ ; turbid liquid crystalline ◯ .

55

Figure 6. Ternary phase diagram. Clear ○ ; turbid ○ ; turbid liquid crystalline ⊙ .

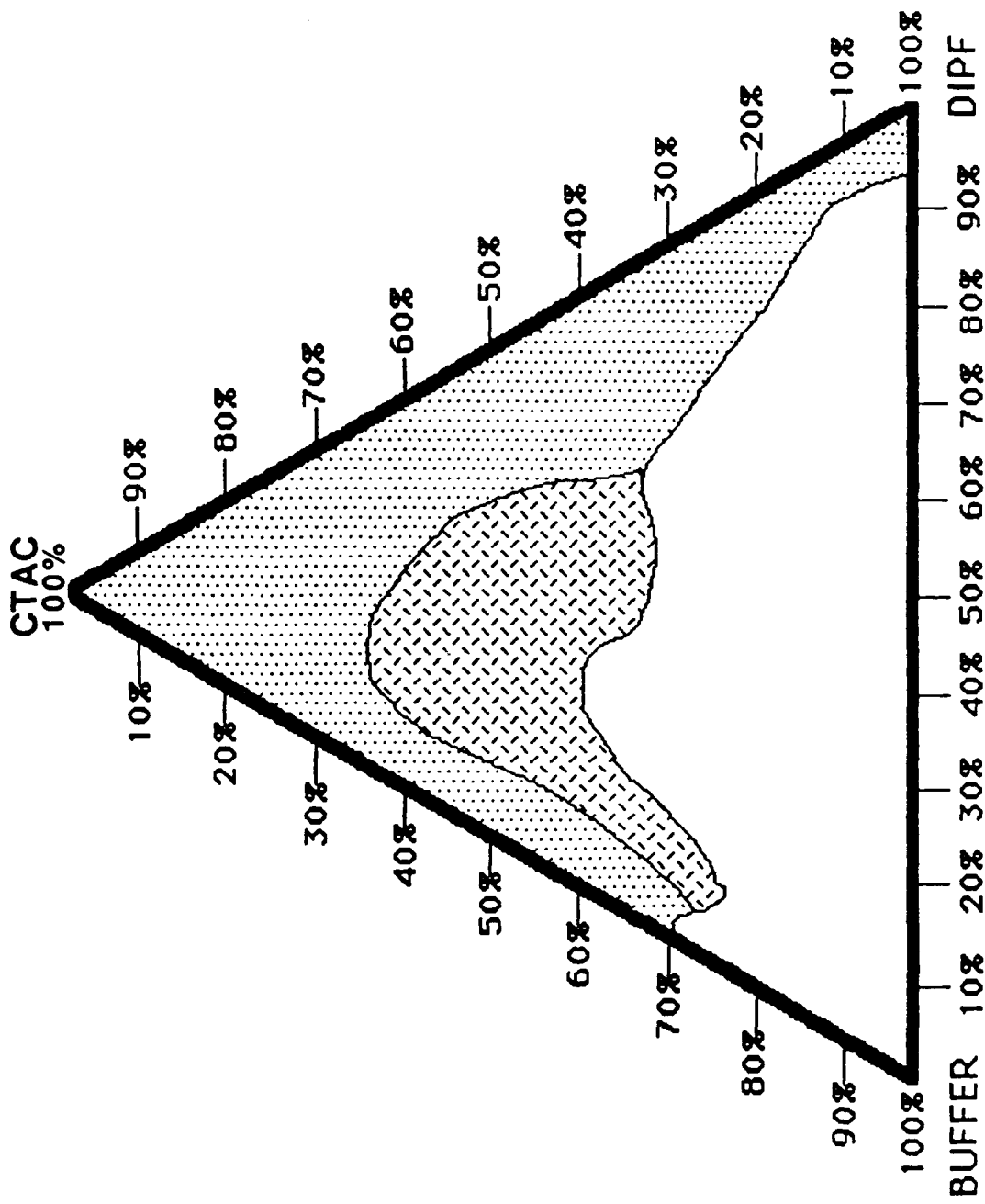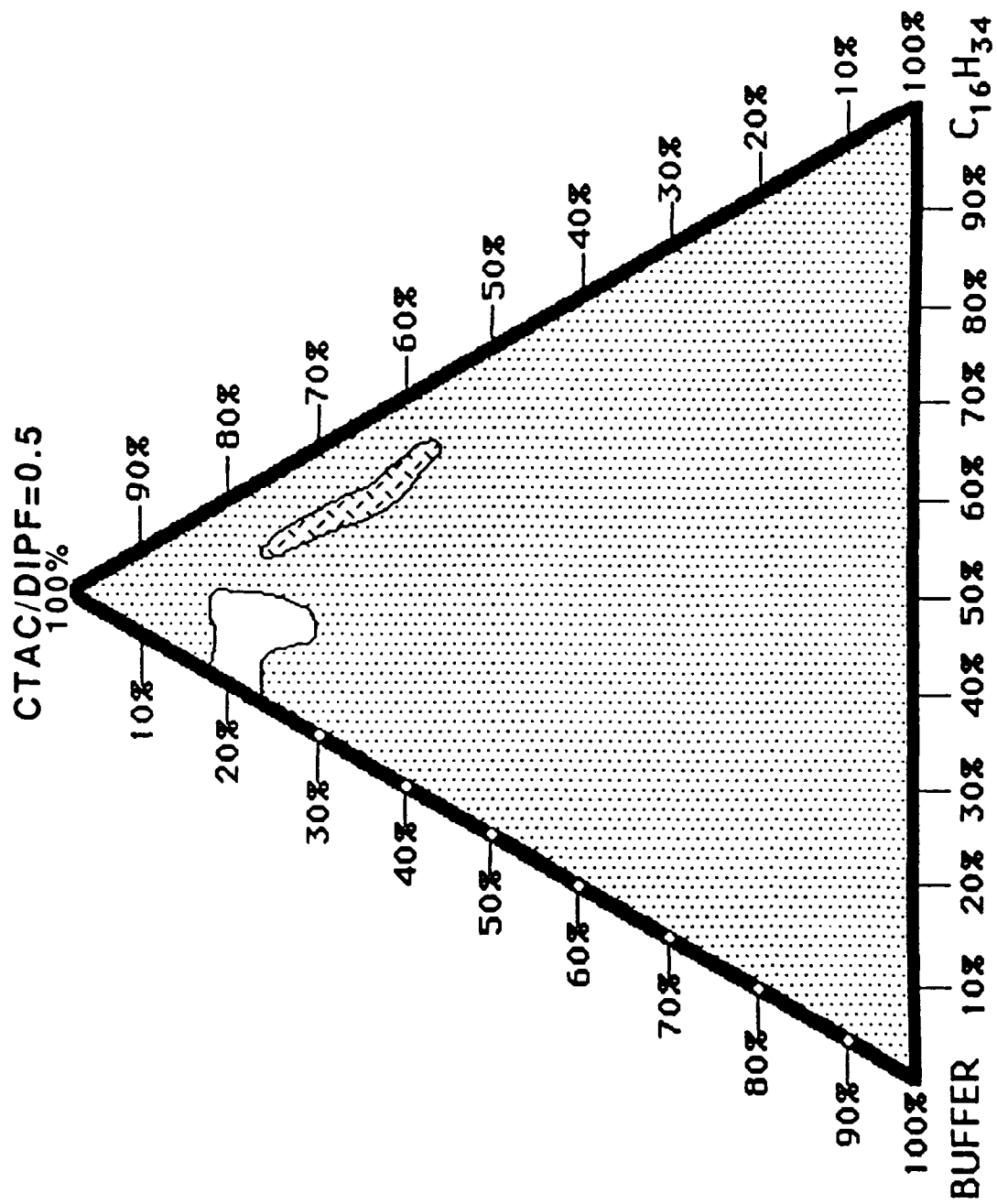Figure 7. Pseudo-ternary phase map. Clear ◯; turbid ◯; turbid ☺; turbid liquid crystalline ☺.
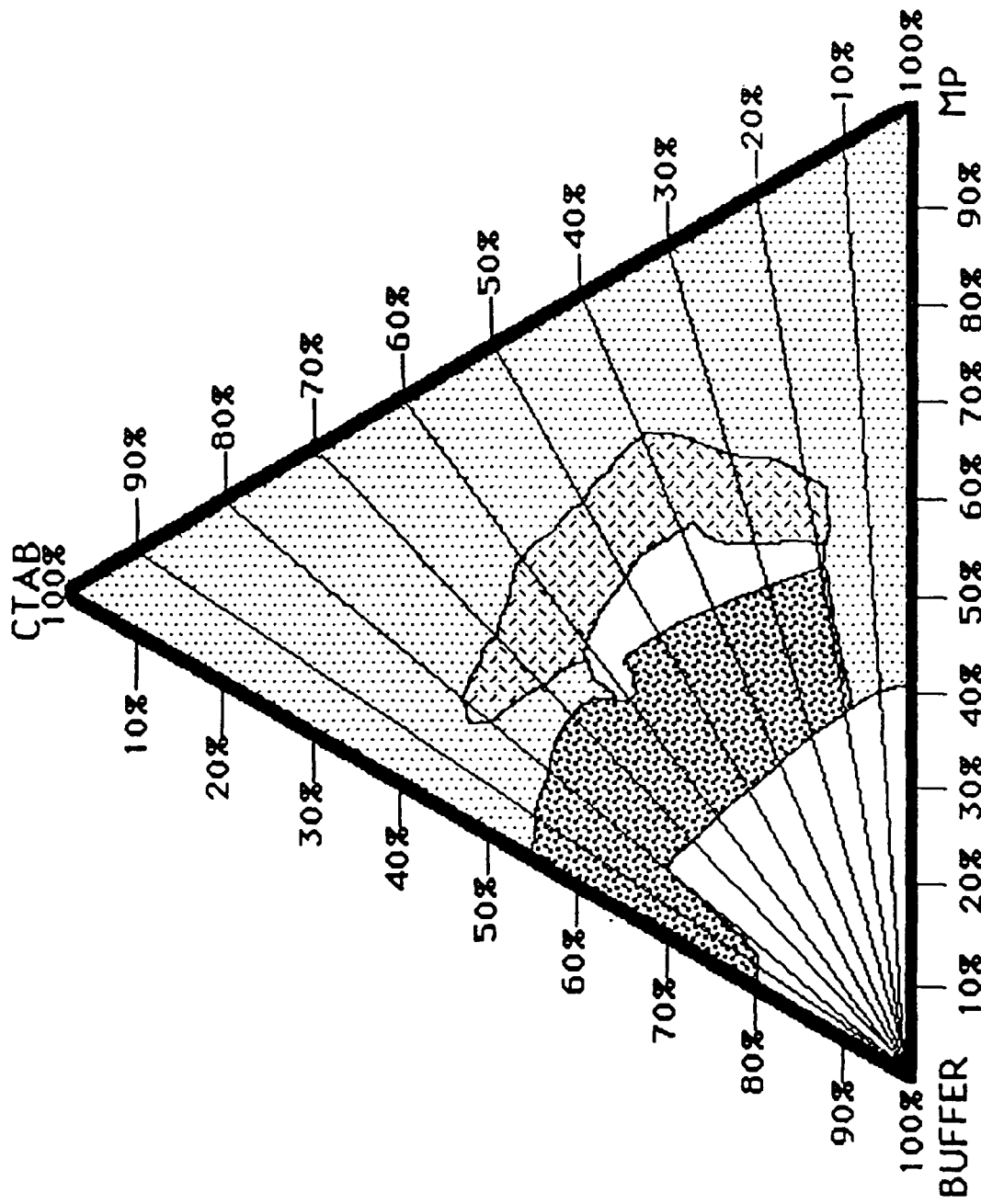
Figure 8. Ternary phase diagram. Constant mass ratios of CTAB / MP are titrated with AQ. Clear ◯ : turbid ◯ ; gel ⊛ ; turbid liquid crystalline ⊘ .
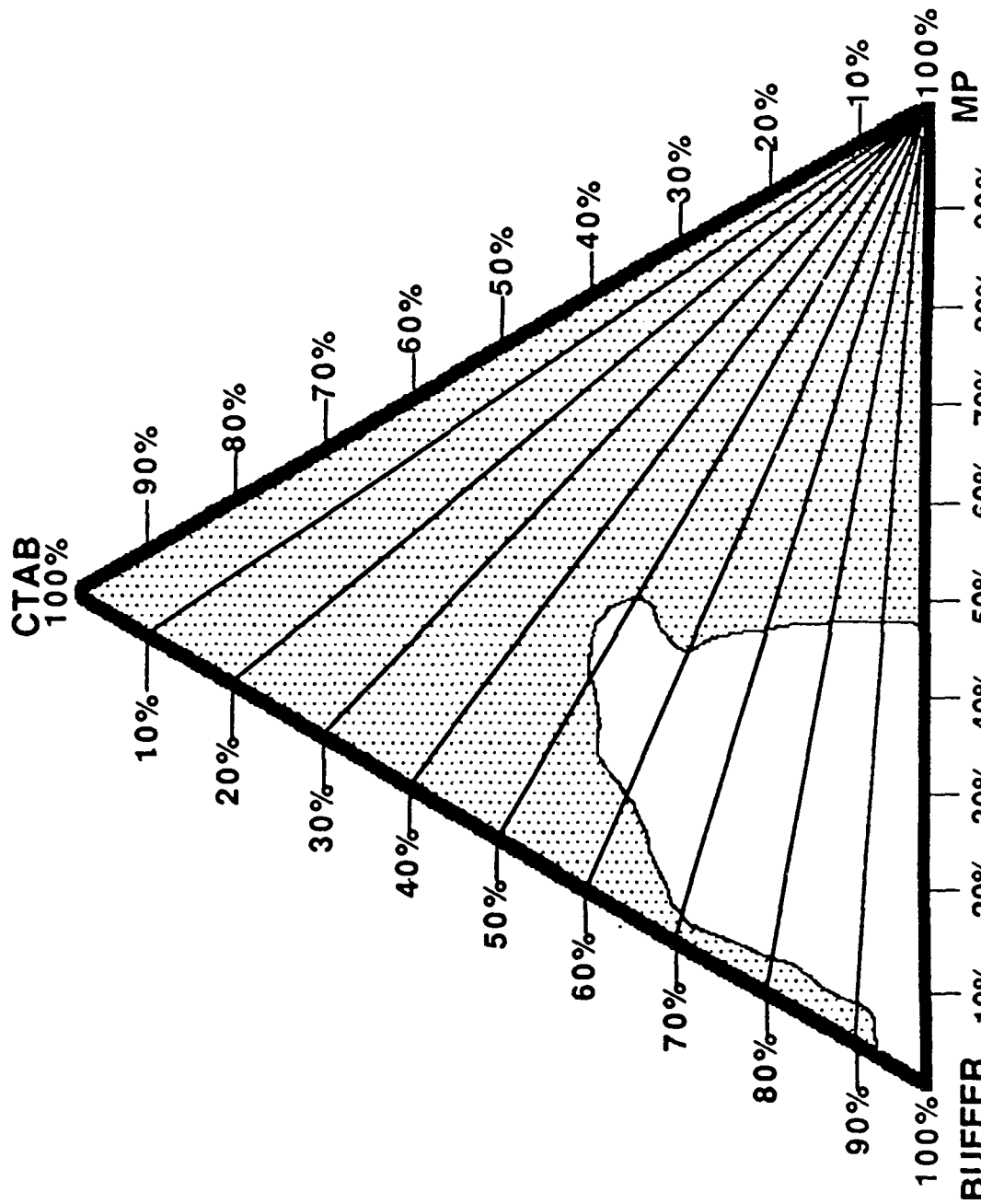
Figure 9. Ternary phase diagram. Constant mass ratios of CTAB / MP are titrated with MP. Clear ◯; turbid ◯.
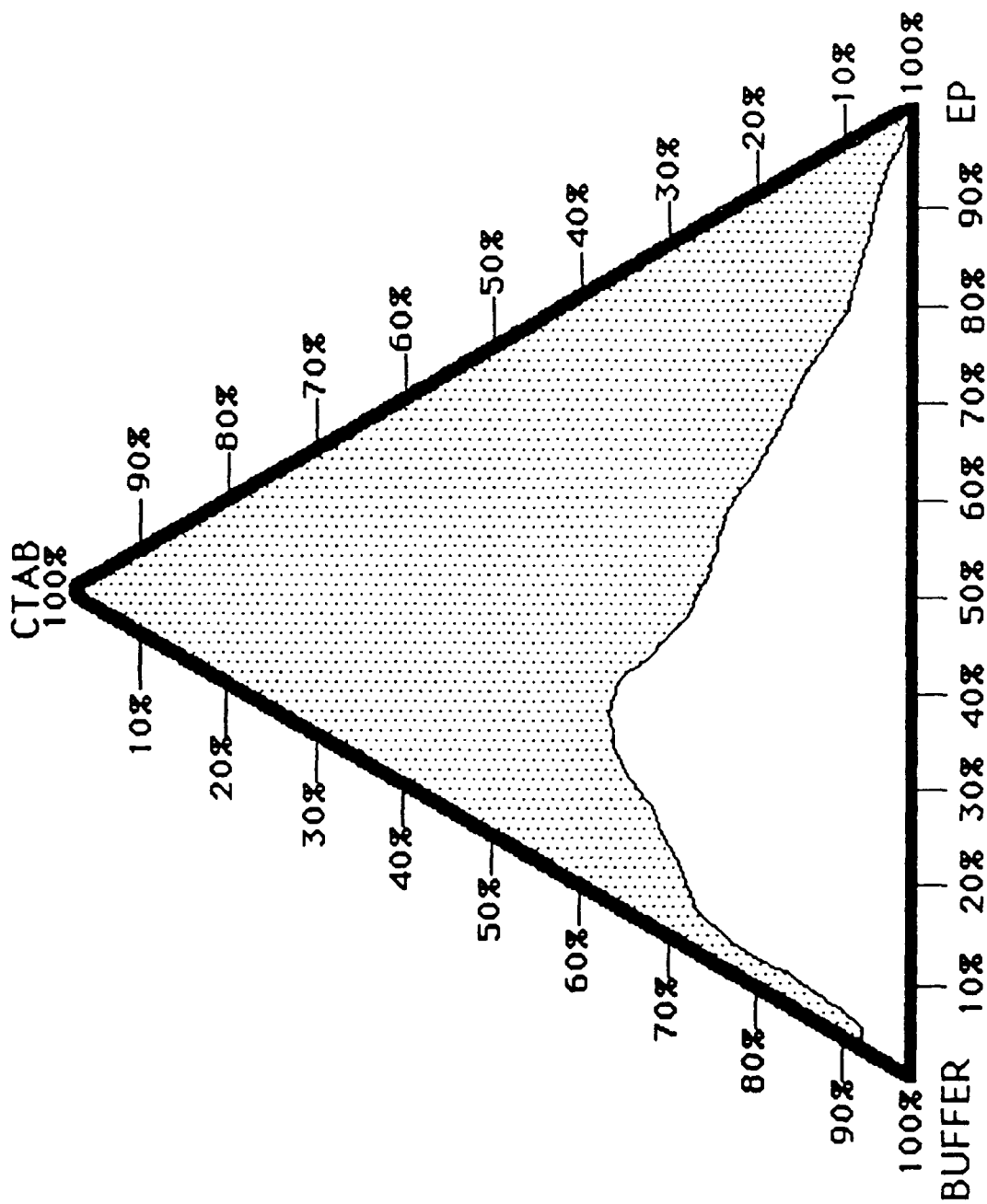
Figure 10. Ternary phase diagram. Clear ◯; turbid ◯.

60
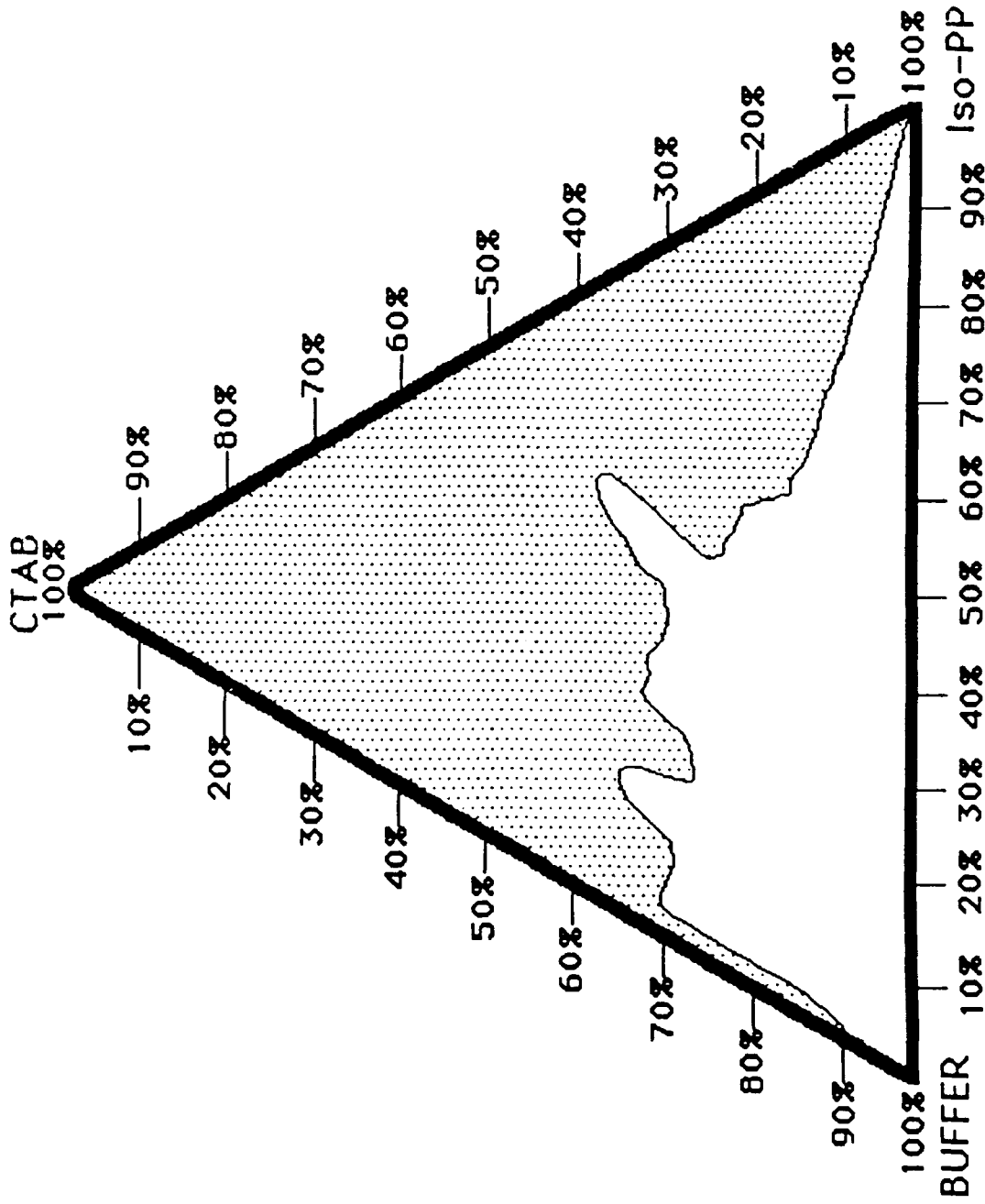
Figure 11. Ternary phase diagram. Clear ○; turbid ○.

61

Figure 12 Ternary phase diagram. Clear ◯ ; turbid ◯ .

62

CTAB/Iso-PP=1.0

Figure 13. Pseudo-ternary phase map. Clear ◯; turbid ◉.

63
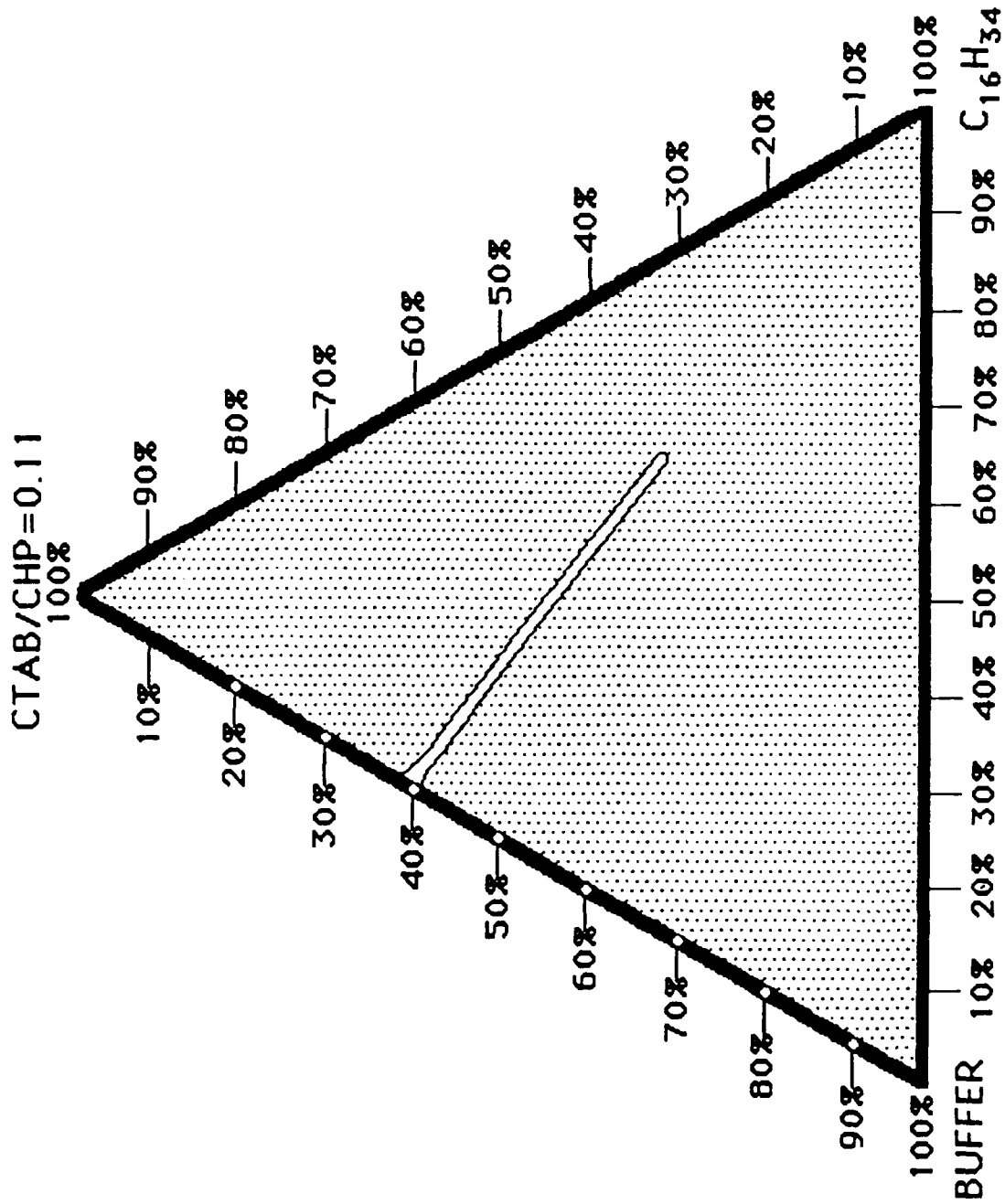
Figure 14. Pseudo-ternary phase map. Clear ◯; turbid ◯.

CTAB/CHP=0.11

BUFFER

$C_{16}H_{34}$
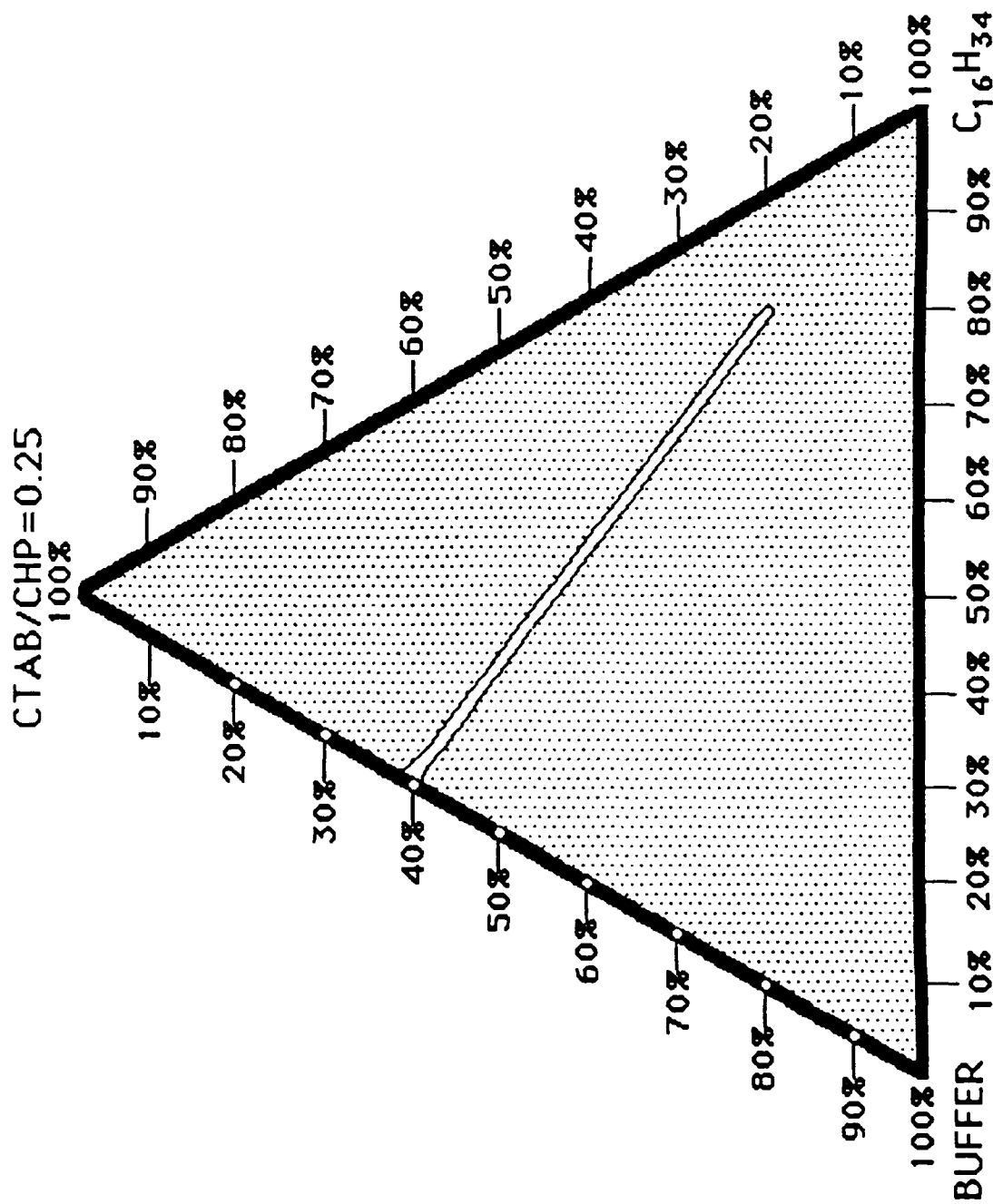
Figure 15. Pseudo-ternary phase map. Clear ◯; turbid ◯.

CTAB/CHP=0.25

BUFFER

$C_{16}H_{34}$
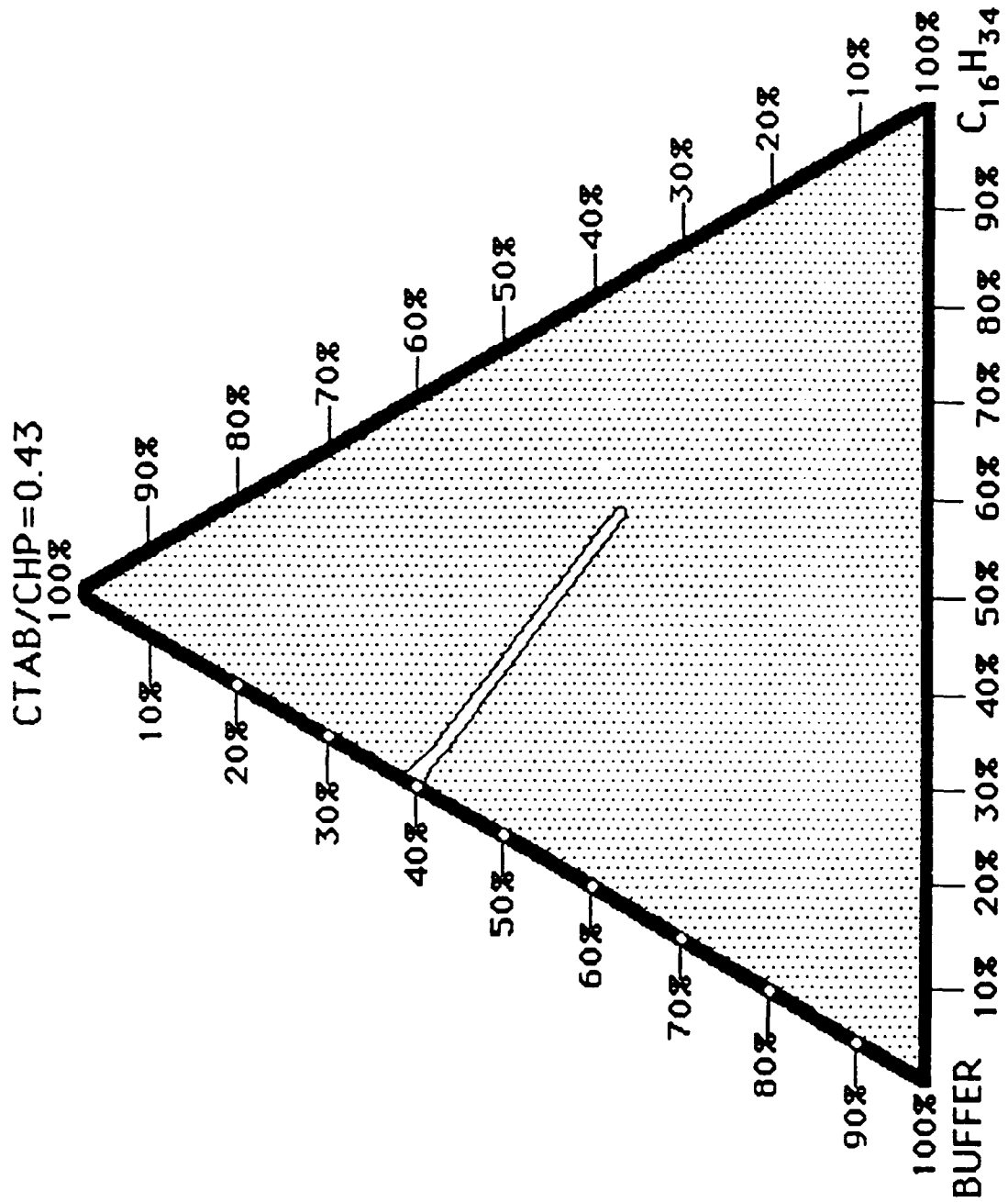
Figure 16. Pseudo-ternary phase map. Clear ◯; turbid ◯.

CTAB/CHP=0.43

100%

BUFFER

$C_{16}H_{34}$

66
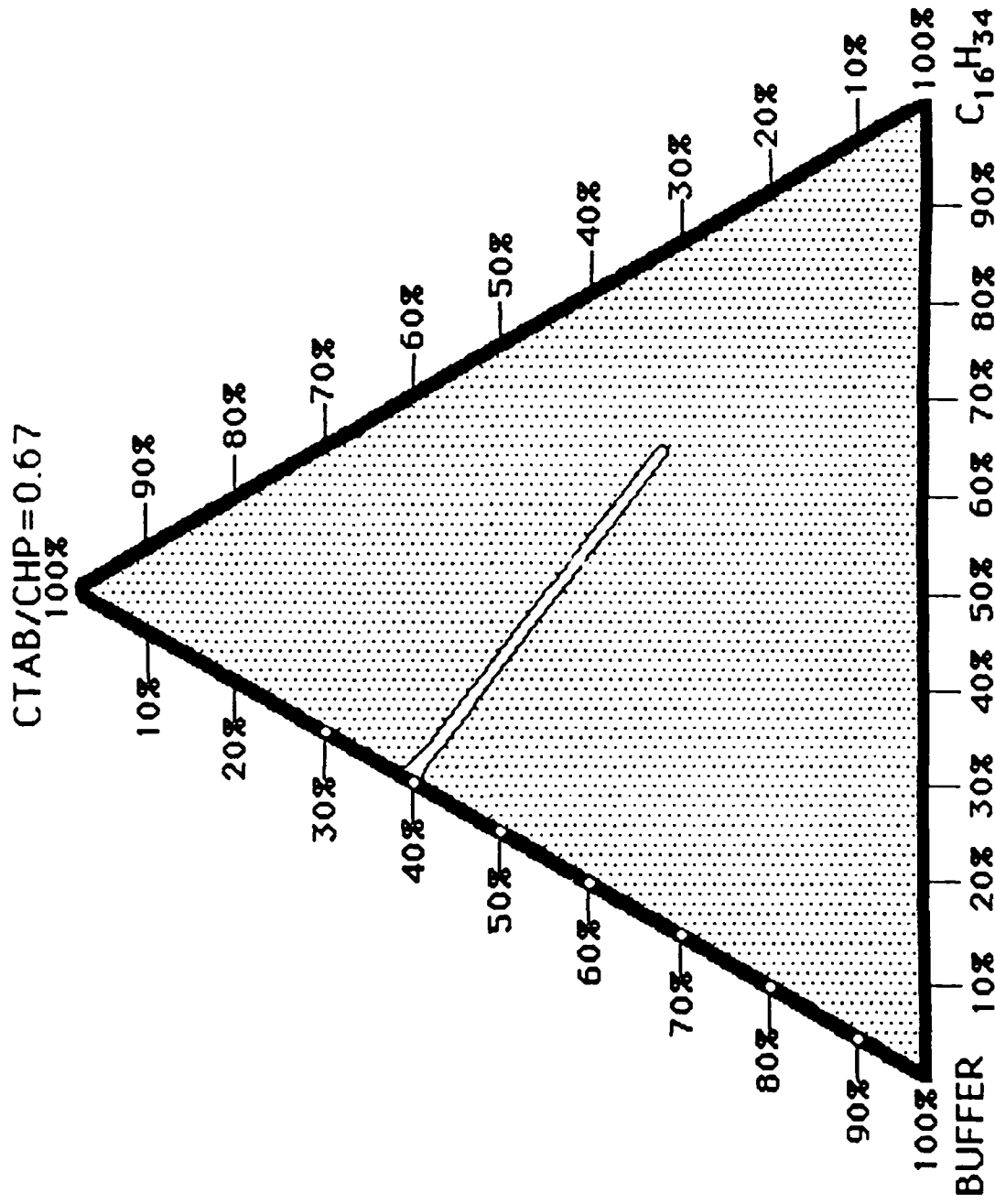
Figure 17. Pseudo-ternary phase map. Clear ◯; turbid ◯.
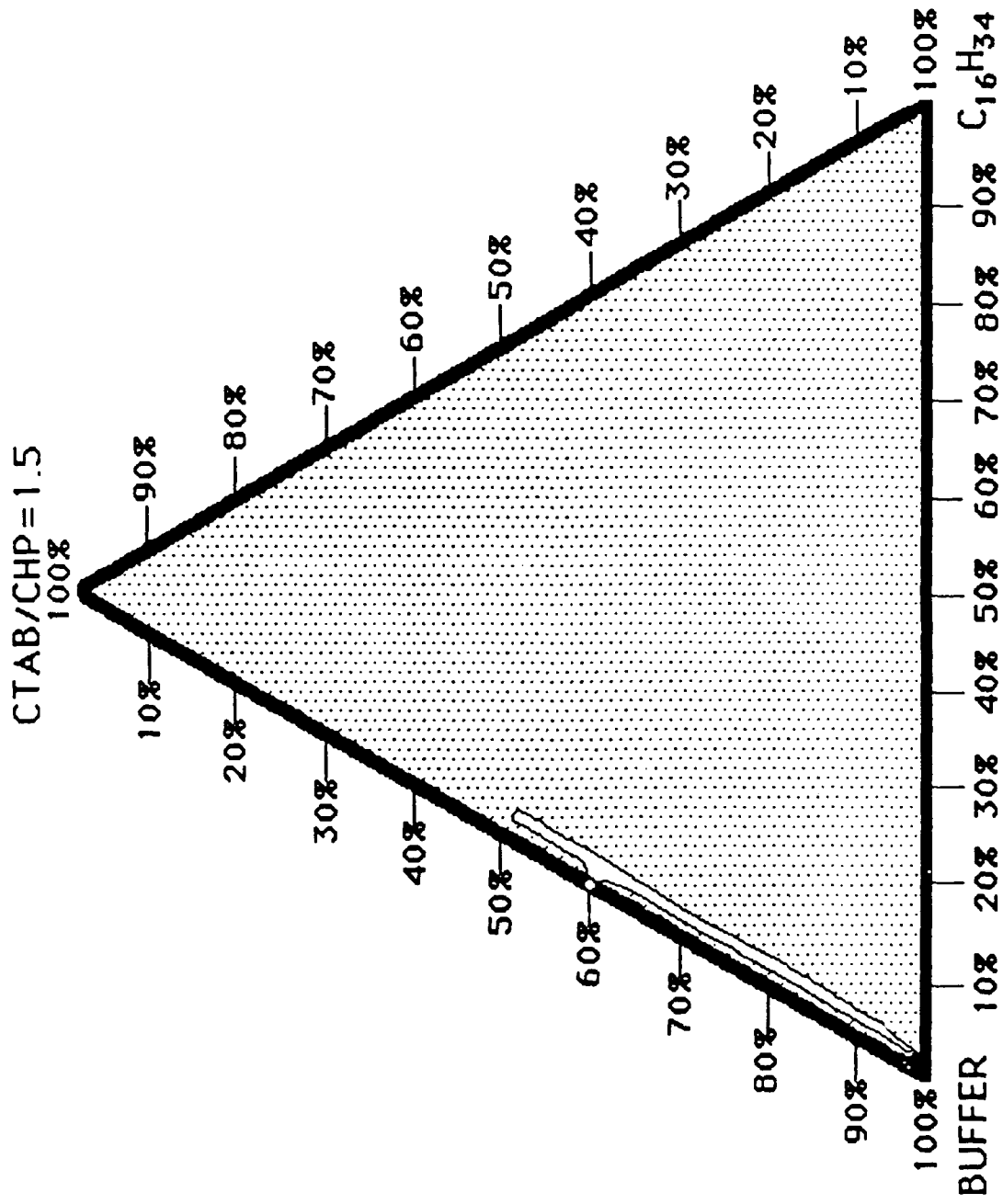
Figure 18. Pseudo-ternary phase map. Clear $\bigcirc$; turbid $\bigcirc$.

CTAB/CHP=1.5

$C_{16}H_{34}$

BUFFER

68
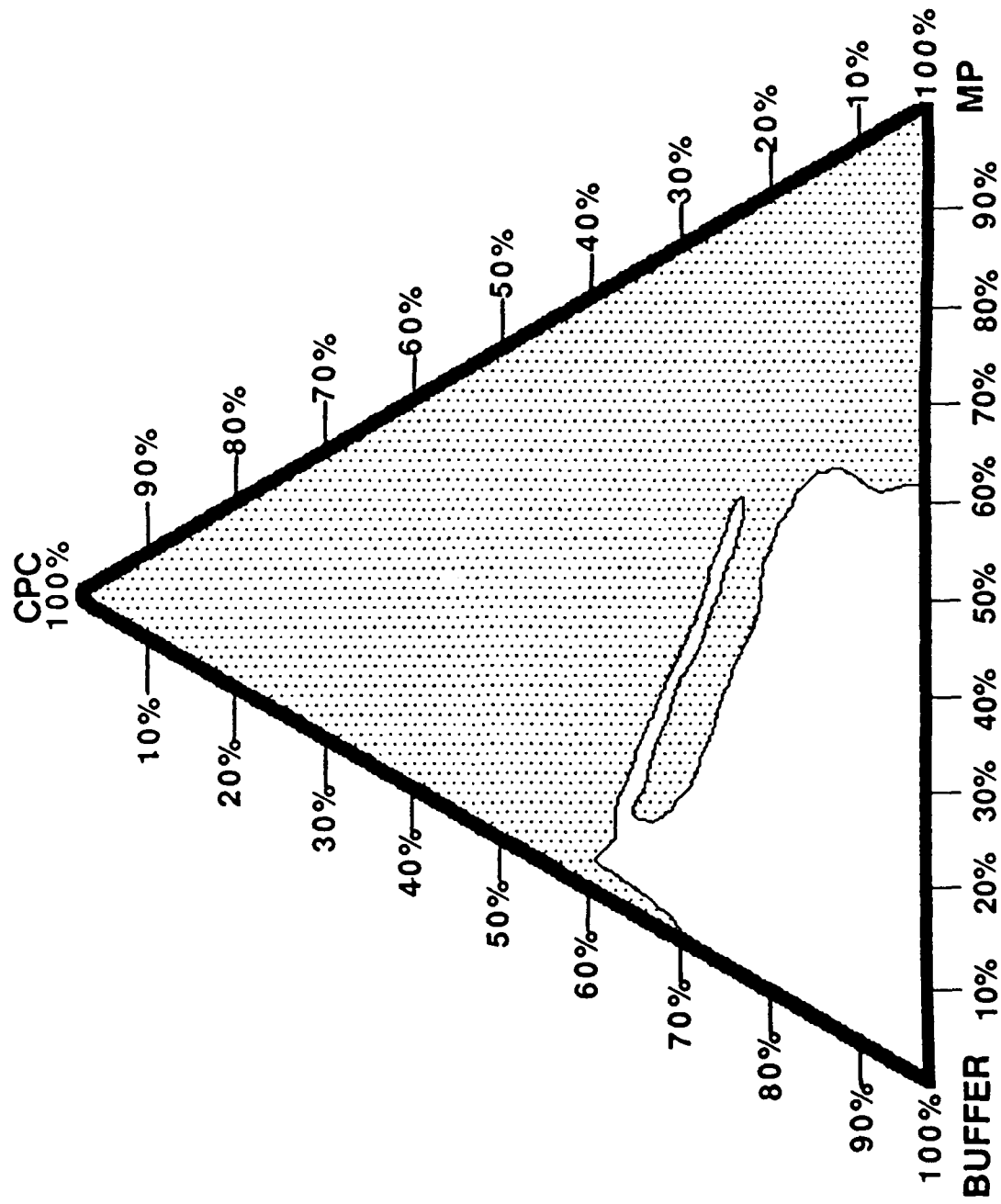
Figure 19. Ternary phase diagram. Clear ◯; turbid ◯.

69
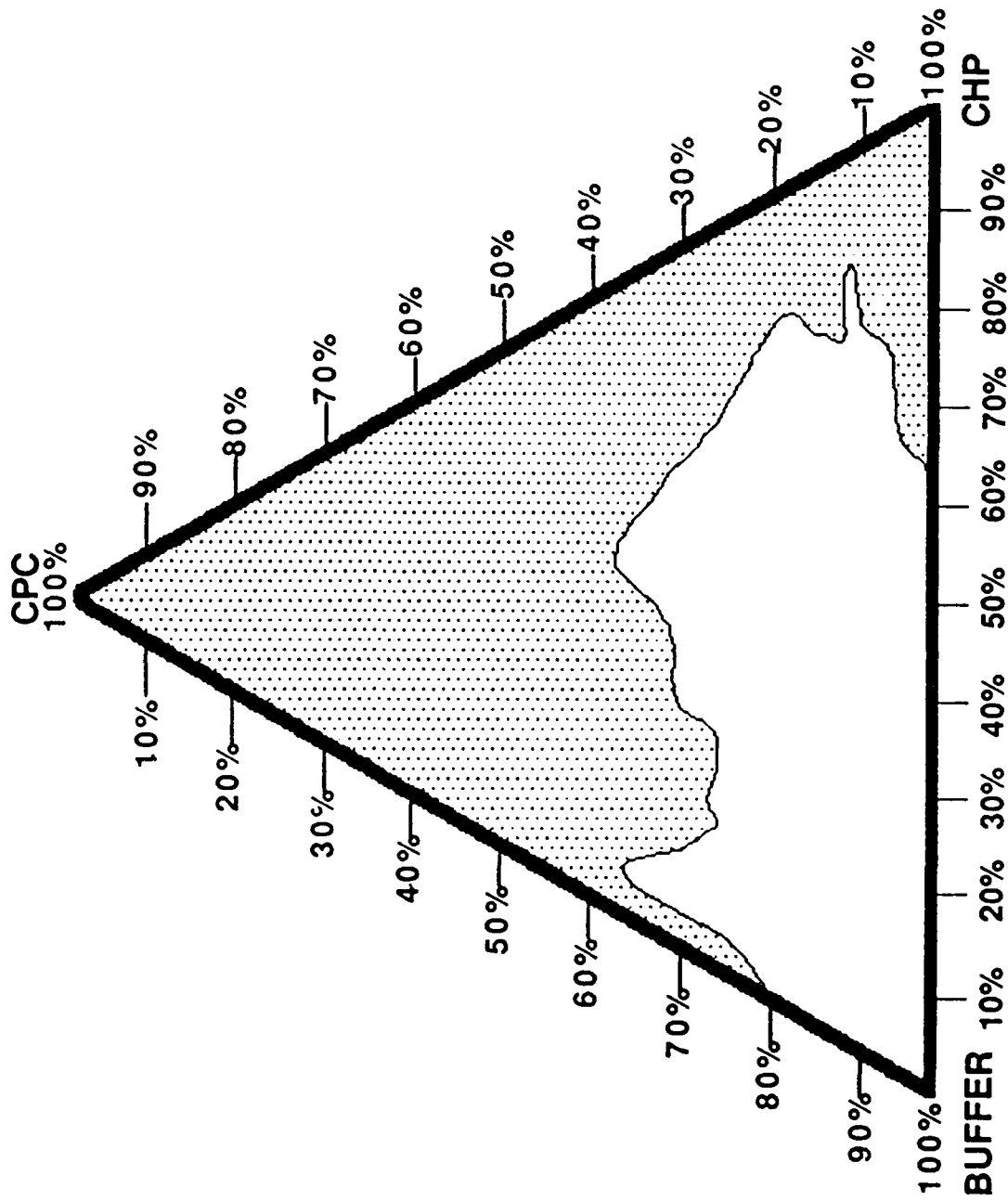
Figure 20. Ternary phase diagram. Clear ◯; turbid ◯.

CTAB/MP=0.5

TOL

BUFFER
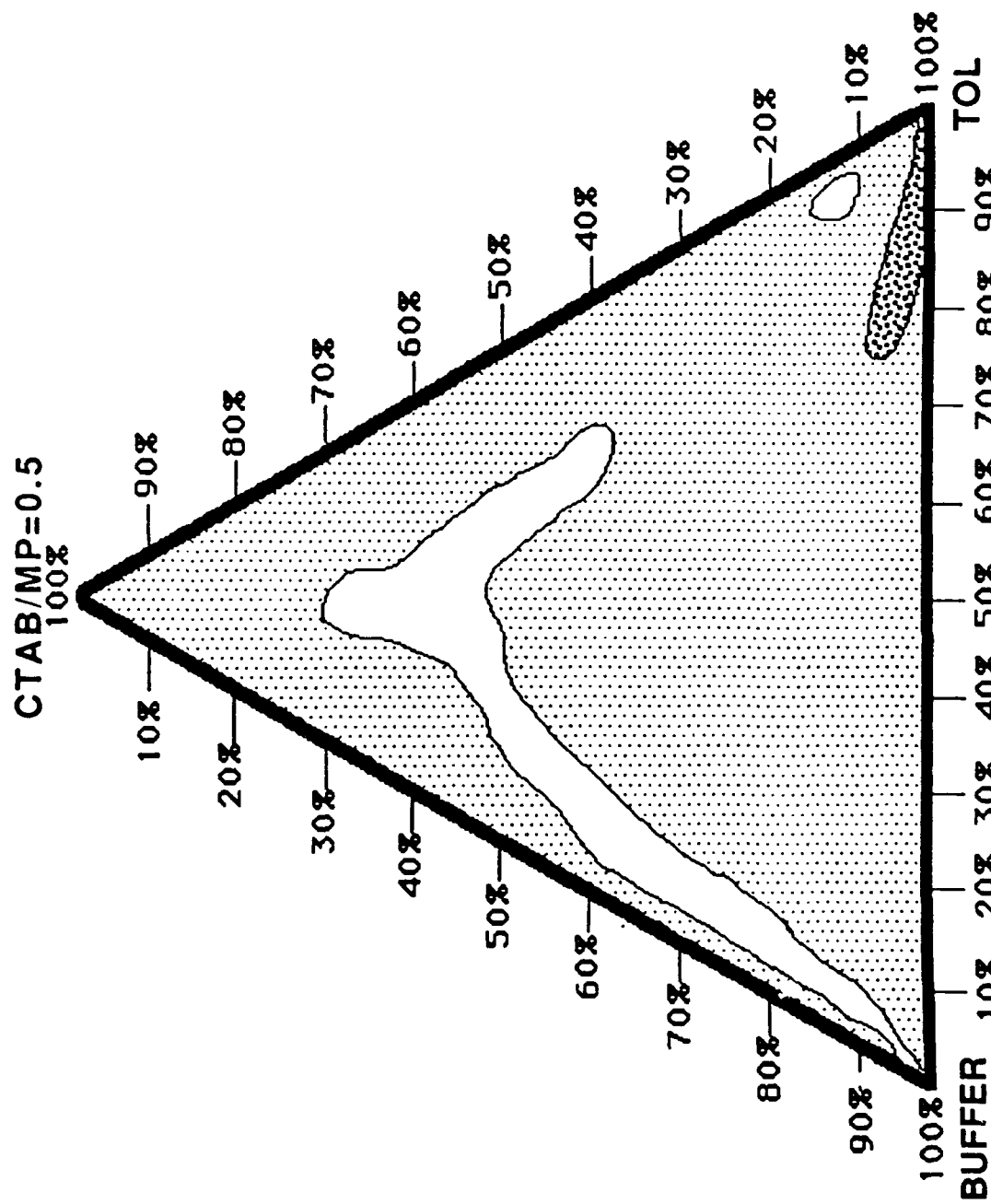
Figure 21. Pseudo-ternary phase map. Clear ◯; turbid ◯; gel ⊗ .

71

CTAB/MP=0.76
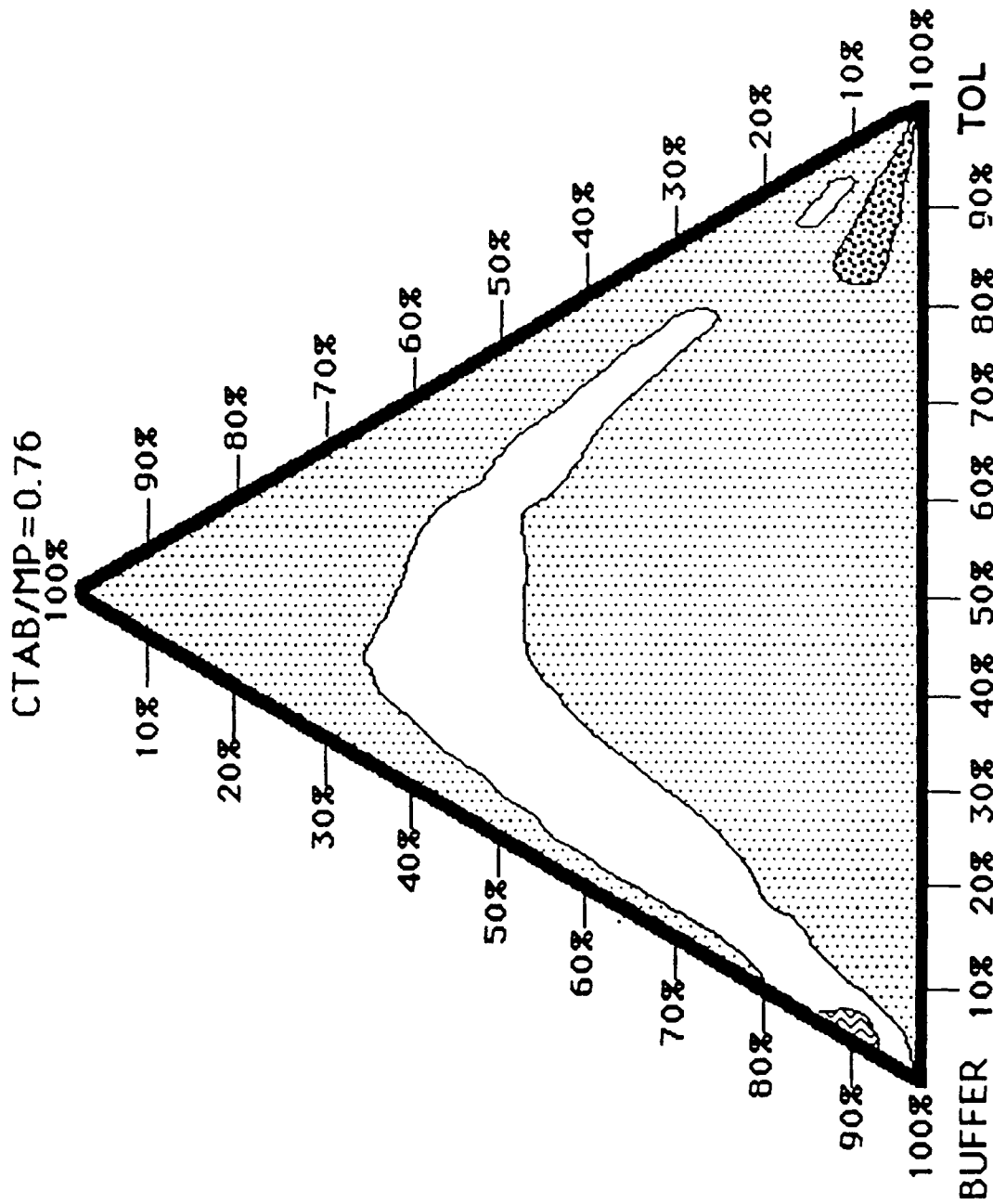
Figure 22. Pseudo-ternary phase map. Clear ◯; turbid ◌; gel ◉; clear liquid crystalline ◉ .
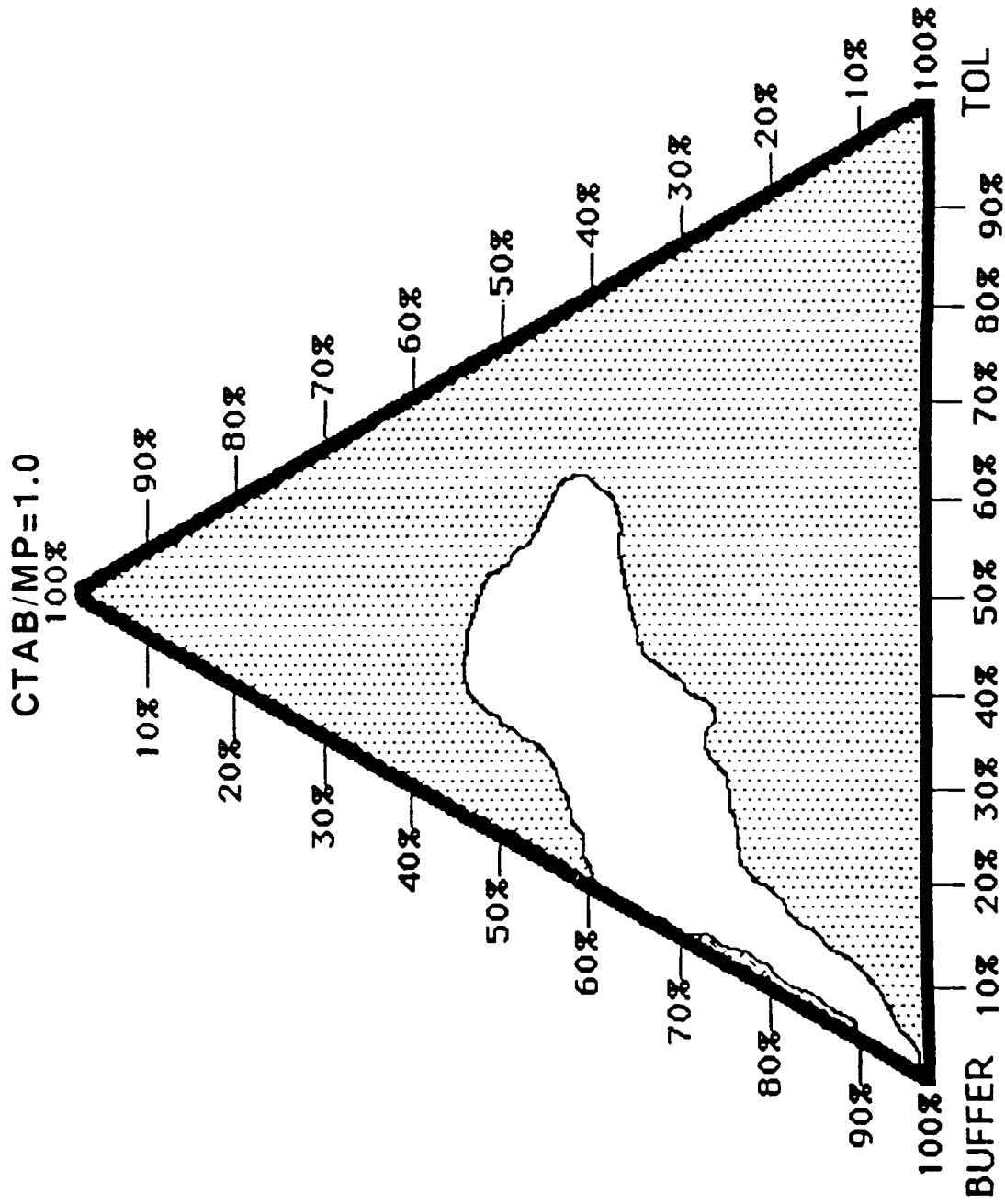
Figure 23. Pseudo-ternary phase map. Clear ◯; turbid ◯; turbid liquid crystalline ⊗.
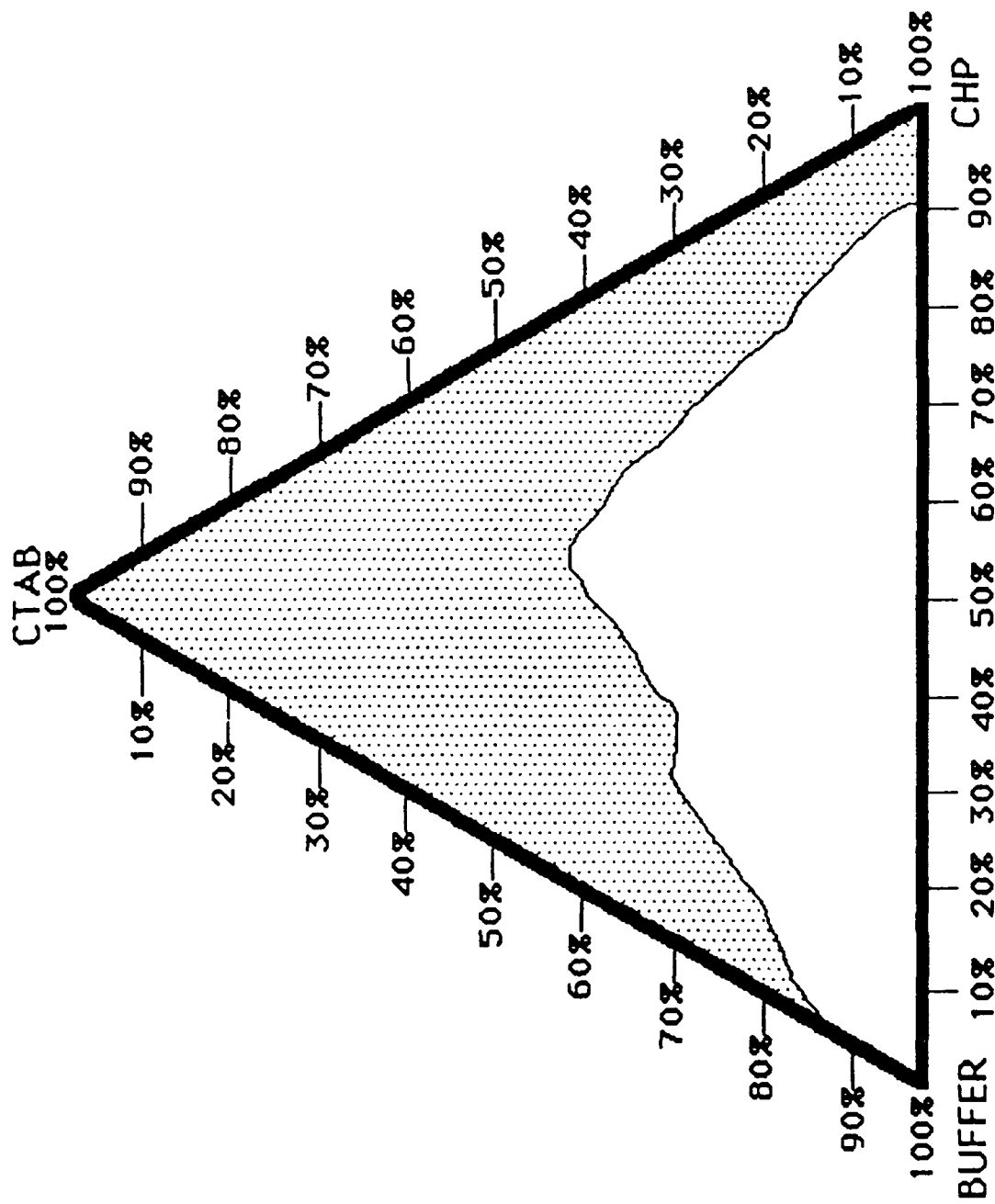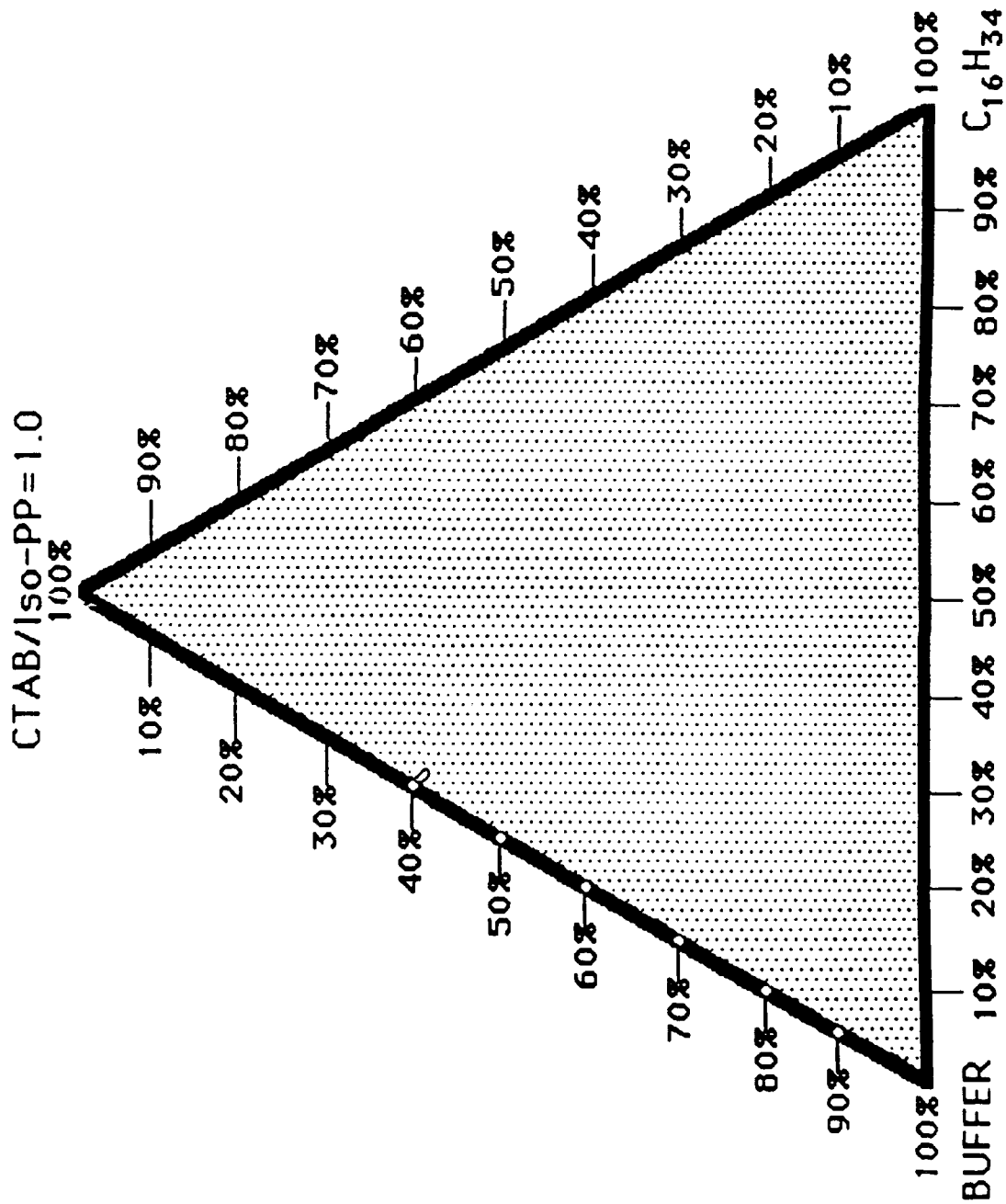
73
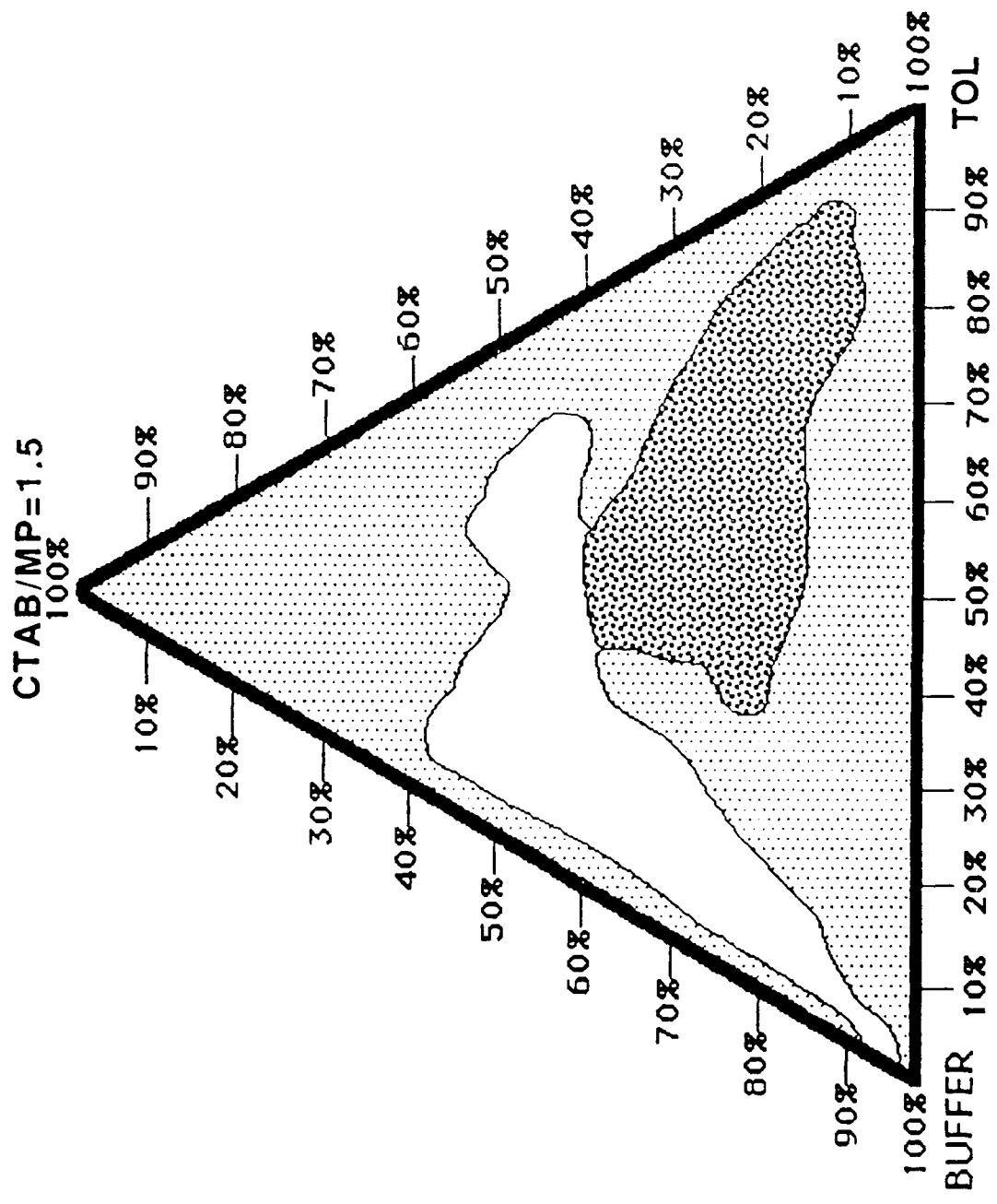
Figure 24 . Pseudo-ternary phase map. Clear ◯; turbid ◯; gel ⊛.
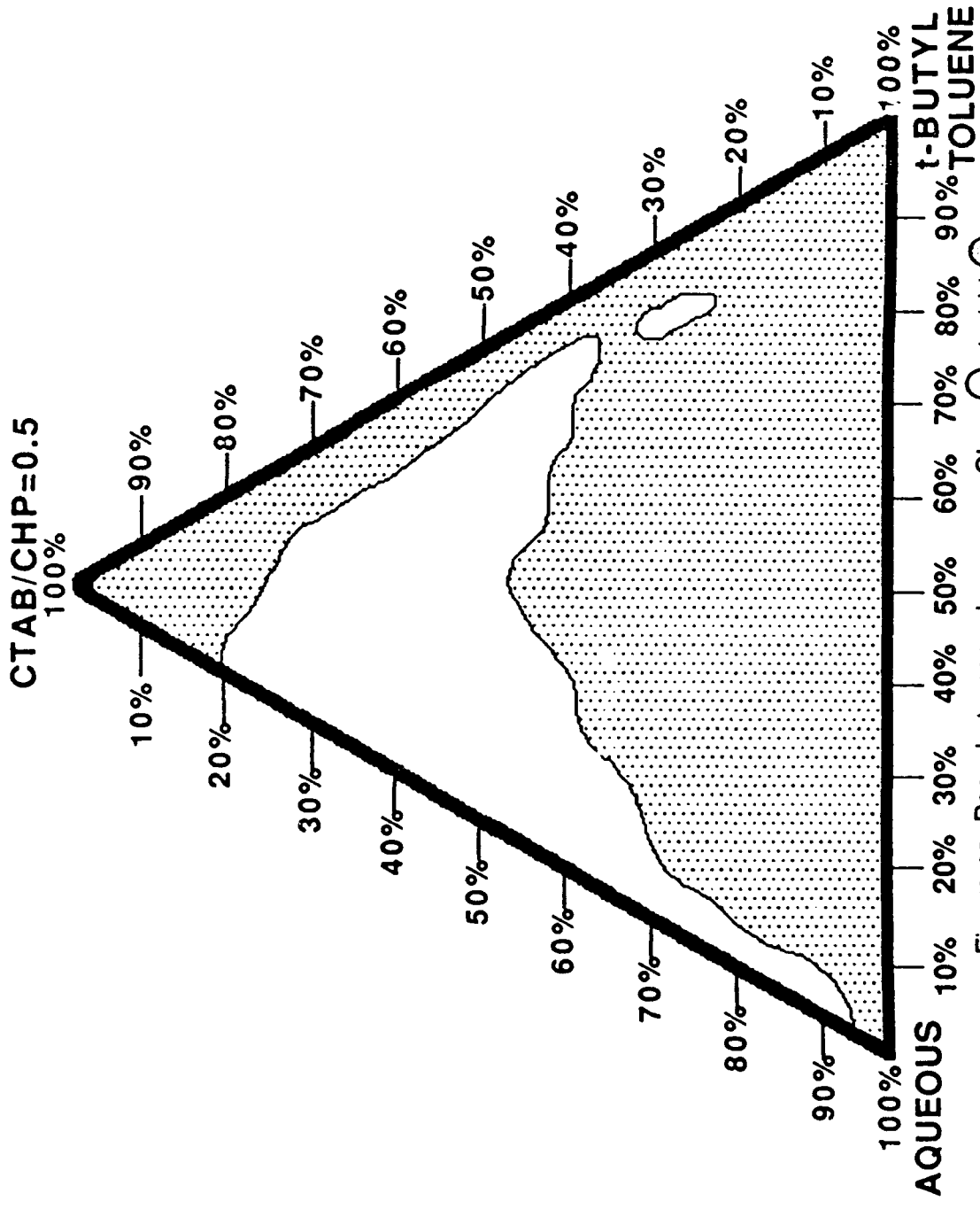
Figure 25. Pseudo-ternary phase map. Clear ○; turbid ○.
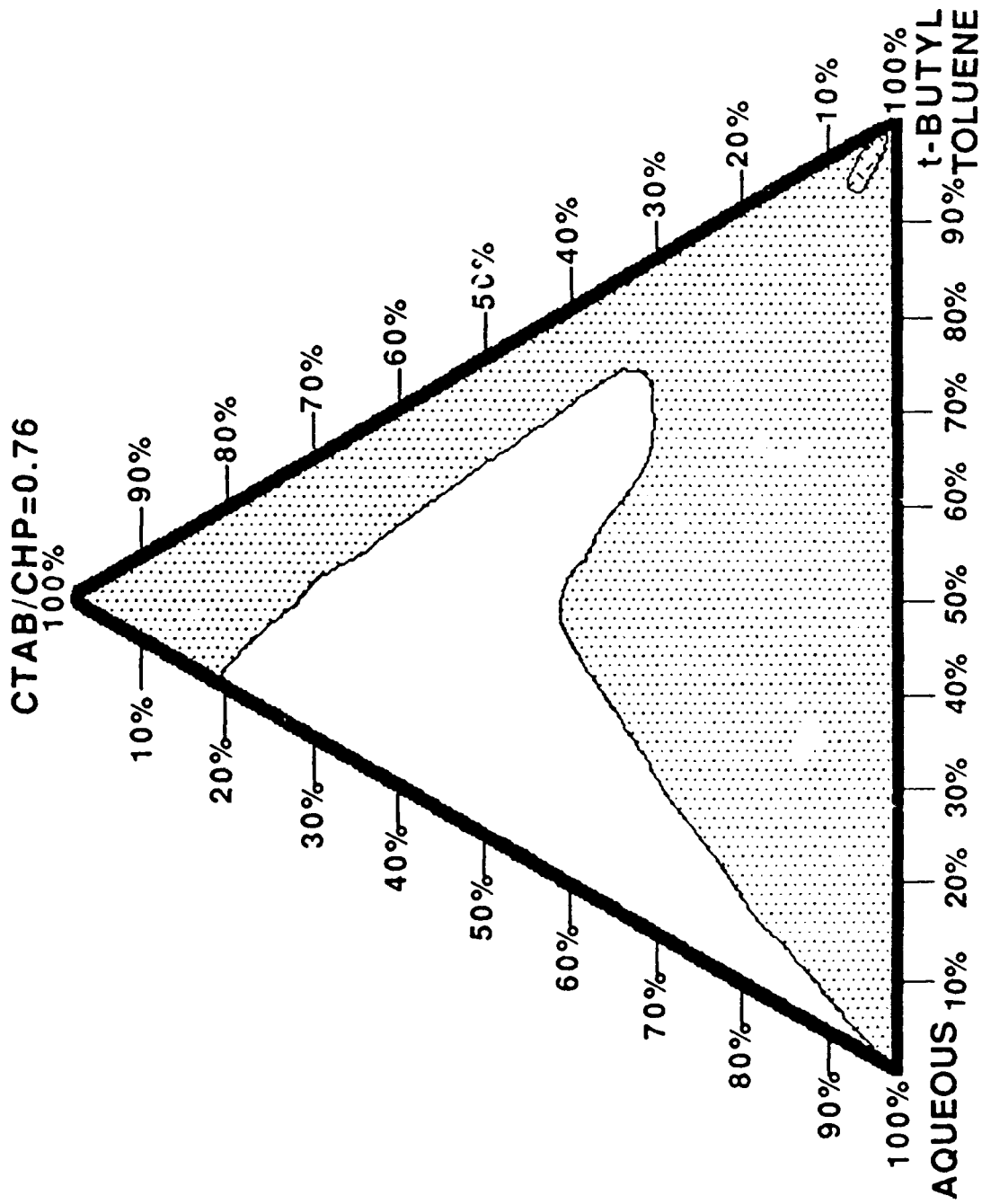
Figure 26. Pseudo-ternary phase map. Clear ◯; turbid ◯; turbid liquid crystalline ◯.

CTAB/CHP=1.0

t-BUTYL TOLUENE

AQUEOUS

Figure 27. Pseudo-ternary phase map. Clear ○; turbid ○; gel ◉ .

77
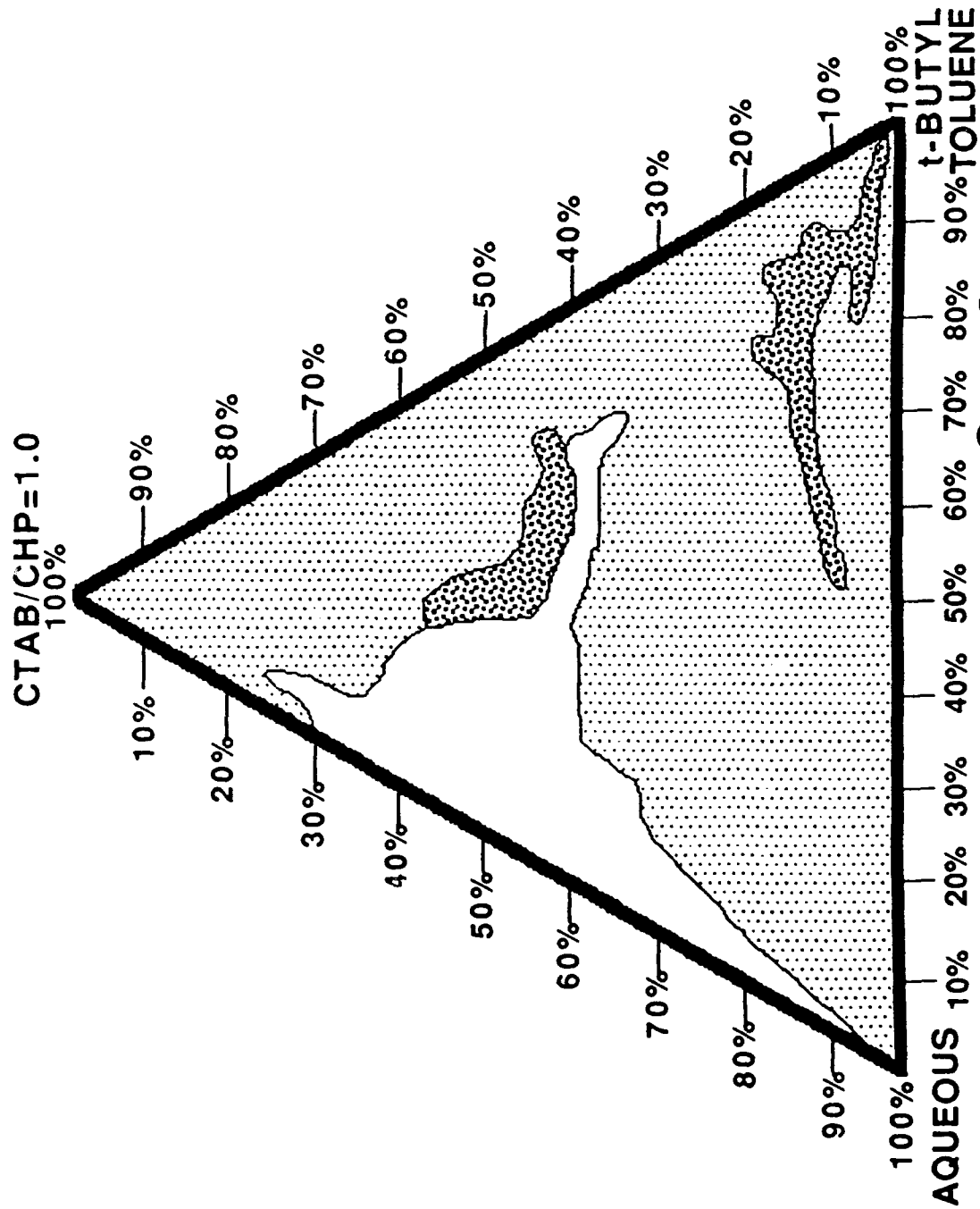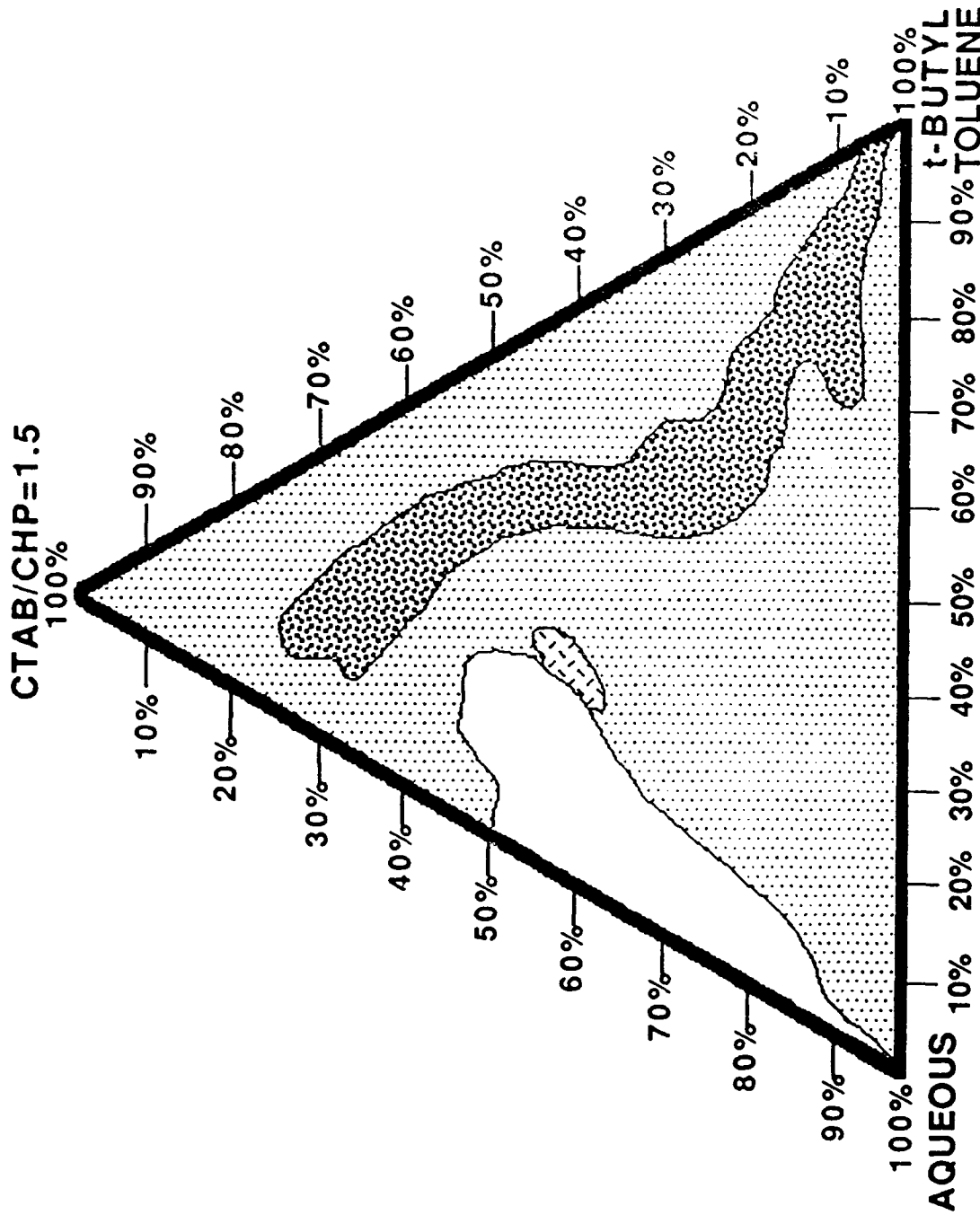
Figure 28 . Pseudo-ternary phase map. Clear ◯; turbid ◯; gel 🔵; turbid liquid crystalline 🔵
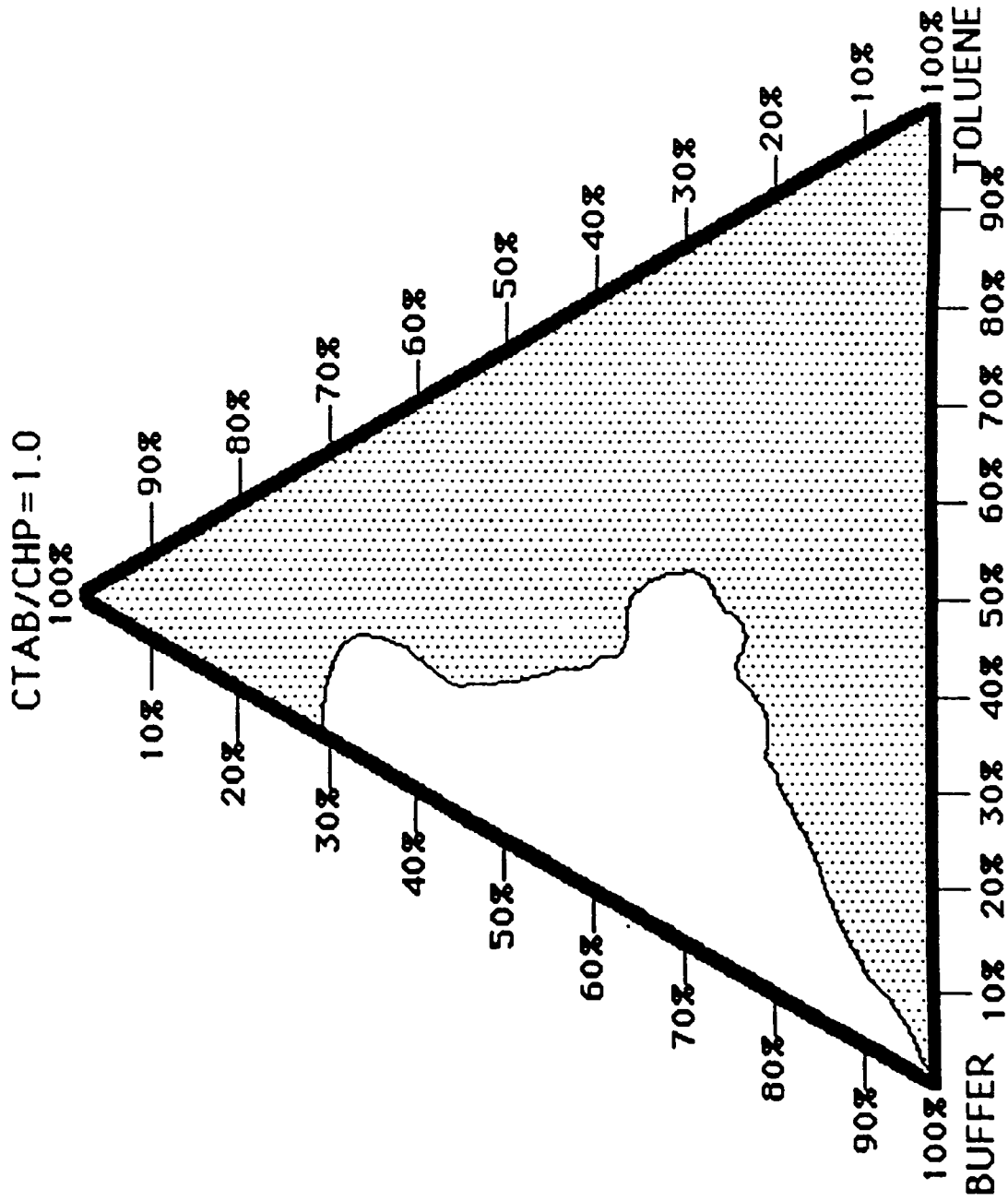
Figure 29. Pseudo-ternary phase map. Clear ◯; turbid ◯.

79
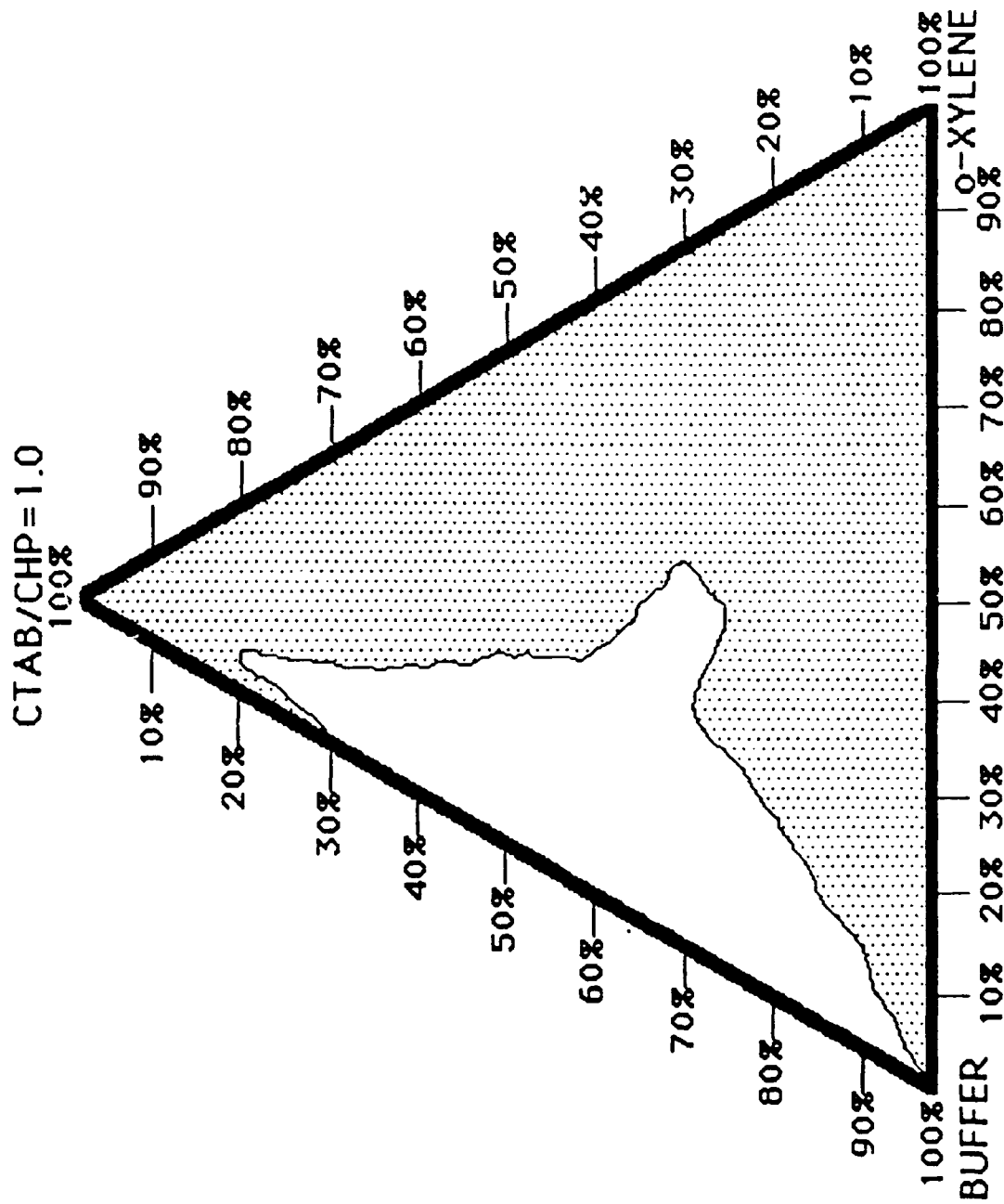
Figure 30. Pseudo-ternary phase map. Clear ◯; turbid ◯.

CTAB/CHP=1.0

O-XYLENE

BUFFER
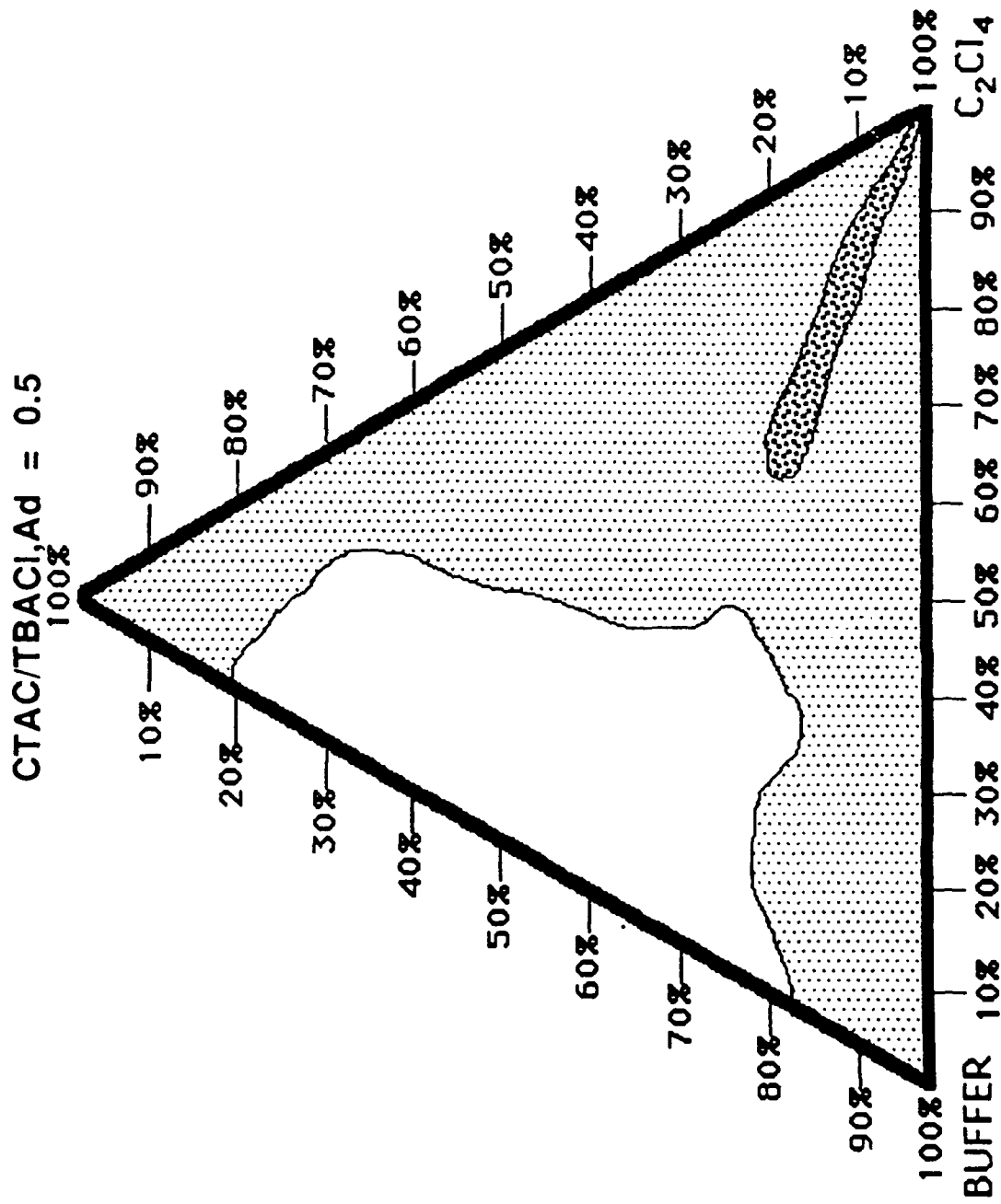
Figure 31. Pseudo-ternary phase map. Clear ◯; gel 🌑; turbid ◯.

81
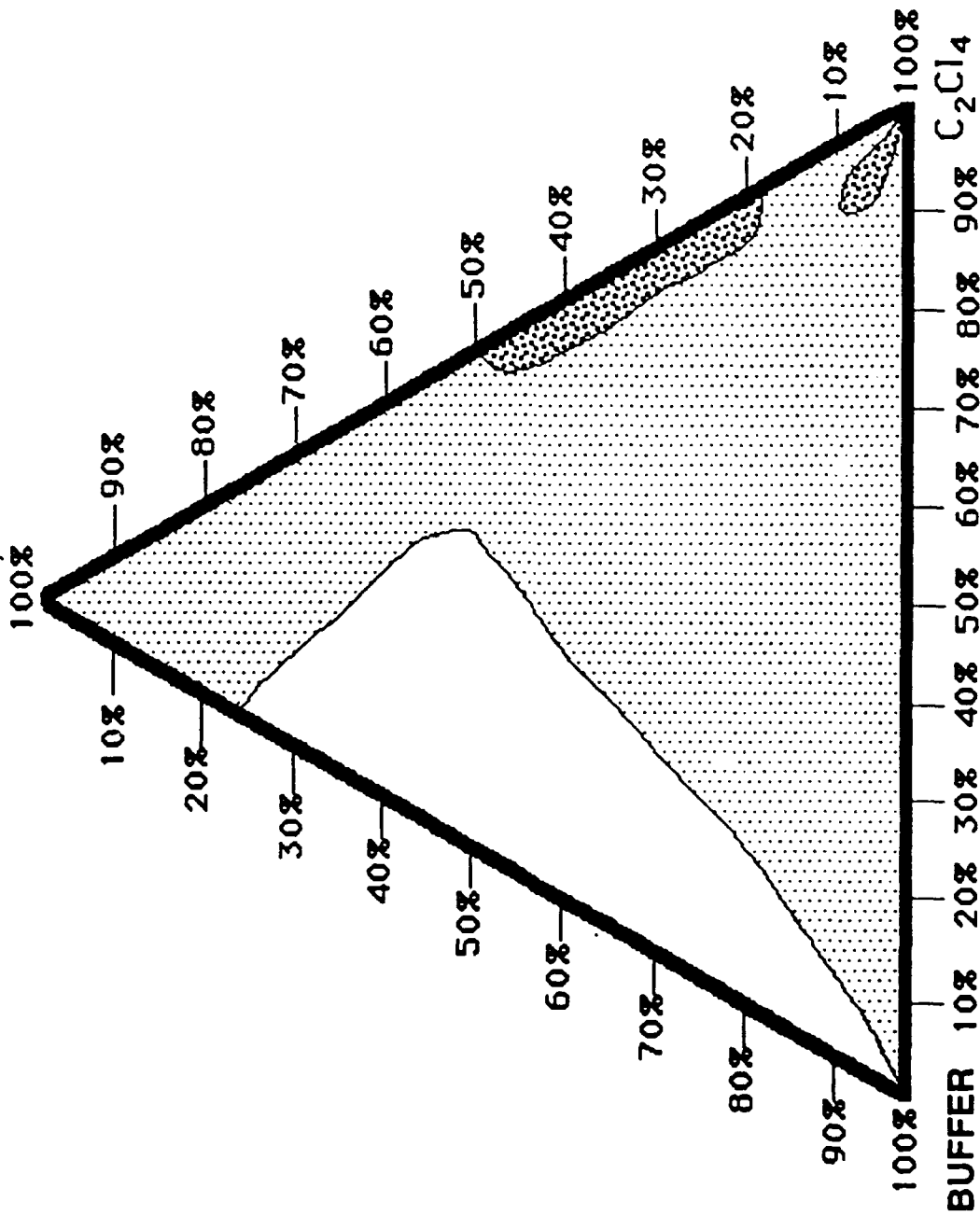
CTAC/TBACl,Ad = 0.76

Figure 32. Pseudo-ternary phase map. Clear ○, gel ⊛, turbid ○.

82
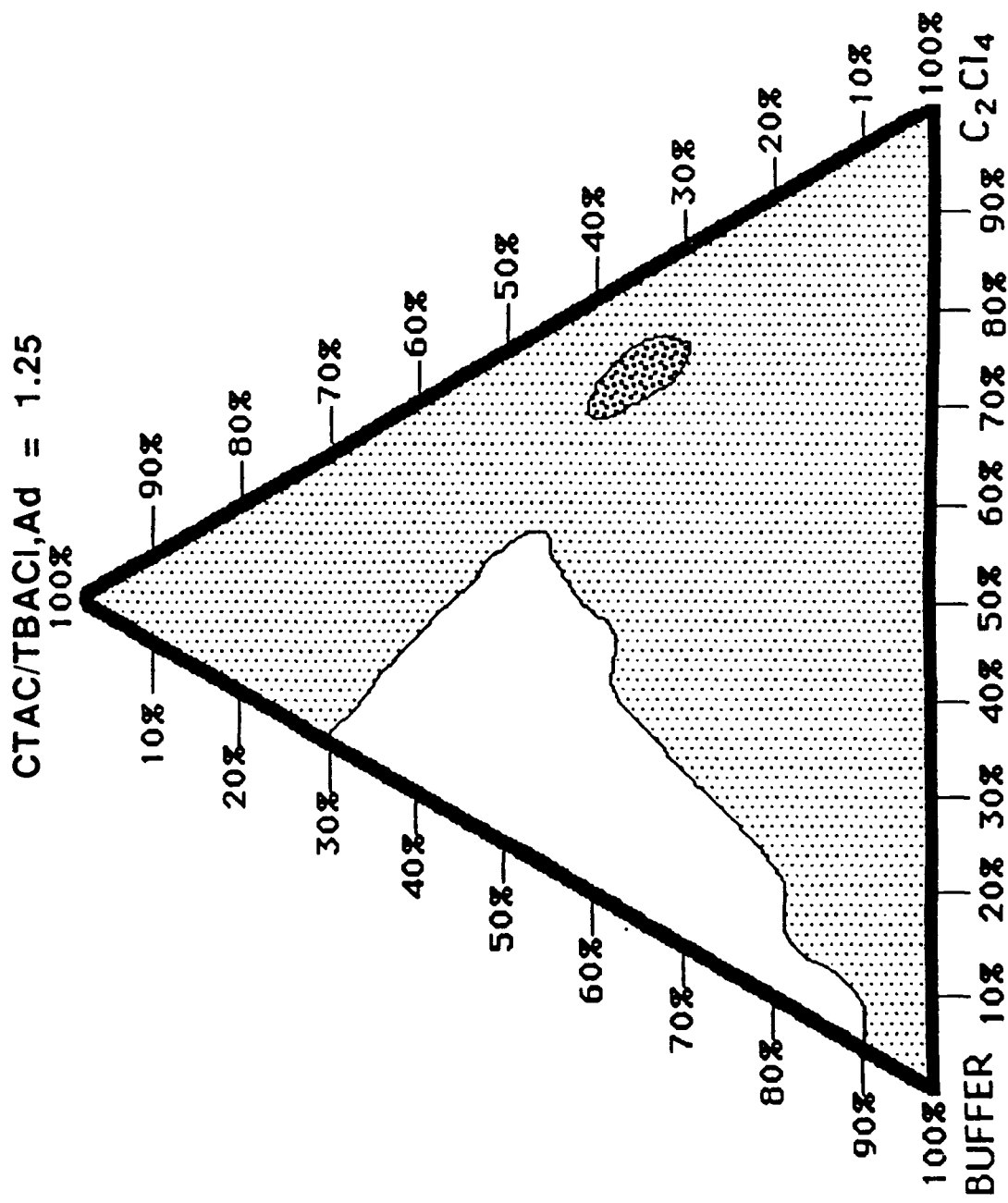
CTAC/TBACl,Ad = 1.25

Figure 33. Pseudo-ternary phase map. Clear ◯; gel ◯; turbid ◯.

83
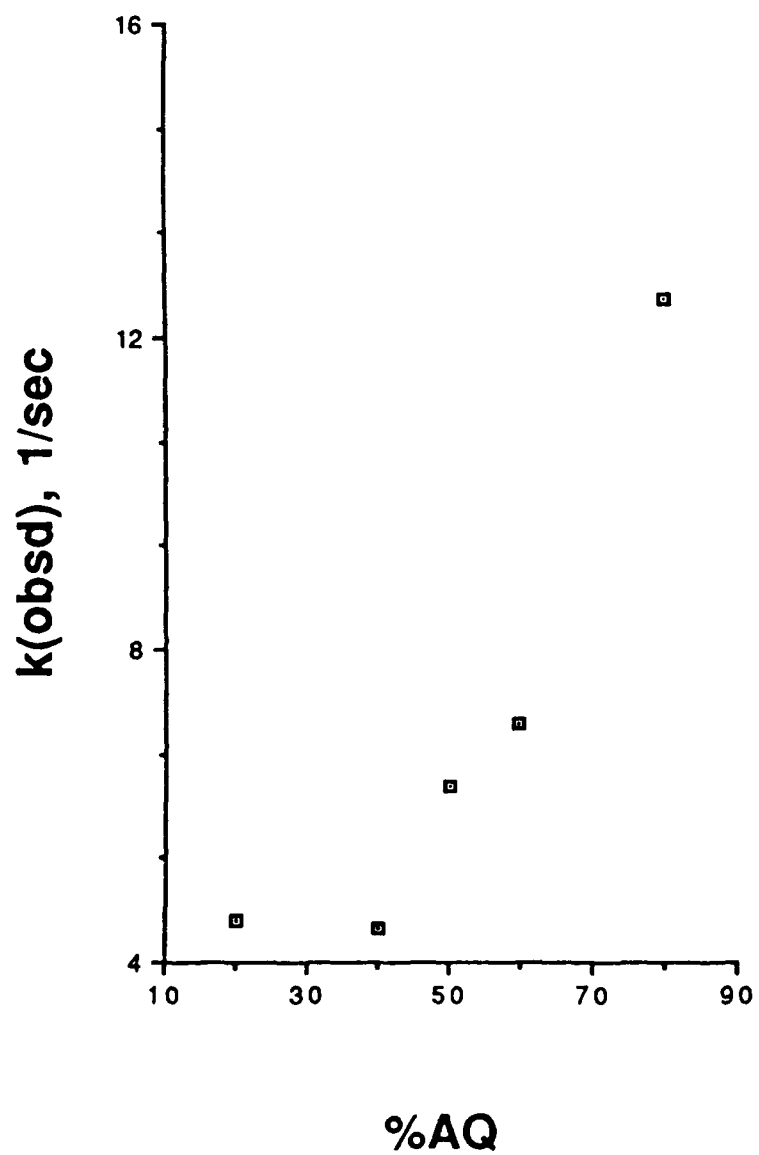
Figure 34. Plot of k_{IBA} versus % AQ for the CTAC / TBACl, Ad / PERC / AQ system. The mass ratio of TBACl to Ad is 8.2.
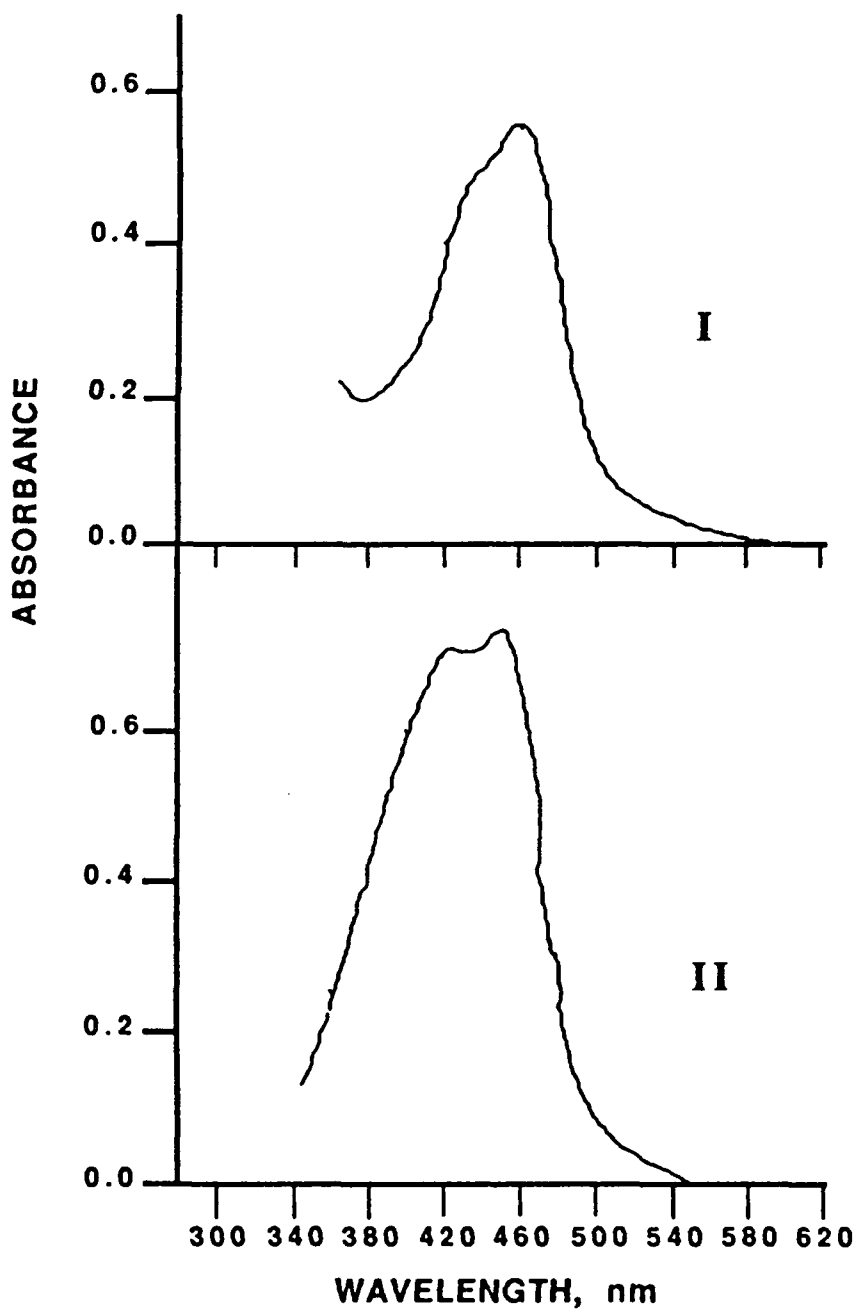
Figure 35. Absorption spectrum of donor molecules I and II in water.

85
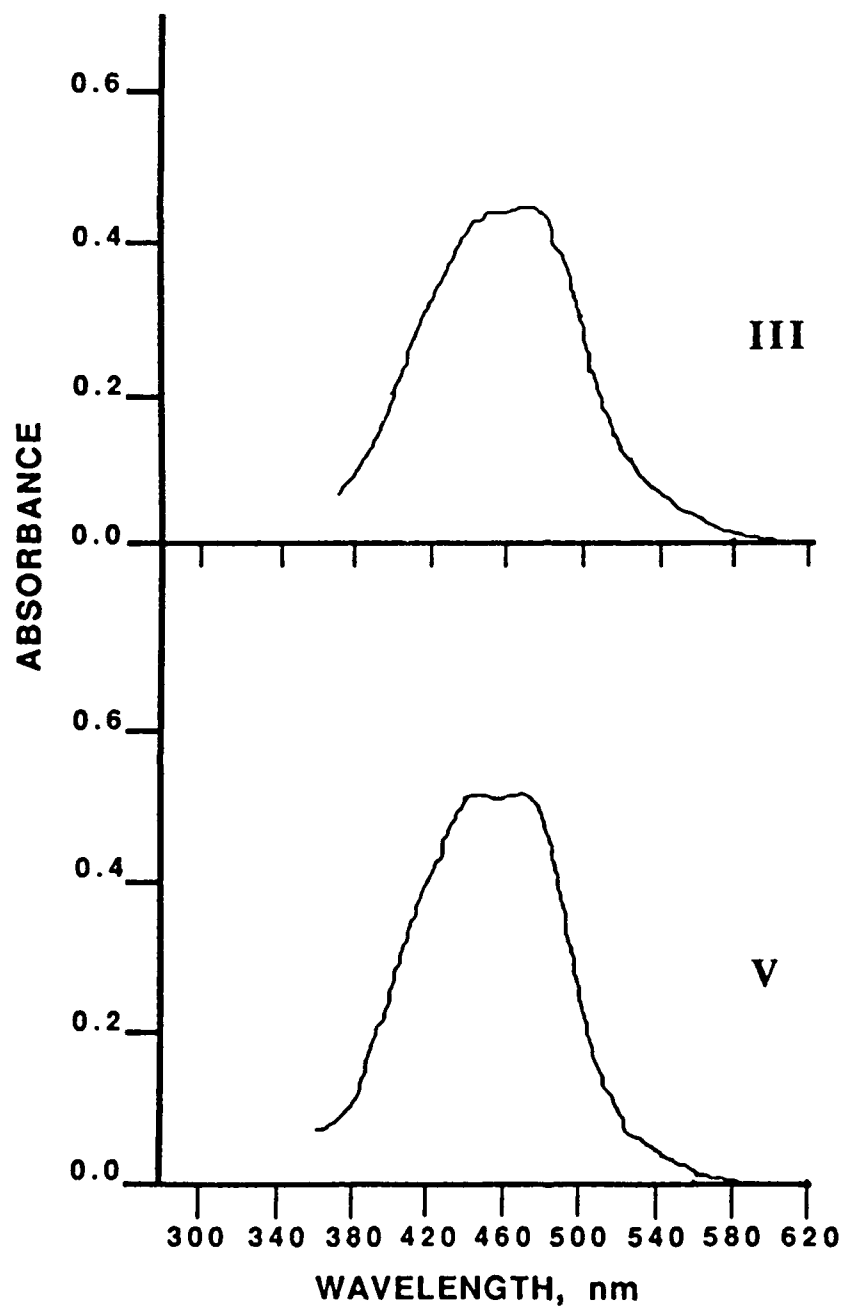
Figure 36. Absorption spectrum of donor molecules III in MP, and V in water.

Tables

Table 1. Second order rate constants for the catalyzed hydrolysis of PNDP in the CTAC / DMF / AQ system. [IBA] ranged from 5 x 10^{-4} M to 6.25 x 10^{-5} M.

% Surfactant	% Cosurfactant	% AQ	pH	k_{IBA} ($sec^{-1} M^{-1}$)
27.0	3.0	70.0	9.4	8.53 ± 0.05
15.0	15.0	70.0	9.4	10.23 ± 0.06
3.0	27.0	70.0	9.2	21.47 ± 0.27

Table 2. Second order rate constants for the catalyzed hydrolysis of PNDP in 8 % CTAB / 8 %N,N - dialkylformamide / 4 % TOL / 80 % AQ systems.

Cosurfactant	k_{IBA} ($sec^{-1} M^{-1}$)
DMF	12.76
DEF	8.71
DIPF	3.83
DBF	-

Table 3. Values of k_{IBA}, k_{OH}, and k_{hyd} in three component systems containing CTAB as surfactant (S) and 0.03 M borate buffer as the aqueous phase (AQ). The cosurfactant (CoS) is either 1-methyl-2-pyrrolidinone (MP), 1-ethyl-2-pyrrolidinone (EP), 1-isopropyl-2-pyrrolidinone (Iso-PP), or 1-cyclohexyl-2-pyrrolidinone (CHP).

%S	CoS	%CoS	%AQ	pH	k_{IBA} (sec⁻¹M⁻¹)	k_{OH} (sec⁻¹M⁻¹)	k_{hyd} x 10⁺⁵ (sec⁻¹M⁻¹)
12.0	MP	10.0	78.0	9.2	14.05 ± 0.35	---	---
12.0	EP	10.0	78.0	9.3	10.76 ± 0.01	0.290 ± 0.007	52.1 ± 0.06
12.0	Iso-PP	10.0	78.0	9.2	10.90 ± 0.02	---	---
12.0	CHP	10.0	78.0	9.5	5.67 ± 0.04	0.315 ± 0.011	49.2 ± 1.7
10.0	EP	40.0	50.0	10.8	3.67 ± 0.05	---	---
10.0	EP	50.0	40.0	10.2	2.52 ± 0.05	---	---
10.0	CHP	40.0	50.0	9.6	1.77 ± 0.01	---	---

Table 4. Values of rate constants for the hydrolysis of p-nitrophenyldiphenyl phosphate in microemulsion media containing CTAB as surfactant (S), 1-cyclohexyl-2-pyrrolidinone as cosurfactant, 0.03 M borate buffer as the aqueous phase (AQ), and hexadecane as oil.

%S	%CoS	%AQ	%Oil	pH	k_{IBA} ($sec^{-1}M^{-1}$)	k_{OH} ($sec^{-1}M^{-1}$)	$k_{hyd} \times 10^{+5}$ ($sec^{-1}M^{-1}$)
5.7	51.6	36.3	6.4	10.4	1.46 ± 0.01	0.067 ± 0.010	9.39 ± 0.36
11.4	45.6	36.7	6.3	10.4	1.88 ± 0.01	---	---
17.3	40.4	35.9	6.4	10.3	2.16 ± 0.03	0.066 ± 0.006	7.98 ± 0.64
23.2	34.8	35.5	6.5	10.3	2.73 ± 0.04	---	---
25.6	17.0	55.0	2.2	9.6	4.03 ± 0.01	---	---

Table 5. Composition of CTAB / 1-alkyl-2-pyrrolidinone / PhHEX / AQ systems.

% S	CoS	% CoS	E Ratio	% Oil	% AQ
26.4	MP	21.0	1.26	2.5	50.1
29.2	MP	14.7	1.99	7.4	48.7
18.5	MP	23.3	0.79	2.8	55.4
24.4	iso-PP	16.3	1.50	2.3	57.0
10.0	CHP	17.5	0.57	6.0	66.5

Table 6. Second order rate constants in 8 % CTAB / 8 % 1-alkyl-2-pyrrolidinone / 4 % TOL / 80 % AQ microemulsions. The pH range is 9.3 to 9.6.

CoS	k_{IBA} ($sec^{-1}M^{-1}$)
2-P	10.62 ± 0.11
MP	11.06 ± 0.11
EP	9.90 ± 0.04
iso-PP	9.09 ± 0.07
AP	8.33 ± 0.04
CHP	5.51 ± 0.09
VP	5.01 ± 0.10

Table 7. Second order rate constants in 8 %CTAB / 0.8073 M 1-alkyl-2-pyrrolidinone / 4 % TOL / AQ system. The pH range is 9.4 to 9.7.

CoS	%CoS	%AQ	k_{IBA}($sec^{-1}M^{-1}$)
CHP	13.5	74.5	3.26 ± 0.01
VP	9.0	79.0	3.61 ± 0.01
AP	10.1	77.9	5.25 ± 0.10
iso-PP	10.3	77.8	5.65 ± 0.10
EP	9.1	78.8	8.20 ± 0.12
2-P	6.9	81.1	8.70 ± 0.10
MP	8.0	80.0	11.06 ± 0.11

Table 8. Values of the first order rate constant, k_{obsd}, for the catalyzed hydrolysis of PNDP in 8 % CTAB / 1-alkyl-2-pyrrolidinone / 4 % TOL / AQ systems. The pH range is 9.4 to 9.7, and [IBA] is 5 x 10^{-4} M.

MP Cosurfactant

% MP	% AQ	k_{obsd} x 10^{+3} (sec^{-1})
6.9	81.1	5.73
8.0	80.0	5.64
9.0	79.0	5.50
9.1	78.8	5.44
10.1	77.9	5.31
13.5	74.5	4.99

Different Cosurfactants

% CoS	% AQ	k_{obsd} x 10^{+3} (sec^{-1})
6.9 (2-P)	81.1	4.84
9.0 (VP)	79.0	---
9.1 (EP)	78.8	3.97
10.3 (iso-PP)	77.8	2.92
10.1 (AP)	77.9	2.64
13.5 (CHP)	74.5	1.66

Table 9. Values of k_{IBA} for the hydrolysis of PNDP in CTAB / MP / TOL / AQ systems. The k_{IBA} values,①, ② result when t-BuTOL is substituted for TOL.

% S	%CoS	E Ratio	%AQ	%Oil	pH	$k_{IBA}(sM)^{-1}$
In Order of Increasing E Ratio						
15.0	30.0	0.50	50.0	5.0	9.3	4.71 ± 0.03
19.4	25.6	0.76	50.0	5.0	9.3	4.50 ± 0.17
22.5	22.5	1.00	50.0	5.0	9.2	4.46 ± 0.07
27.0	18.0	1.50	50.0	5.0	9.3	4.95 ± 0.16
28.6	16.4	1.75	50.0	5.0	9.1	5.10 ± 0.08
In Order of Increasing % AQ						
24.4	24.4	1.00	35.0	16.2	10.8	4.01 ± 0.13
20.6	20.6	1.00	45.0	13.8	10.4	5.11 ± 0.15
22.5	22.5	1.00	50.0	5.0	9.2	4.46 ± 0.07 ①
16.9	16.9	1.00	55.0	11.2	10.1	6.08 ± 0.11
18.0	18.0	1.00	60.0	4.0	9.3	6.34 ± 0.18
13.1	13.1	1.00	65.0	8.8	9.9	7.31 ± 0.13
13.5	13.5	1.00	70.0	3.0	9.3	8.62 ± 0.12 ②
9.4	9.4	1.00	75.0	6.2	9.7	11.6 ± 0.28
9.0	9.0	1.00	80.0	2.0	9.3	12.4 ± 0.55
5.6	5.6	1.00	85.0	3.8	9.6	17.3 ± 0.19
4.5	4.5	1.00	90.0	1.0	9.4	25.1 ± 0.26
In Order of Increasing % Oil						
21.0	21.0	1.00	47.0	11.0	9.3	3.66 ± 0.09
16.5	16.5	1.00	54.0	12.0	9.3	3.08 ± 0.15
26.0	26.0	1.00	31.0	17.0	9.3	2.67 ± 0.05
21.5	21.5	1.00	33.0	23.0	9.3	2.00 ± 0.02

① 6.35 $s^{-1}M^{-1}$; ② 7.41 $s^{-1}M^{-1}$

Table 10. Values of k_{IBA} for the hydrolysis of PNDP in microemulsion consisting of CTAB (S) / CHP (CoS) / 4-tert- butyltoluene (Oil) / borate buffer (AQ). The emulsifier ratios (E Ratio) are listed. The footnoted k_{IBA} values result when toluene is substituted for 4-tert - butyltoluene. [IBA] = 10^{-3} - 10^{-4} M.

%S	%CoS	E Ratio	%AQ	%Oil	pH	$k_{IBA}(sM)^{-1}$
In Order of Increasing E Ratio						
15.0	30.0	0.50	50.0	5.0	9.5	2.33 ± 0.01
19.4	25.6	0.76	50.0	5.0	9.4	2.86 ± 0.01
22.5	22.5	1.00	50.0	5.0	9.4	3.05 ± 0.02
27.0	18.0	1.50	50.0	5.0	9.3	4.32 ± 0.07
28.0	17.0	1.65	50.0	5.0	9.3	3.34 ± 0.13
28.6	16.4	1.75	50.0	5.0	9.1	3.37 ± 0.20
In Order of Increasing % AQ						
36.0	36.0	1.00	20.0	8.0	9.6	3.43 ± 0.06
31.5	31.5	1.00	30.0	7.0	9.6	3.01 ± 0.03
27.0	27.0	1.00	40.0	6.0	9.5	2.98 ± 0.06
22.5	22.5	1.00	50.0	5.0	9.4	3.05 ± 0.02
18.0	18.0	1.00	60.0	4.0	9.4	3.94 ± 0.08 [1]
13.5	13.5	1.00	70.0	3.0	9.3	4.39 ± 0.15
9.0	9.0	1.00	80.0	2.0	9.2	6.66 ± 0.03 [2]
4.5	4.5	1.00	90.0	1.0	9.4	12.6 ± 1.0
In Order of Increasing % Oil						
21.0	21.0	1.00	47.0	11.0	9.4	2.78 ± 0.04
16.5	16.5	1.00	54.0	12.0	9.4	3.55 ± 0.26
26.0	26.0	1.00	31.0	17.0	9.4	2.45 ± 0.03
21.5	21.5	1.00	33.0	23.0	9.4	2.94 ± 0.01

[1] 3.73 $s^{-1}M^{-1}$

[2] 6.88 $s^{-1}M^{-1}$

Table 11. Values of k_{IBA} for the hydrolysis of PNDP in CTAB / CHP / OIL / AQ systems. The oil is either TOL, o-XY, or CUM. The pH ranges from 9.2 to 9.4.

% S	% CoS	% AQ	% OIL	k_{IBA} (sec^{-1}M^{-1})
Toluene				
17.5	17.5	50.0	15.0	2.47 ± 0.01
10.0	10.0	70.0	10.0	3.12 ± 0.04
10.0	10.0	75.0	5.0	4.39 ± 0.04
o-Xylene				
17.5	17.5	50.0	15.0	2.41 ± 0.01
10.0	10.0	70.0	10.0	2.51 ± 0.01
10.0	10.0	75.0	5.0	5.38 ± 0.04
Cumene				
17.5	17.5	50.0	15.0	2.61 ± 0.02
10.0	10.0	70.0	10.0	3.33 ± 0.03
10.0	10.0	75.0	5.0	4.99 ± 0.11

Table 12. Values of rate constants in 8 % CTAB / 8 % or 0.8073 M CoS / 4 % TOL / AQ systems containing additional cosurfactants at pH 9.2.

CoS	k_{IBA} (sec^{-1}M^{-1})	
	8 % CoS	0.8073 M CoS
DMP	11.67 ± 0.37	8.92 ± 0.05
DMIZ	11.26 ± 0.40	10.00 ± 0.10
DMAC	10.73 ± 0.11	12.56 ± 0.14
TMU	10.57 ± 0.24	9.35 ± 0.11
1-PC	9.11 ± 0.07	9.11 ± 0.07
DEF	7.95 ± 0.02	8.71 ± 0.11
1-FP	6.00 ± 0.01	6.07 ± 0.03
DIPF	3.83 ± 0.06	3.11 ± 0.06
MP	11.06 ± 0.11	11.06 ± 0.11

Table 13. Values of k_{IBA} for the hydrolysis of PNDP in CTAC (S) / TBACI, Ad (CoS) / PERC / AQ microemulsions The mass ratio of TBACI / Adogen is 8.2. The emulsifier ratios (E Ratio) are listed, and the pH range is 9.3 to 9.5.

%S	%CoS	E Ratio	%AQ	%Oil	$k_{IBA}(\underline{sM})^{-1}$
In Order of Increasing E Ratio					
13.3	26.7	0.50	50.0	10.0	4.99 ± 0.18
17.3	22.8	0.76	49.9	10.0	6.24 ± 0.21
22.1	18.2	1.25	49.7	10.0	6.37 ± 0.05
10.7	21.3	0.50	60.0	8.0	5.90 ± 0.12
13.8	18.4	0.76	59.8	8.0	7.05 ± 0.23
17.7	14.7	1.25	59.6	8.0	8.05 ± 0.13
In Order of Increasing % AQ					
28.0	36.0	0.76	20.0	16.0	4.53 ± 0.09
18.4	29.6	0.76	40.0	12.0	4.43 ± 0.12
17.3	22.8	0.76	49.9	10.0	6.24 ± 0.21
13.8	18.4	0.76	59.8	8.0	7.05 ± 0.23
6.9	9.4	0.76	79.7	4.0	12.5 ± 0.83

Table 14. A comparison of k_{IBA} values obtained in several microemulsions.

% CTAC	% CoS	% Oil	% AQ	pH	k_{IBA} ($\underline{sM}$)$^{-1}$
16.5	11.6 TBAOH 1.4 Ad	7.5 PERC	63.0	11.3	17.6
16.5	11.6 TBACl 1.4 Ad	7.5 PERC	63.0	9.4	10.1
21.2	1.8 Ad	9.6 PERC	67.4	9.4	< 7
15.9	4.8 TBACl	8.5 PERC	70.8	9.4	13.3
---	13.0 TBACl	----	87.0	9.4	1.67
8.0 CTAB	11.6 TBAOH 8.0 MP	4.0 TOL	68.4	11.2	10.3

Table 15. Values of k_{obsd} for the hydrolysis of PNDP in 0.03 M borate buffer, pH 9.2, as a function of mass % TBACl. The IBA concentration is 1×10^{-3} M.

% TBACl	[TBACl]	$k_{obsd} \times 10^{+4}$ ($\underline{sec}^{-1}$)
0	0	4.63
0.5	0.017	4.52
1.0	0.035	6.08
2.0	0.069	7.03
4.0	0.138	12.4
5.0	0.173	12.7
7.0	0.242	11.2
9.0	0.311	11.8
11.0	0.380	11.1
13.0	0.449	11.5
15.0	0.518	12.0

Table 16. Absorbances at 402 nm following incubation of solid PNDP in 0.03 M borate buffer with and without 13 % TBACl at pH 9.4 and 11.2.

	pH	TBACl	Absorbance
10 min.			
	9.4	-	0.457
	9.4	+	0.416
	11.2	-	0.471
	11.2	+	0.585
60 min.			
	9.4	-	0.538
	9.4	+	0.604
	11.2	-	0.541
	11.2	+	0.852
180 min.			
	9.4	-	0.590
	9.4	+	0.678
	11.2	-	0.550
	11.2	+	0.963

Table 17. Values of k_{IBA} in CTAC / Tetraalkylammonium halide / PERC / AQ systems. Several systems contain a mass ratio of TBACl / Adogen of 8.2 as the cosurfactant. The pH range is 9.2 to 9.4.

% S	CoS	% CoS	% AQ	% Oil	k_{IBA} ($sec^{-1}M^{-1}$)
15.9	TMACl	4.8	70.8	8.5	----
15.9	TEACl	4.8	70.8	8.5	11.8 ± 1.8
15.9	TPrCl	4.8	70.8	8.5	13.0 ± 0.15
15.9	TBACl	4.8	70.8	8.5	13.3 ± 0.10
15.9	TBACl, Ad	4.8	70.8	8.5	13.8 ± 0.22
16.5	TBACl, Ad	13.0	63.0	7.5	10.1 ± 0.06
17.6	TBABr	3.1	70.8	8.5	12.0 ± 0.26
15.9	TBABr	4.8	70.8	8.5	12.7 ± 0.14
15.9	TPABr	4.8	70.8	8.5	10.2 ± 0.17
15.9	THACl	4.8	70.8	8.5	10.9 ± 0.33
15.8	THABr	1.1	75.2	7.9	10.7 ± 0.22
15.9	THABr	4.8	70.8	8.5	9.4 ± 0.19
15.9	TOABr	0.6	75.5	8.0	10.2 ± 0.05
15.8	TOABr	1.4	74.9	7.9	10.4 ± 0.35
16.4	TOABr	2.5	72.6	8.5	10.8 ± 0.22

Table 18. Previous work involving catalyzed hydrolysis of phosphate esters by IBA, IBX, and their derivatives. Aqueous buffer is designated by AQ.

Catalyst	Substrates	System
IBA[a]	PNDP[c]	CTAC/AQ[2,40]
IBA, IBX,[b] OXIBA[f]	PNDP, PNPAc,[d] PNPH[e]	CTAC/AQ[39]
CHDA-IBA[g]	PNDP, PNDEP,[h] PNDB[i]	CTAC/AQ[48]
IBA, OXIBA, 5-NIBA[k]	PNDP	CTAB/1-BuOH/HEX /AQ[2,16,45,5i]
OXIBA	PNDP	CTAC/AQ[51]
IBA, 5-NIBA,4-CXIBA,[l] 4-NIBA,[m] OXIBA, 4-MIBX[n]	PNDP	CTAC/Ad/HEX/ AQ[45,44]
5-BXIBA,[p] 5-NIBA, 5-DDXIBA,[q] 5-BXIBX,[r] 5-NIBX,[s] 5-DDXIBX[t] 5-MIBA[u]	PNDP, PNPH, NPIPP[v]	CTAC/AQ[41,43]
IBA, OXIBA, 5-MXIBA,[w] 5-NIBA, CHDA-IBA	PNDP, GA,[x] GB,[y] GD,[z] VX[aa]	CTAC/AQ[41,42]

[a] o -iodosobenzoate
[b] o -iodoxybenzoate
[c] p-nitrophenyldiphenyl phosphate
[d] p-nitrophenyl acetate
[e] p-nitrophenyl hexanoate
[f] 5-(n-octyloxy)-2-iodosobenzoate
[g] 4-(cetyl-2-hydroxyethyldimethyl ammonium)-2-iodosobenzoate
[h] p-nitrophenyldiethyl phosphate
[i] p-nitrophenyldibutyl phosphonate
[k] 5-nitro-2-iodosobenzoate
[l] 5-carboxy-2-iodosobenzoate
[m] 4-nitro-2-iodosobenzoate
[n] 4-methyl-2-iodoxybenzoate
[p] 5-(n -butoxy)-2-iodosobenzoate
[q] 5-(n -dodecyloxy)-2-iodosobenzoate
[r] 5-(n -butoxy)-2-iodoxybenzoate
[s] 5-(n -octyloxy)-2-iodoxybenzoate
[t] 5-(n -dodecyloxy)-2-iodoxybenzoate
[u] 5-methyl-2-iodosobenzoate
[v] p-nitrophenylisopropylphenyl phosphinate
[w] 5-(methoxy)-2-iodosobenzoate
[x,y,z,aa] tabun, sarin, soman (See Fig. 4)

Table 19. Comparison of second order rate constants for PNDP hydrolysis.

Catalyst	Second Order Rate Constants ($s^{-1}M^{-1}$) Reference						
	41[a]	43[b]	16[c]	51	48[f]	45	39
IBA	260		9.4	1.2[d]		1550[g]	645[b]
5-BXIBA	4575						
5-OXIBA	4526		6.5	6038[e]		1.4[d]	14426[h]
5-DDXIBA	4864						
CHDA-IBA					28500		
4-NIBA	1032		11.4				
5-NIBA	588	616	3.5	0.9[d]			
4-CXIBA	146						
5-CXIBA			2.0				
5-MXIBA		546					
5-MIBA	774						
IBX							178[i]
4-MIBX			8.0				
5-MIBX	564						
5-BXIBX	4450						
5-OXIBX	4494						
5-DDXIBX	4012						
4-NIBX	1089						
5-NIBX	494						

[a] 1mM CTAC/borate buffer; pH 8.5; 25 °C

[b] 1 mM CTAC/0.02 M phosphate buffer, μ = 0.0ᶠ (NaCl); pH 8.0; 25 °C

[c] 15.5 % CTAC / 14.0 % Ad / 9.0 % HEX / 61.5 % AQ; 0.03 M borate buffer; pH 9.2; 25 °C

[d] 18.0 % CTAB / 18.0 % 1-BuOH / 4 % HEX / 60 % AQ; 0.03 M borate buffer; pH ~ 9; 25 °C

[e] 1 mM CTAC/0.03 M borate buffer; pH 9.2; 25 °C

[f] 5 mM CTAC/0.01 M tris buffer, μ = 0.01 (KCl); pH 8.0; 25 °C

[g] 0.82 M CTAC/0.03 M borate buffer; pH 9.2; 25 °C

[h] 0.20 mM CTAC/0.02 M phosphate buffer, μ = 0.08 M NaCl; pH 8.0; 25 °C

[i] 0.80 M CTAC/0.02 M phosphate buffer, μ = 0.08 M NaCl; pH 8.0; 25 °C

Table 20. Second order rate constants for the catalyzed hydrolysis of PNDP in the 8 % CTAB / 8 % MP / 4 % TOL / 80 % AQ system. The pH range is 9.2 - 9.4, and the catalyst concentration ranges from 8.75×10^{-5} to 5.0×10^{-4} M.

Catalyst	k_{IBA} ($sec^{-1}M^{-1}$)
2-iodoso benzoate	12.4 ± 0.55
2-iodoso-4-methylbenzoate	18.6 ± 0.36
2-iodoso-4-ethylbenzoate	22.9 ± 0.38
2-iodoso-4-n-propylbenzoate	0.01 ± 0.01
2-iodoso-4-n-pentyl benzoate	0.03 ± 0.01
2-iodoso-4-n-octyl benzoate	---

Table 21. Second order rate constants[47] for hydrolysis of PNDP in 18 % CTAB / 18 % 1-BuOH / 4 % HEX / 60 % AQ. The pH is 9.2.

Catalyst	Rate Constant ($sec^{-1}M^{-1}$)
o-IBA	1.2[59]
m-IBA [47]	1.9×10^{-3}
p-IBA [47]	6.9×10^{-6}

Table 22. Pseudo first order rate constants, k_{obsd}, for the hydrolysis of PNDP in CTAB/1-BuOH/HEX/AQ microemulsion media following exposure to low intensity radiation.

Time (min)	k_{obsd} x 10^4 (sec^{-1})
0	5.6
4	3.6
8	2.3
12	1.5
20	0.91
25	0.72
30	0.43
35	0.36
40	0.33
60	0.29
70	0.25
90	0.24
110	0.23
130	0.24

Table 23. Pseudo first order rate constants, k_{obsd}, for the hvdrolysis of PNDP in CTAB/1-BuOH/HEX/AQ microemulsion media following e   )sure to high intensity radiation.

Time (sec)	k_{obsd} x 10^4 (sec^{-1})
0	5.8
30	4.9
60	4.2
120	3.6
180	2.6
240	2.1
360	1.5
480	1.0
600	0.73
720	0.51
900	0.38
960	0.29
1080	0.28
1200	0.25
1500	0.25

Table 24. Measured and reported values of absorption (Abs.) maxima and donor lifetimes in water at 25 °C (unless indicated below).

Donor	Abs. Maxima (nm)		Donor Lifetimes (μs)	
	Measured	Reported	Measured	Reported
I	429, 453	452, 458[50] 423[53] 452,[8,54] 453[57,53] 455[58,55]	0.593	0.576[60] 0.60[8]
II	422, 448	425, 465[56] 421, 447[8,50] 422, 447.5[9] 447[200]	----	0.908[60] 0.92[8]
III	455, 478*	460[8]	— 455[55]	4.68[8] 3.58[60]
V	447, 470	----	3.79	3.73[60]

* Absorption spectrum for donor III was measured in MP.
[50] 4.75 M $HClO_4$; 30 °C
[57] 1.0 M $HClO_4$
[56] 2 parts diethylether, 2 parts 3-methylpentane, 1 part 100 % ethanol; 82 °K

Table 25. Aggregation numbers (N) determined from steady-state luminescence quenching measurements in microemulsion media.

% CTAB	CoS	% CoS	Oil	% Oil	% AQ	N
8.0	MP	8.0	TOL	4.0	80.0	164,182
8.0	2-P	6.9	TOL	4.0	81.1	243,252,210
8.0	EP	9.1	TOL	4.0	78.8	206,190,156
8.0	iso-PP	10.3	TOL	4.0	77.8	241,163
8.0	AP	10.1	TOL	4.0	77.9	230,207
8.0	VP	9.0	TOL	4.0	79.0	253,176
8.0	CHP	13.5	TOL	4.0	74.5	277,289,248
15.0	MP	30.0	TOL	5.0	50.0	427,357,288
19.4	MP	25.6	TOL	5.0	50.0	427,424,380
22.5	MP	22.5	TOL	5.0	50.0	613,339
27.0	MP	18.0	TOL	5.0	50.0	595,457,629
28.6	MP	16.4	TOL	5.0	50.0	750
18.0	MP	18.0	TOL	4.0	60.0	457
13.5	MP	13.5	TOL	3.0	70.0	310
9.0	MP	9.0	TOL	2.0	80.0	231
4.5	MP	4.5	TOL	1.0	90.0	156
17.0	MP	17.0	TOL	12.0	54.0	546
26.0	MP	26.0	TOL	17.0	31.0	897
22.0	MP	22.0	TOL	23.0	33.0	722
9.4	MP	9.4	TOL	6.2	75.0	268
15.0	CHP	30.0	t-BuTOL	5.0	50.0	343
19.4	CHP	25.6	t-BuTOL	5.0	50.0	416,456
22.5	CHP	22.5	t-BuTOL	5.0	50.0	550
27.0	CHP	18.0	t-BuTOL	5.0	50.0	666
28.6	CHP	16.4	t-BuTOL	5.0	50.0	576
36.0	CHP	36.0	t-BuTOL	8.0	20.0	654
31.5	CHP	31.5	t-BuTOL	7.0	30.0	499
27.0	CHP	27.0	t-BuTOL	6.0	40.0	611
22.5	CHP	22.5	t-BuTOL	5.0	50.0	535
18.0	CHP	18.0	t-BuTOL	4.0	60.0	404
13.5	CHP	13.5	t-BuTOL	3.0	70.0	456
9.0	CHP	9.0	t-BuTOL	2.0	80.0	240
4.5	CHP	4.5	t-BuTOL	1.0	90.0	111,109
17.0	CHP	17.0	t-BuTOL	12.0	54.0	336
26.0	CHP	26.0	t-BuTOL	17.0	31.0	607
22.0	CHP	22.0	t-BuTOL	23.0	33.0	609
21.0	CHP	21.0	t-BuTOL	11.0	47.0	216
8.9	1-BuOH	9.1	HEX	2.0	80.0	341,387
4.5	1-BuOH	4.5	HEX	1.0	90.0	151
18.0	1-BuOH	18.0	HEX	4.0	60.0	469
24.1	1-BuOH	24.1	HEX	47.5	4.3	608

Table 26. Lifetimes of donors V and I (AμE) in microemulsion media (no Q).

	% CTAB	CoS	% CoS	Oil	% Oil	% AQ	τ (μs)
1)	8.0	MP	8.0	TOL	4.0	80.0	3.36 ± 0.77
2)	8.0	CHP	13.5	TOL	4.0	74.5	4.30 ± 0.19
3)	4.5	MP	4.5	TOL	1.0	90.0	4.89 ± 0.21
4)	4.5	CHP	4.5	t-BuTOL	1.0	90.0	4.06 ± 0.65
5)	8.9	1-BuOH	9.1	HEX	2.0	80.0	4.75 ± 0.20
6)	4.5	1-BuOH	4.5	HEX	1.0	90.0	3.77 ± 0.36
7)	4.5	DMF	4.5	TOL	1.0	90.0	4.50 ± 0.58
8)	4.5	DEF	4.5	TOL	1.0	90.0	3.67 ± 0.22
9)	4.5	DIPF	4.5	TOL	1.0	90.0	4.10 ± 0.37
10)	4.5 CTAC	Ad	4.5	HEX	1.0	90.0	3.72 ± 0.16
11)	5.53 SDS	C_5H_{12}	10.28	DDEC	5.14	79.05	0.701±0.01

Table 27. Aggregation numbers (N) determined from time-resolved luminescence quenching measurements in microemulsion media (Table 26).

μE	η	k_q($\times 10^6$)/s	N (T-R)	N (S-S)
1	0.63 ± 0.15	1.13 ± 0.34	273 ± 64	173 ± 12.7
2	----	----	----	271 ± 21.0
3	0.72 ± 0.12	1.25 ± 0.31	174 ± 30	156
4	1.11 ± 0.55	0.21 ± 0.18	269 ± 134	110 ± 1.4
5	----	----	----	364 ± 33.0
6	0.63 ± 0.08	0.94 ± 0.41	154 ± 19	151
7	1.02 ± 0.05	0.88 ± 0.10	247 ± 12	124
8	0.51 ± 0.07	1.39 ± 0.13	124 ± 17	115
9	1.13 ± 0.56	0.19 ± 0.16	275 ± 137	135
10	1.77	0.31	740 ± 32	221
11	1.30 ± 0.83	1.29 ± 0.62	484 ± 308	142 ± 16.0

Table 28. Combined data from Tables 25, 26, and 27.

%CTAB	CoS	%CoS	Oil	%Oil	%AQ	N(T-R)	N(S-S)
1. 8.0	MP	8.0	TOL	4.0	80.0	273±64	173±13
2. 8.0	CHP	13.5	TOL	4.0	74.5	----	271±21
3. 4.5	MP	4.5	TOL	1.0	90.0	174±30	156
4. 4.5	CHP	4.5	t-BuTOL	1.0	90.0	269±134	110±1
5. 8.9	1-BuOH	9.1	HEX	2.0	80.0	----	364±33
6. 4.5	1-BuOH	4.5	HEX	1.0	90.0	154±19	151
7. 4.5	DMF	4.5	TOL	1.0	90.0	247±12	124
8. 4.5	DEF	4.5	TOL	1.0	90.0	124±17	115
9. 4.5	DIPF	4.5	TOL	1.0	90.0	275±137	135
10. 4.5CTAC	Ad	4.5	HEX	1.0	90.0	740±43	221
11. 5.53SDS	C_5H_{12}	10.28	DDEC	5.14	79.05	484±308	142±16